Cover page for final technical report

Project Title:	Atmospheric CO_2 Capture and Membrane Delivery
Project Period:	Oct 1, 2015 – Sept. 30, 2018
Reporting Period:	Oct 1, 2015 – Sept. 30, 2018
Reporting Frequency:	Final
Recipient:	Arizona State University
Website:	www.asu.edu
Award Number:	DE-EE0007093
Awarding Agency:	DOE EERE – Bioenergy Technology Office: Targeted Algal Biofuels and Bioproducts (TABB)
Working Partners:	N/A
Cost-Sharing Partners:	N/A
Principal Investigator:	Dr. Bruce Rittmann Regents' Professor of Environmental Engineering Director of the Biodesign Swette Center for Environmental Biotechnology (480)727-0434 Rittmann@asu.edu
Submitted by:	N/A
DOE Contracting Officer:	Lalida Crawford
DOE Project Manager:	Christy Sterner

4/26/2019

Signature **Date**

Acknowledgment: This material is based upon work supported by the Department of Energy's Office of Energy Efficiency and Renewable Energy under the Bioenergy Technologies Office, Award Number EE0007093.

Table of Contents

Executive Summary

Motivation

A major bottleneck for growing microalgae as a sustainable alternative to fossil carbon in economically producing fuels and chemical products is the cost of delivering CO_2 in sufficient concentrations for it not to limit growth. This project sought to develop and integrate two innovative technologies for capturing and concentrating CO_2 from air and delivering it to microalgae with high efficiency into an Atmospheric CO_2 Enrichment and Delivery (ACED) system (**Figure 1**). The CO_2 capture technology is based on moisture swing sorption (MSS), where specialized resin materials selectively capture CO_2 when dry and release it when wet into a confined space where the concentration can be increased up to 500-fold. The CO_2-delivery technology is based on membrane carbonation (MC), which uses hollow fiber membranes that allow CO_2 to diffuse into the algae-containing liquid without forming bubbles, achieving nearly 100% delivery efficiency. The project objectives, work performed, and key findings are described next.

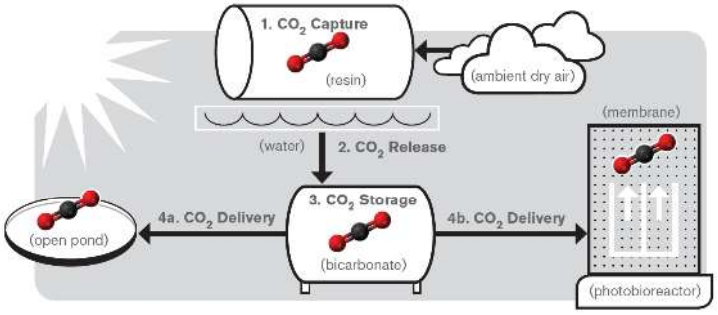

Figure 1. Schematic illustrating the Atmospheric CO_2 Enrichment and Delivery (ACED) system.

Objectives

1. Develop the MC technology to deliver CO_2 efficiently to microalgal cultures when the CO_2 concentration in the supply gas is <100% CO_2; this objective includes indoor and outdoor testing.
2. Develop the MSS technology to capture CO_2 from the atmosphere and concentrate it to a level suitable for delivery by MC to microalgae; this objective includes indoor and outdoor operation.
3. Develop an intermediate system to store captured CO_2 to buffer differences in supply and demand, further concentrate the CO_2 and integrate the MSS and MC technologies.
4. Develop a model for MC, MSS, and the integrated system for economic projections.

Work completed

1. **Subsystem design, construction, and characterization** [Months 1-6]. ACED integration requirements were defined; prototype MSS and MC sub-systems were constructed to conform to these requirements and characterized independently.
2. **Subsystem optimization and evaluation** [Months 7-12]. An iterative process of operating and upgrading each subsystem at lab scale, leading to compatibility at full integration.
3. **System Integration with open raceway, testing, and modeling** [Months 13-24]. Operation and testing of the integrated ACED system in an open raceway pond and modeling.

Key findings and achievements

Membrane carbonation (MC) CO_2 delivery using hollow fiber membranes

1. Biomass productivities were equal and pH control was superior with MC, compared to sparging.
2. ~100% delivery efficiency and 3-fold higher Carbon Utilization Efficiency (CUE) (versus sparging) were achieved with MC.

3. CO_2 delivery rates by MC were not adversely affected by months of operation outdoors.
4. Effective strategies were developed to relieve inert gas accumulation when delivering < 100% CO_2. This concept will be further evaluated to deliver industrial gases as part of award DE-EE0008517.
5. MC reduces the cost of supplying CO_2 by at least 40–50% for current operators who pay $120–500 / tonne for CO_2.
6. MC should reduce total CO_2 costs by 15–20% at the large scales envisioned by BETO.

Moisture swing sorption (MSS) CO_2 capture with anion exchange resin

1. CO_2 capture from ambient air was demonstrated in the lab and for outdoor conditions.
2. Over 10% of CO_2 in air was captured by dry resin in lab wind tunnel tests at 1 m/s.
3. A MSS prototype was constructed for outdoor evaluation.
4. Performance data were collected periodically over 6 month and for up to 11 consecutive days; the extent of data collection was limited by hardware, software, and weather issues.
5. Outdoor performance was best when temperature >25 ^{o}C, wind speed >2 km/h wind, and < 25% relative humidity.
6. Wetting the resin by temporarily flooding the regeneration chamber to release CO_2 made sorbent filters too wet. This slowed drying times, reducing performance and wasting water.
7. Adding sodium bicarbonate to supply water mitigated performance reduction from anions in tap water.
8. System, and especially the sorbent material, survived nearly nine months under outdoor conditions, and remained intact.

CO_2 storage within carbonate/bicarbonate brine tanks

1. A low-energy system for storage of CO_2 in carbonate/bicarbonate brines was demonstrated.
2. Heating the storage brine to near 100^{o}C releases gas with >90% CO_2 on lab scale and >70% outdoors.
3. A transfer mechanism using wetted fabrics was demonstrated for dissolving captured CO_2 into storage brine.
4. The concept to capture CO_2 was demonstrated over a range of concentrations into multiple brine tanks.
5. Software emerged as a major bottleneck in technology development. Software frequently terminated CO_2 delivery into storage prematurely, reducing production.
6. CO_2 flux into storage is highly dependent on the air flow rate and brine composition.

Broader impacts

The ACED research program added to our understanding of 1) MC technology's (i.e., hollow fiber membranes) utility for transferring pure CO_2 and CO_2 gas mixtures into microlagal cultures in laboratory and outdoor environments, 2) the first-of-a-kind MSS technology to capture CO_2 from ambient outdoor air, and 3) methods for storing captured CO_2 in carbonate/bicarbonate brines from which the CO_2 can be retrieved at high concentration (> 90%). Near-term commercial opportunities were outlined for the MC technology for small scale algae cultivation with high CO_2 costs (> $100/ton) and larger scale operators with continued development. This will help reduce costs for producing sustainable fuels and products and reduce cost for microalgal research for developing new applications. Research areas were identified for MSS technology to achieve cost competitive CO_2 produced from ambient air ($100/ton) as a means

for closing the carbon cycle to make products from atmospheric CO_2 instead of fossil fuels and remove CO_2 from air to mitigate climate change.

Project Overview

Introduction

2.5 billion years ago, photosynthetic microorganisms completely transformed our planet by using solar energy to capture huge amounts of CO_2 from the atmosphere for growth and releasing O_2. Today, these microalgae have the potential to produce fuels and products with significant economic value. Key to making microalgal technologies economically attractive is increasing the per-area productivity so that capital costs are offset by a large income stream. Despite atmospheric CO_2 levels rising at an alarming rate from anthropogenic fossil fuel combustion, current levels (i.e., ~ 410 ppmv) present a significant limitation for technologies that rely on microalgal growth. One way to increase the areal microalgal productivity is to deliver CO_2 at a concentration much higher than in ambient air. Our goal is to deliver enriched CO_2 in a cost-effective manner and to be able to do it at any location.

While flue gas from a power plant is an appealing source of CO_2-enriched gas, its usefulness is compromised by four factors. First, the sunny places ideal for growing microalgae (e.g., the rural Southwest) have few major flue-gas sources, and high CO_2-transportation costs constrain viable growing areas to near the CO_2 source (Quinn et al. 2012). Second, flue gas contains a wide range of contaminants (e.g., heavy metals, arsenic, selenium) that can be toxic to microalgae and can contaminate fuel or high-value products (e.g., cosmetics, nutrition supplements). Third, microalgae companies may become responsible for the emission of CO_2 and the release of all other air pollutants in the exhaust streams from their systems. Fourth, fuels produced from microalgae grown using flue gas will ultimately lead to fossil CO_2 being released into the atmosphere preventing such fuel from reaching true carbon neutrality. Having a cost-effective strategy to capture and concentrate CO_2 directly from the air for delivery to microalgae-growth systems will overcome all four limitations. It will enable high microalgae productivity on available land in any sunny location.

CO_2-enriched gas is typically delivered to microalgae by sparging. A tradeoff is encountered between sparging fast enough to avoid slow growth, but slow enough to avoid off-gas CO_2, which wastes resources and money. Cost-effective bubble-less membrane delivery of gases to microorganisms can dramatically increase the efficiency of gas transfer and is critical to increasing the growth rate and CO_2 utilization of microalgae.

The project goal has been to combine novel CO_2-capture and -delivery technologies to boost microalgal productivity and cost-effectiveness for any location and for all microalgae products. The two technologies are Moisture Swing Sorption (MSS) and Membrane Carbonation (MC), and we call the integrated system **A**tmospheric **C**O_2 **E**nrichment and **D**elivery (**ACED**). As illustrated in **Fig. 1,** MSS enriches CO_2 directly from the atmosphere using a novel moisture-based sorption system. The CO_2 is stored on site and delivered precisely and efficiently by the novel MC system.

Project Goal

This project combined two innovative technologies, integrating them into a single system while simultaneously advancing each. The project moved in stages. In the first stage, we advanced each sub-system toward integration in the second stage. The sizing of each sub-system and the handoff of CO_2 will maximize the performance of the system overall.

For example, design of the integrated system needed to take into account that the cost of the MSS system increases as the CO_2 concentration exceeds 3%, while the membrane area of the MC system increases as the CO_2 partial pressure is lowered. Optimization must balance cost of adding membranes, increasing CO_2 concentration, and raising overall pressure. The MSS system also must account for the specific CO_2 demands of microalgae, by adding storage capacity for excess production at night and increasing CO_2 concentration as technically and economically feasible.

Our primary goal has been to demonstrate the feasibility of this approach. In this we succeeded. We deployed all units outdoors to feed CO_2 from the air to an outdoor algae growth system. This is an early prototype, with minimal integration.

We demonstrated the ACED system in outdoor microalgae growth systems. For that, we used 1500-L open raceway ponds for demonstrations. We installed appropriately sized MC modules in the raceway ponds and documented the efficient delivery of CO_2 to microalgae using feed streams that the MSS could deliver.

For the ACED system to become practical, costs will have to be reduced and processes will have to be streamlined. Nevertheless, we have shown that it is possible to use enriched CO_2 obtained locally from the atmosphere. In particular, we demonstrated that MSS can capture and concentrate atmospheric CO_2 to a concentration range of 3% to 90% and that delivering the CO_2 by MC leads to nearly 100% use of CO_2 in the microalgae system. Much work needs to be done on system integration and on increasing the reliability of the MSS system.

Key Concepts

1. Dry resin selectively collected atmospheric CO_2 (~ 410 ppm).
2. Wetting the CO_2-loaded resin released CO_2 at a concentration of ~1%; this illustrates why the technology is called Moisture Swing Sorption (MSS). We fell short of our initial goal of 5%, because the dead volume of the chamber proved to be too large. Further optimization will be needed to achieve 5%, which has been exceeded under laboratory conditions.
3. The CO_2 stream released from MSS has been successfully directed to a carbonate brine that stores the CO_2 as bicarbonate (HCO_3^-).
4. Heating the brine released the stored HCO_3^- to produce a much more concentrated CO_2 supply. Under practical operations, which was hampered by air contamination, we achieved 70% CO_2 concentration. Indoor test runs on a smaller scale yielded 90% CO_2.
5. This concentrated CO_2 stream was compressed and delivered to the Membrane Carbonation (MC) technology.
6. MC delivered CO_2 to the microalgal culture on an on-demand basis that was determined by a pH controller.

7. MC provided CO_2-delivery rates and pH control at least as good as sparging, but with much higher CO_2-delivery efficiency.

Other Findings

Membrane carbonation (MC) delivery of CO_2 using hollow fiber membranes

1. The correct rate of CO_2 delivery and the desired pH could be achieved by opening and closing the gas-supply valve based on a pH set point.
2. Completely closing the distal end of fibers has the advantage of 100% deliver efficiency, but the buildup of inert gases within fibers reduces CO_2 flux.
3. Allowing the distal end of fiber to be completely open avoided the buildup of inert gases and allowed a high CO_2 flux, but also allowed major loss of CO_2 in the vented gas. Future designs could recover the lost CO_2 and return it to the MSS carbonator subsystem.
4. High CO_2-delivery efficiency and high CO_2 could be achieved simultaneously by restricting the flow of vented gas from the distal end. The optimal gas-flow rate from the fibers' distal ends must be further evaluated as a function of inlet gas composition and will be part of EERE award number DE-EE0008517.
5. TechnoEconomic Analysis (TEA) identified important economic value created by MC
    - A near-term opportunity is to sell MC modules to small-scale operators paying significant cost for CO_2, as the cost saving emanating from MC's much higher CO_2-utilization efficiency (CUE) overwhelms the costs of installing MC.
    - Over the longer term, technology advancements that lower the costs of installing MC will make MC advantageous at large scale, even if the cost of CO_2 is low.

Moisture swing sorption (MSS) CO_2 capture with anion exchange resin

1. Anions in tap water reduced resin collection efficiency; but this was overcome by adding bicarbonates to the make-up water so that the bicarbonate concentration exceeded other anion concentrations by 10- to 100-fold.
2. Challenges that still need to be overcome:
    - Storage adds significant cost when going from gas to liquid back to gas.
    - MSS hardware construction and software development and control were complex and slowed implementation of MSS.

CO_2 storage within carbonate/bicarbonate brine tanks

1. CO_2 was successfully transferred from the CO_2 collector into a CO_2 storage tank that used an energy-efficient gas-liquid contactor to make the transfer.
    - The use of multiple reservoirs to accommodate the dropping concentration of CO_2 in the sweep gas was successfully demonstrated.
    - Further optimization of the design is necessary.
2. Gas liquid transfer proved to be energetically far more favorable than the originally intended sparging of low concentration CO_2 into a brine.
3. Thermal release achieved > 90% CO2 on lab scale, but only > 70% outdoors

Summary of activities and key outcomes

A summary of each research activity and key outcomes is now presented. This is not an exhaustive compilation of what was performed, and more details can be found within the quarterly and annual reports. Tasks are presented in order except for TEA tasks, which are summarized together after other tasks. A full TEA report of MC and MSS technologies are included as appendices.

Task 0 - Process and Data Validation. [Go/No Go]

The ASU team worked with DOE and NREL advisors who visited ASU to assess the technology readiness level of the key technologies and key project metrics. The key performance parameter for productivity was reduced from 25 g AFDW m^2 d^{-1} to 5–10 g AFDW m^2 d^{-1}, which is in line with seasonally adjusted state of microalgae technology. This change recognized that increasing productivity was not the major goal of this project; instead, the goals were capturing atmospheric CO_2 and delivering it efficiently to microalgae.

Key Outcome: The project review yielded a Go approval to proceed with the project as planned.

Task 1 – Define subsystems. [Go/No Go]

The Team created requirements and specifications for each subsystem that, if met, would ensure that the integrated system could provide its intended function in a safe manner. The system was then designed to meet those specifications. Data on each subsystem was presented to DOE during a site visit, with approval given. One key recommendation was to forgo the originally planned experiments to integrate MSS and MC in 75-L rooftop photobioreactors; instead, integration was focused on 1500-L raceway ponds.

Key Outcome: Design documents were prepared for each subsystem and complete system. System integration requirements were met for all subsystems. A Go approval was issued to proceed with year 2 project activities.

Task 2 – Design continuous-operating CO_2-capture subsystem.

The Team designed, built, and tested lab-scale filter units (**Figure 2, inset**) that passively collect CO_2 from the air when dry and releases it when wet. A prototype filter unit was tested in a wind tunnel at a windspeed of 1 m/s, where it initially collected > 10% of the CO_2 from the air stream before declining in performance as the resin loaded up (**Figure 2**). The prototype unit consisted of a set of flat sorbent sheets held apart by spacers. The frontal area of the prototype was 10 cm by 10 cm, as compared to 100 cm by 50 cm for the full scale design (**Figure 3**). However the spacing and depth of the sheets comprising the filter were very close to those used in the full apparatus. An apparatus was constructed to repeatedly test the filter unit at the lab scale (**Figure 4**). This apparatus was comprised of a chamber, a water reservoir, a framework to hold the cube, and a mechanism to move the cube from the fully extended (exposed) position to the fully retracted (enclosed) position, where the filter was held within the regeneration chamber. In these early experiments, the CO_2 released from the resin was pumped through a sparger into a carbonate storage solution. **Figure 5** shows the rate of CO_2 delivery into storage. Techno-economic analysis later revealed the high cost of compressing and pumping dilute CO_2 captured into storage; hence, an alternative design was constructed consisting of fabric sheets soaked in

storage solution that would create a high surface area to passively take up captured CO_2; the fabric contactor is shown in **Figure 6**. Finally the filter unit design was scaled up into a collection panel (**Figure 3**) comprising 25 double-wide filter units to support the larger scale, outdoor experiments.

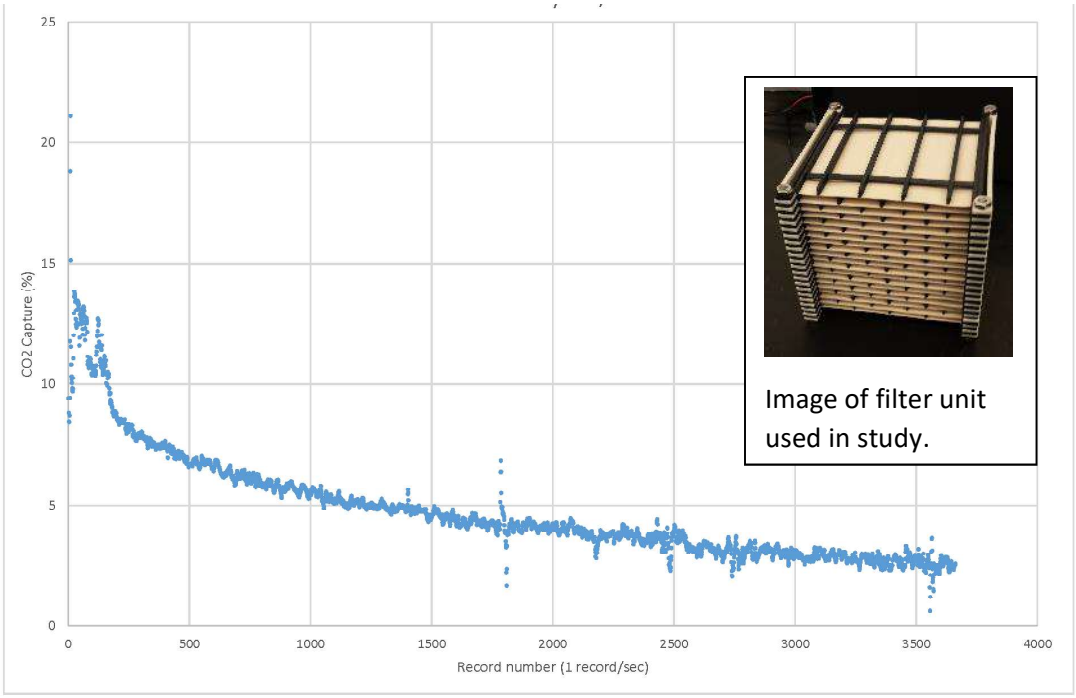

Image of filter unit used in study.

Figure 2. Fraction of CO_2 removed from ambient air flowing through filter unit at 1 m/s as it loads up.

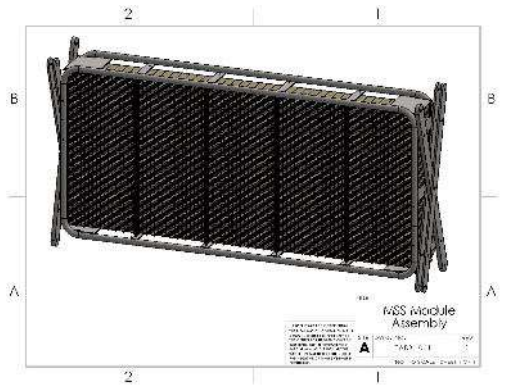

Figure 3. Design drawing of the CO_2 capture apparatus (collection panel), composed of 25 double-wide filter units.

Figure 4. Schematic illustrating the apparatus designed to test CO_2 capture and delivery into the storage brine of a single cube filter unit.

Key Outcome: The collector initially removed > 10% CO_2 from air at 1 m/s and operated for successive wet-dry cycles.

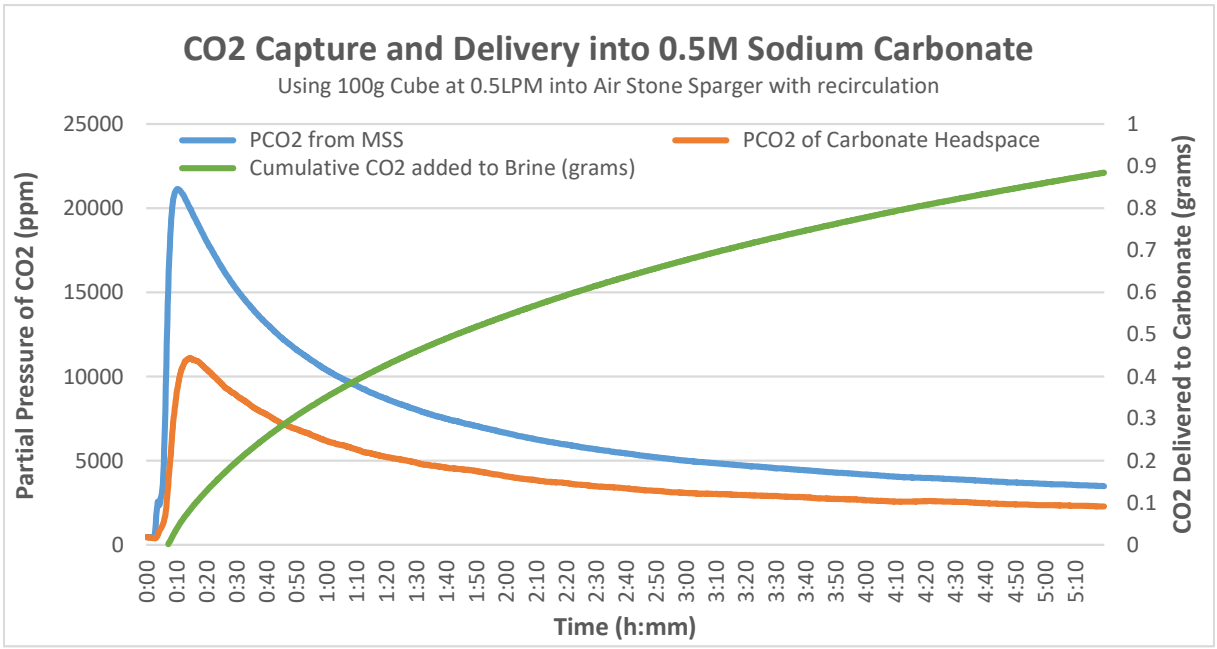

Figure 5. CO_2 released from filter unit delivered into a carbonate storage solution by sparging.

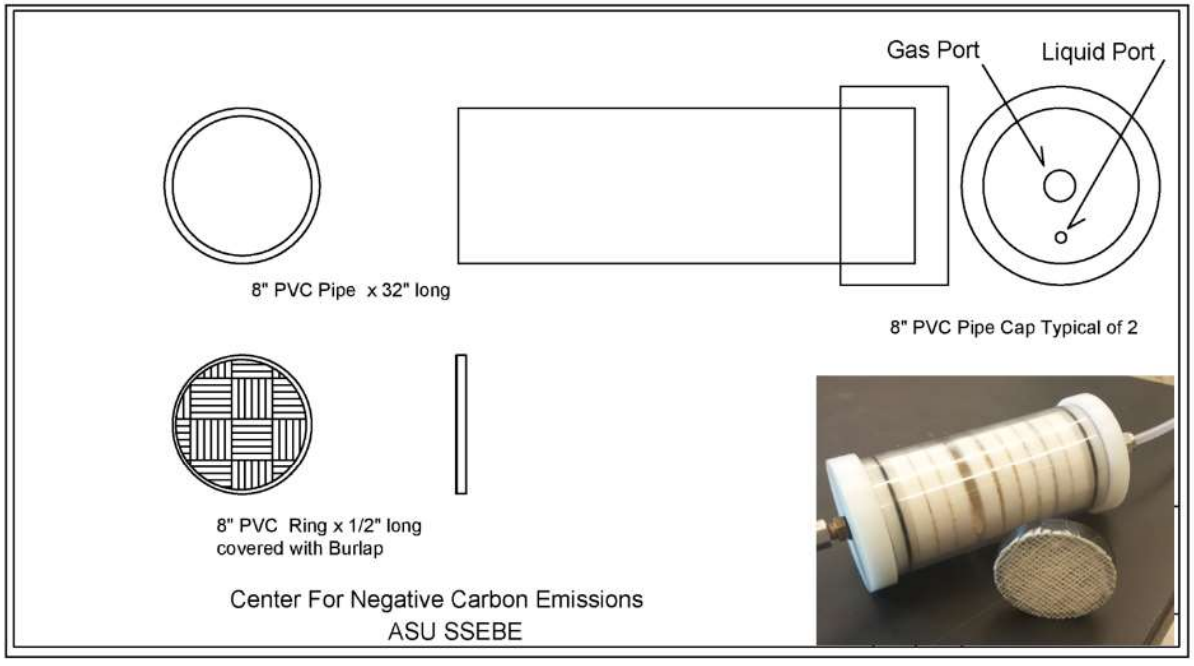

Figure 6. Schematic of the fabric contactor carbonator design and photo of a prototype system.. The prototype has fewer disks and a smaller diameter than the ultimate design.

Task 3 – Design and testing of bicarbonate storage and CO_2 delivery.

The MSS Team designed a thermal release column for extracting CO_2 from carbonate bicarbonate brines. It included a large single-stage distillation column and a multi-tray distillation column, condensing out water vapor with a cold trap to concentrations exceeding 90% CO_2, and then compressing the gas to pressures required by the MC system for delivery to the microalgae. We determined at this point that adding a vacuum stage to induce CO_2 extraction at lower temperatures was not cost effective. Finally, the thermal release column was integrated with the collector at the lab scale.

Key Outcome: The testing of the bicarbonate prototype showed that CO_2 delivery was possible, and that the system could produce CO_2 with > 90% concentration (**Figure 7**). Taken together, the collector can take CO_2 out of the atmosphere, deliver it in a nearly quantitative fashion to a carbonate/bicarbonate brine, from which it can once again be recovered by a distillation process.

Task 4 – Characterize CO_2-delivery rates of MC membranes in PBRs

The CO_2-delivery rate of the MC system was comprehensively evaluated as a function of CO_2 concentration and total applied pressure of the supplied gas using a special abiotic protocol and also when cultivating microalgae at the bench scale.

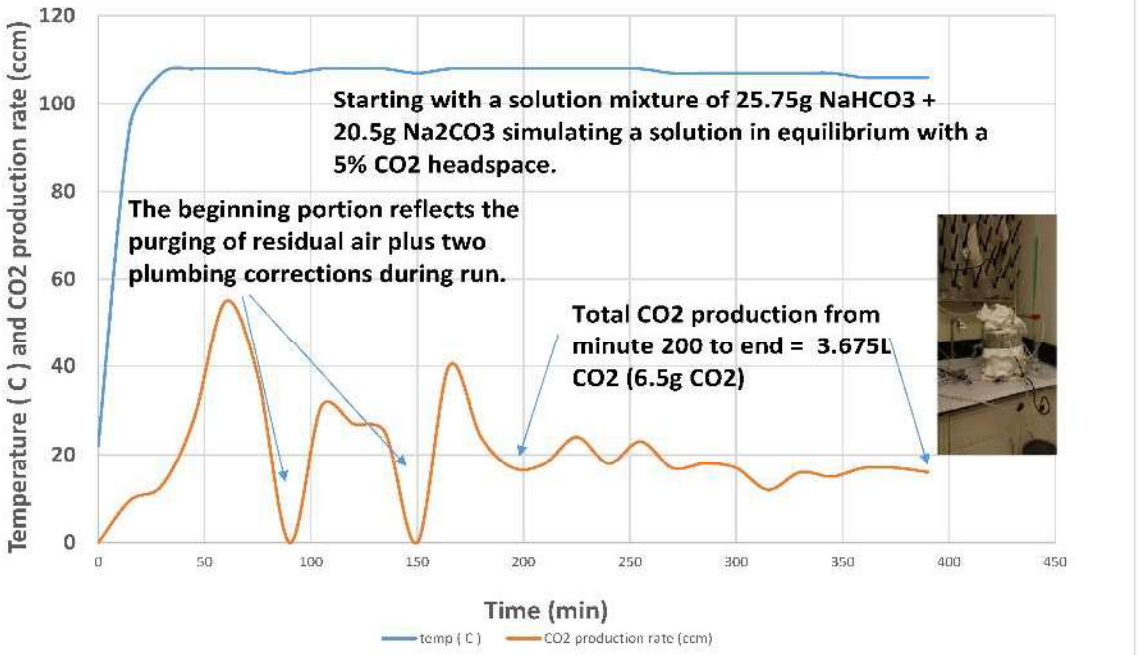

Figure 7. 90–95% CO_2 thermally released from the storage brine after condensing out water.

pH-model predicted DIC flux

We developed a mathematical model to compute the dissolved organic carbon (DIC) concentration in real time using pH measurements in abiotic tests. The DIC concentrations were then used to compute the rate of CO_2 transfer from the Hollow fiber membranes (HFM) to the liquid medium in abiotic experiments. **Figure 8** presents the results for an experiment in which we measured the DIC concentration in parallel to the pH measurements to evaluate the accuracy of the model. The model-predicted DIC concentrations matched the measured DIC values for pH values down to approximately 7.5, when the experimental data deviated from the predicted DIC concentrations. Low pH caused the liquid's CO_2 concentration to be super-saturated compared to its concentration in equilibrium with atmospheric carbon dioxide (~410 ppm), and CO_2 off-gassed before the sample could be analyzed. Additionally, the solution could absorb CO_2 from the atmosphere at very high pH, although the result in **Figure 8** does not indicate significant absorption. For these reasons, we restricted the pH range for computing DIC and the mass transfer kinetics to be from 10 to 8, where model-predicted DIC values definitely were accurate.

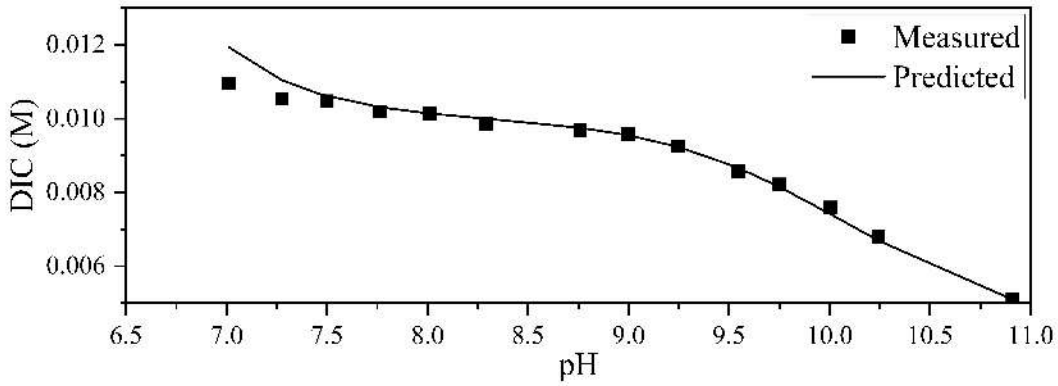

Figure 8. Comparison of DIC concentrations predicted by the model versus measured values using open-end HFM modules of 32 fibers, 0.18 m in length supplied with 90% CO_2 and diluting samples with DI water.

Open- vs Closed-End Operation

For the abiotic tests, we summarize the results in **Figure 9** and **Table 1** for the changes in CO_2 concentration, total gas pressure, and closed-end versus open-end configurations. The first trend is that the CO_2 flux increased as a function of gas inlet pressures in all cases. For example, with 100% CO_2 and closed-end operation, the CO_2 flux increased from 1500 to 6000 g CO_2/m^2-day as the lumen pressure rose from 5 to 20 psig (1.3 to 2.4 atm absolute pressure).

The two characteristic methods of operating the HFM are open end, in which the gas is passed through the fiber at a high rate to create a nearly uniform CO_2 concentration across the fiber, and closed-end, in which all gas that enters the HFM must diffuse from the lumen into the surrounding medium. In closed-end operation, the CO_2 concentration decreases in the fiber lumen the further it travels from the source gas due to selective transfer of CO_2 to the medium; thus, inert gases accumulate in the lumen. Accumulation of inert gases is accentuated when the inlet gas has substantially less that 100% CO_2, but it occurs to some degree even with a pure-CO_2 feed, due to the diffusion of inert gases from the solution into the lumen. As a result of inert-gas accumulation, the distal end of the membrane

lumen may lose its ability to transfer CO_2 to the liquid, and the average CO_2 flux out of the fibers is reduced. The impact of inert gases is more pronounced when the input gas is less than 100% CO_2, since the input inert gases accumulate in the lumen.

In contrast, open-end operation has a high gas velocity through the lumen. Thus, bulk mass transport through the lumen overwhelms diffusive mass transport across the membrane wall. This allows a uniform CO_2-concentration profile to be maintained in the membrane lumen, allowing CO_2 diffusion to occur uniformly throughout the lumen, since inert gases are vented out; however, it has two disadvantages. The first disadvantage of an open-end module is that a large amount of CO_2 is vented; this prevents the CO_2-transfer efficiency from approaching 100%. The second disadvantage is that the high gas-velocity through the lumen can lead to a pressure drop that lowers the average CO_2 partial pressure, even though inert gases do not accumulate.

In summary, a closed-end module is characterized by a high CO_2-transfer efficiency, but it can have a low CO_2 flux if inert gases accumulate. The opposite can be the case of open-end operation. **Table 1** clearly illustrates that the accumulation of inert gases in the closed-end module was the dominant effect for the set of experiments with 90% CO_2. In contrast, the pressure-drop effect was dominant for feeding 100% CO_2. For 50% CO_2, the trend was opposite: Closed-end operation had markedly lower CO_2 flux. This was an effect we anticipated: Out-diffusion of CO_2 depleted the lumen space of CO_2 near the distal end of the fibers, making some of the fiber surface area ineffective for CO_2 delivery. For example, with 20-psig pressure (2.4 atm), the flux at 50% CO_2 was about 25-fold lower than with 100% CO_2. This dramatic drop-off in transfer rate is the reason we included open-end operation in our evaluation.

Table 1: CO_2-transfer and HFM characteristics were affected by CO_2 inlet concentration and open-end versus closed-end operation. The modules consisted of 32 fibers, 0.18 m in length supplied with gas at 69 kPa-gauge.

CO_2 Content (%)	Operating Condition	Flux ($g\ m^{-2}\ day^{-1)}$	Usable Fiber Length (m)	(%)
90	Open	2150	0.15	83
50	Open	1200	0.15	83
10	Open	200	0.12	65
90	Closed	750	0.04	23
50	Closed	165	0.02	10
10	Closed	53	0.02	10

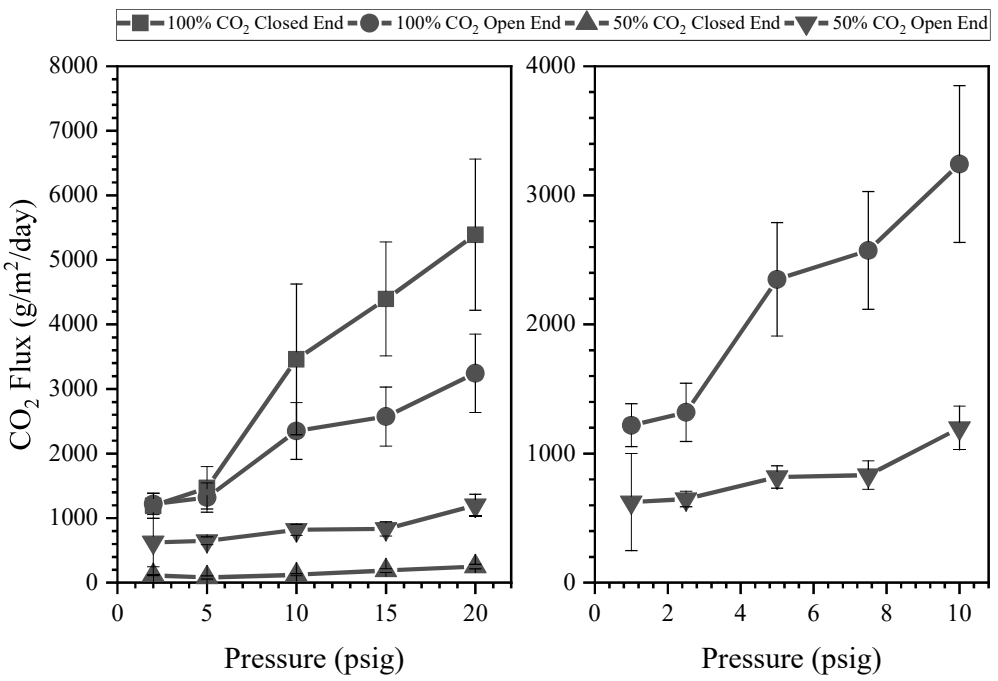

Figure 9. Pressure dependence of CO_2 flux for open-end or closed-end membrane modules consisting of 96 fibers, 0.21 m in length based on a) total gas inlet pressure for closed-end and open-end operation, and b) average total gas pressure across the lumen for open-end operation. Error bars represent the standard deviation of data for each experiment.

Semi-batch PBR operation with MC fibers and *Scenedesmus*:

We used *Scenedesmus acutus* strain LRB0401, obtained from AzCATI, as the model microalga for tests of our pH-stat system with on-demand CO_2 delivery from the fibers as the pH-control mechanism. HFMs were suspended inside 1.8-L glass flasks illuminated by 100 µE/m^2.s fluorescent lamps (**Figure 10**). The fibers had a solenoid valve on the inlet, and it was opened or closed in response to the culture's pH. When the pH was higher than the set point (pH = 8.0), the valve opened for CO_2 delivery. When the pH dropped below the 7.9, the inlet valve closed. A venting valve was located at the distal/outlet end of the fibers. The venting valve opened and closed based on separate pH set points of 8.05 and 8.03, respectively. The objective of opening the vent valve was to clear the membrane lumen of inert gases

when the CO_2 delivery rate was too low. To minimize the loss of CO_2, a bleed-valve was implemented to reduce CO_2 loss during venting by restricting the outflow rate.

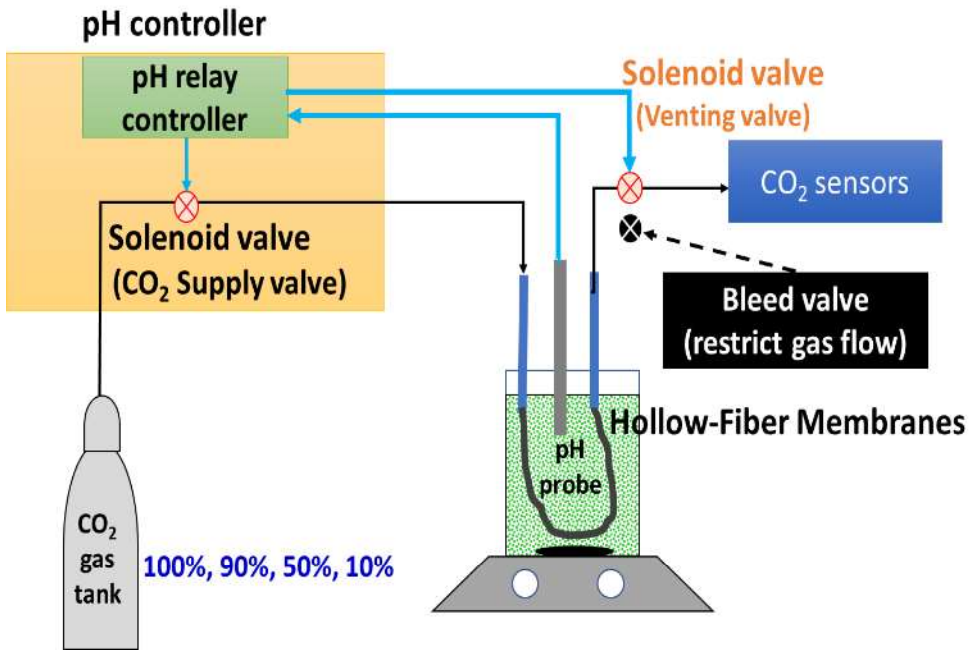

Figure 10. A schematic of the system used for testing CO_2-delivery strategies using gas supplies having CO_2 range from 10–100%.

PBR operation with mixed gasses

Figure 11 shows growth when we delivered 10%, 50%, 90%, and 100% CO_2. To reduce the off-gassing occurring with 10% CO_2, we included a bleed valve, which restricted the exiting flow to 2.2 standard cubic centimeter per minute (SCCM); without the bleed valve (i.e., open-end operation), the exit flow rate was ~1700 SCCM. Open-end operation was able to maintain CO_2 fluxes of 84 ± 20, 150 ± 32 and 170 ± 31 gCO_2/m^2-hr, when using 50%, 90% and 100% CO_2, respectively. The flux dropped to 22 ± 6 gCO_2/m^2-hr for 10% CO_2. For the fully open-end operation at the same gas pressure supply, CO_2 fluxes was proportional to CO_2 percentage.

When operated in the closed-end mode, the CO_2 flux declined only a small amount, to 140 ± 28 gCO_2/m^2-hr for 100% CO_2, but it dropped dramatically, to 1.9 ± 0.8 gCO_2/m^2-hr, for 10% CO_2, because of accumulating inert gases. However, using a bleed valve restored much of the flux for 10% CO_2.

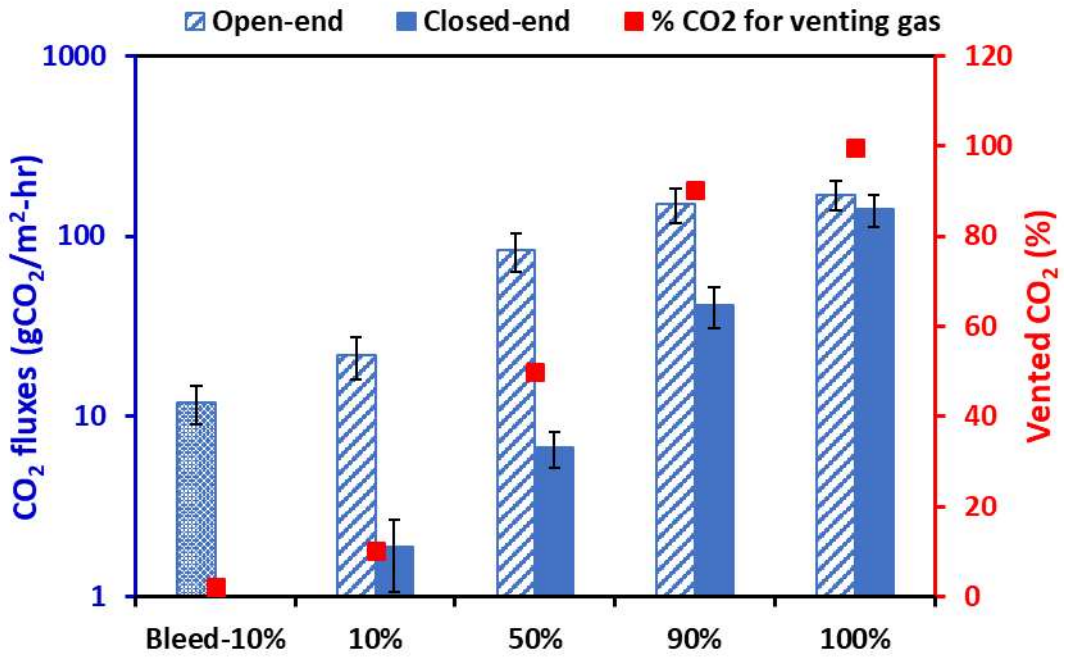

Figure 11. Given gas pressure supply at 10 psig, CO_2 flux (bars) and concentration of CO_2 in exhaust gas when the vent valve is open. Bleed-10% refers to the operational conditions of maintaining a steady exhaust rate of 2.2 SCCM when the main CO_2 valve is open.

Operation with a venting valve or bleed valve minimized CO_2 losses out the distal end of the fibers for 10% CO_2. Using a bleed valve limited CO_2 losses to only 2%, and the venting value kept the lost to 10%.

Figure 12 shows the pH in the medium and the status of the inlet and vent valves during two days of continuous cultivation for various input-CO_2 concentrations. The top panels show the variations of pH around the set-point of 8.0. The bottom panels show when the inlet valve was open (blue line) and when the venting value was open (orange line). 10% CO_2–Bleed means that venting valve remained open but the flow through the gas gauge was restricted.

The first thing that the graphs highlight is that the pH could be maintained within a narrow range for all input-CO_2 concentrations. In fact, pH control was most precise when delivering 10% CO_2. This trend was related directly to the second major trend: a transition from no venting for 100% CO_2 to a high frequency of venting for 10% (orange spikes). The third trend is that the inlet valve turned on less frequently (blue spikes) when delivering 100% CO_2, but was on most the time for 90% CO_2 and almost all the time for ≤ 50%. The inlet valve was on less often for 10%-bleed than for 10% CO_2 (open-end), since higher CO_2 flux could be achieved by using a bleed valve (**Figure 11**).

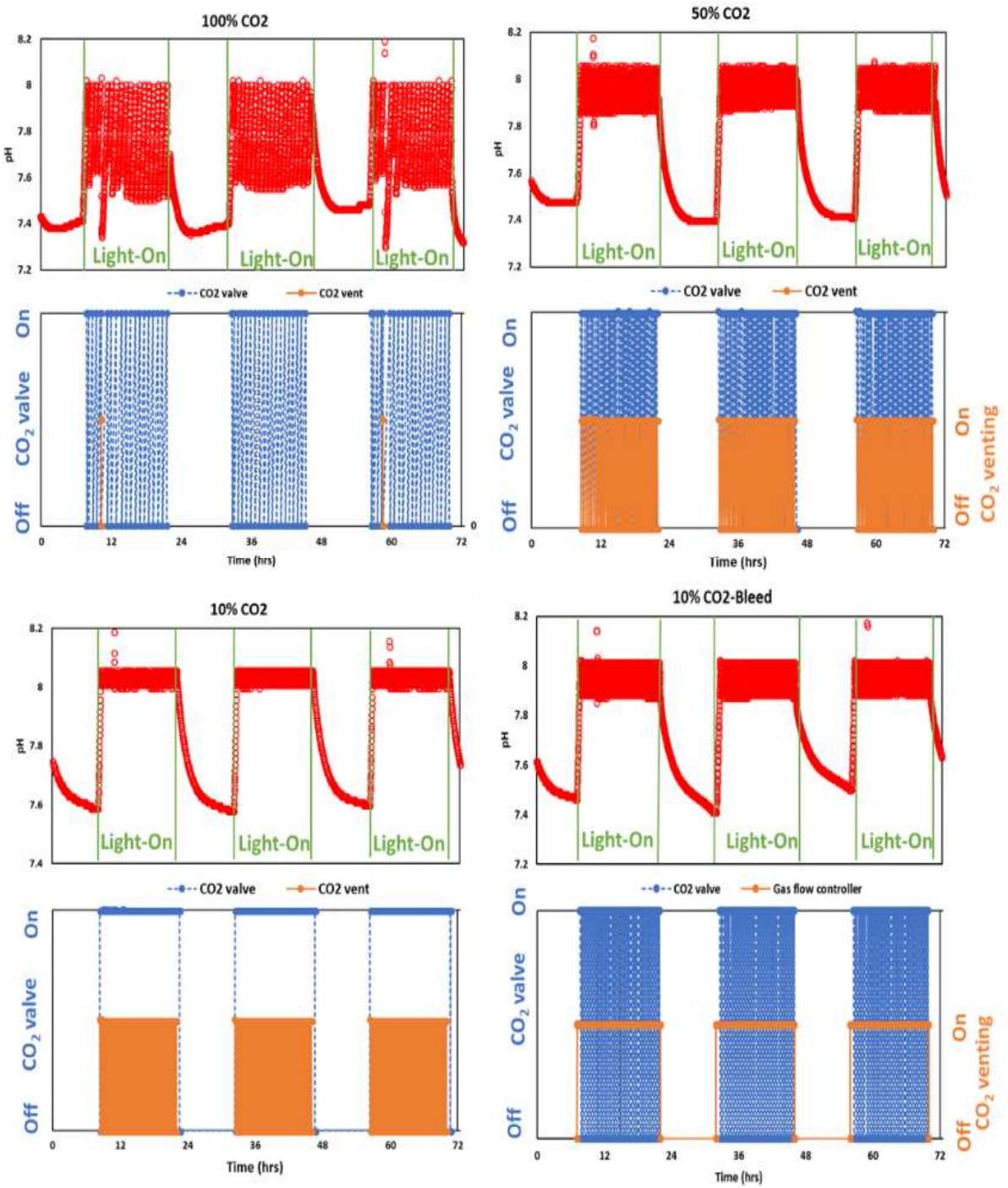

Figure 12. Examples of how pH-controlled operation of inlet and venting allowed precise pH control during the diurnal operation of cultures of *Scenedesmus acutus* in bench-scale PBRs.

Figure 13 shows the distribution of delivered CO_2 into the biomass and DIC in the medium, along with carbon-capture efficiency (CCU), which is defined as the percentage of delivered CO_2-C that is synthesized into biomass-C. The total transfer efficiency (TTE) is a larger value, because some of the

delivered CO_2-C is dissolved in the water as DIC. The distributions of delivered CO_2 were almost the indistinguishable for each operating condition. This was true because all systems have the same biomass-production rate and pH, which reinforces that the various forms of MC and sparging could support biomass growth when the pH was stabilized. Without any venting, MC using 100% CO_2 gave nearly 100% TTE (no venting and no bubbles) and 82% CCU, which was far superior to the 20% CCU with sparging. Delivering 10% CO_2 with the bleed-valve configuration gave a CCU of 60%, a significant improvement over sparging, but less than 82% CO_2 for pure CO_2. The CCUs for 90%, 50% and 10% CO_2 with open venting were less than 15% of CCU. These low values were associated with the small size of our bench-scale reactor (only 1.8 L), which meant that we have practical limits on how low we could restrict of outflow rate. Due to limited restriction of the outlet flow, a significant gas volume was lost each time when the vent valve was opened. Future work at larger scale will minimize the gas losses by venting. Our ability to minimize losses is supported by the results with the 10% bleed-valve, which had a CCU of 60%, and more precise flow control at larger scale will enhance the CCU even further.

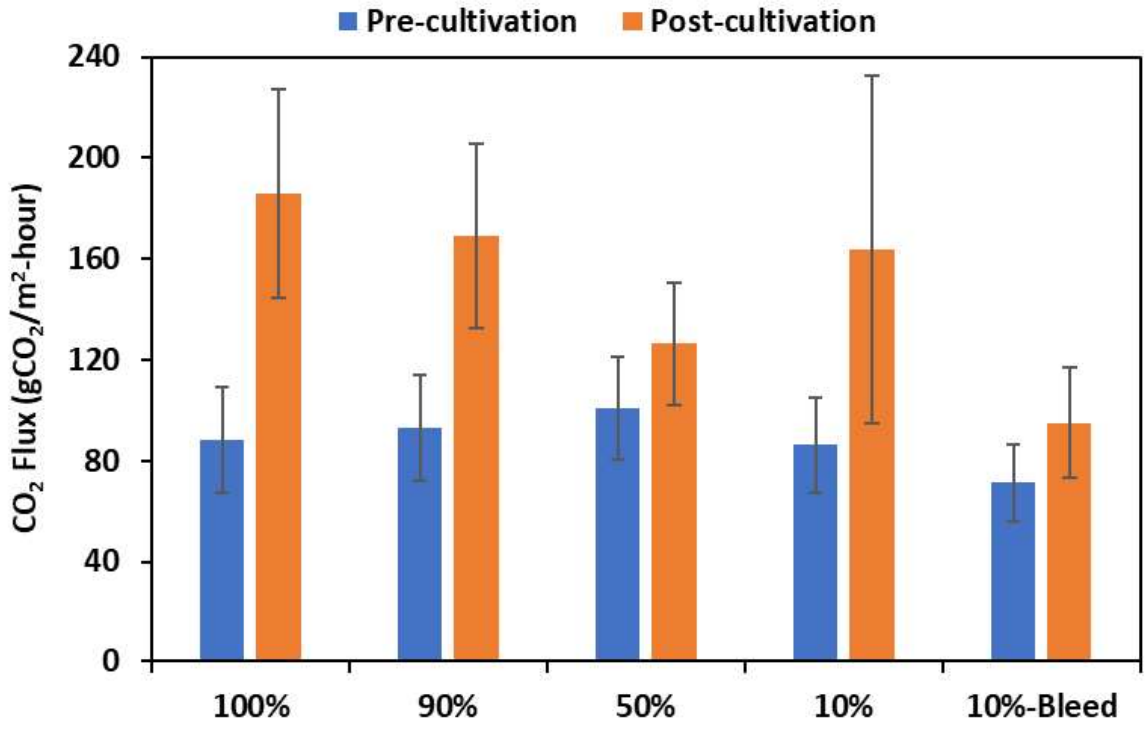

Figure 13. Comparison of CO_2 distribution into biomass and media, along with the calculated CO_2 capture efficiency for different CO_2 concentrations. Net CO_2 added was obtained from the difference between feeding cycle and measured by DIC.

Last but not least, we saw no decline in flux over time; in fact, the fluxes were even higher after cultivation, as shown in **Figure 14**. On the one hand, these results demonstrate that membrane fouling was not a problem. On the other hand, it is possible that the long-term pressurization of the lumen at 10 psig may have expanded internal macropores and thinned the non-porous inner layer. No matter the mechanisms acting, the MC approach was reliable for long-term use.

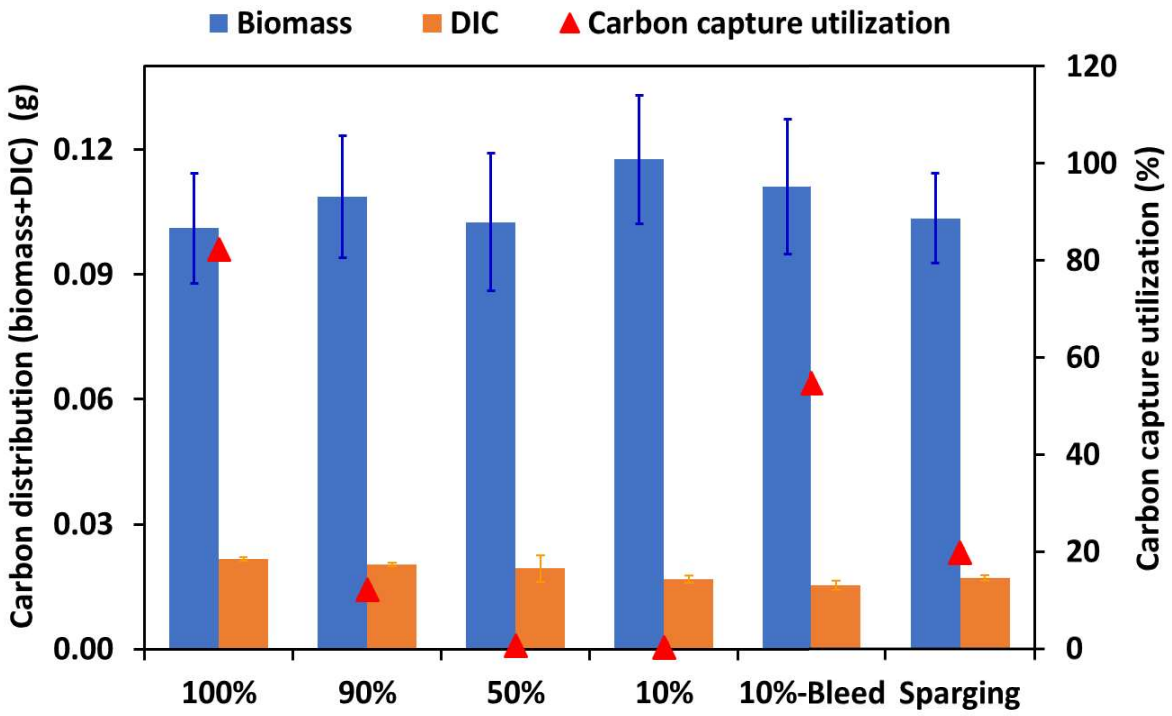

Figure 14. The fiber bundle performance was reevaluated using 90% CO_2 with open-end scenarios (with 10 psig gas supply) after 38-d cultivation

Key Outcomes:

1. Using a venting valve made MC compatible with a wide range of inlet CO_2 gas concentrations.
2. A bleed valve significantly reduced CO_2 loss.
3. Biomass productivities were nearly identical for the range of CO_2 contents from 10% to 100%.
4. Reliable, long-term operation was demonstrated.
5. CO_2-source flexibility, available with MC, opens up the possibility of using a wide range of concentrated sources to enhance the productivity of microalgae culturing.

Task 5 – Scaling up MC to outdoor 75-L PBRs.

A membrane carbonation system was designed for an outdoor 75-L photobioreactor (PBR). **Figure 15** shows the components for the design of MC modules for use inside the 75-L tubular PBRs. In order to insert the MC unit into the PBR, the PBR head was modified to allow the MC unit to be open- or closed-end (**Figure 15a**). CO_2 normally was delivered in the closed-end mode, for which the supplied CO_2 gas cannot exit the fibers except by diffusing through the membrane wall into the culture medium for uptake by the algae. In open-end mode, a regulated stream of gas exits the distal end of the fiber, which purges the MC unit and preclude a buildup of inert gasses, which we showed can slow the transfer rate.

Figure 15b shows that a check valve was added after we determined that the MC fibers could fill with water when not delivering CO_2 at night.

Figure 16 shows the MC module placed inside the 75-L PBRs. A module consisting of short fiber bundles using quick connect fittings to allow for simple replacement should a fiber bundle become faulty. Additionally, the short bundles are placed perpendicular to culture flow to maximize CO_2 transfer into the media. **Figure 16** shows the current design for the 75-L PBR; it consists of 10 fiber bundles each containing 64 fibers at an average length of 3.7 cm. This provides a total length of 23.6 m with a total surface area of 0.021 m^2, making the specific surface area 0.28 m^{-1}.

Key Outcome: We developed a workable design for the cylindrical PBRs, adapted it to open-end or closed-end operation, and overcome the problem of water infiltration at night. Effort was shifted to the raceways by recommendation of DOE.

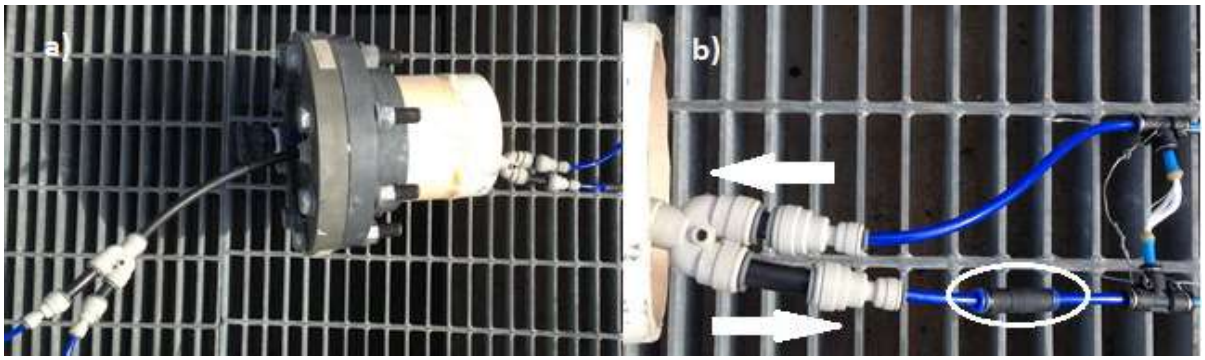

Figure 15: a) The modified PBR head utilizes a ¼" line within a ½" line to allow for gas to flow in and out of the MC unit, while minimizing the potential for leaks and damage to the structural stability of the head. The Y's are utilized to insert the ¼" line into the ½" line, while maintaining a gas tight system. b) Close up of the interior side of the PBR head that interfaces with the MC unit. The arrows indicate the direction of gas flow into (right arrow) and out (left arrow) of the MC unit. The gas flowing into the reactor uses the ¼" line and flow into a check valve to reduce the transfer of water into the MC unit when not in use.

Task 7 – Replicate MSS gas mixture into MC membranes in the 75-L PBR

The gas delivered through the MC fibers was humidified by flowing through water, and a CO_2-concentration of 90% was evaluated during outdoor cultivation in the 75-L PBRs. The focus was on membrane performance for outdoor conditions and utilizing *Scenedesmus acutus* AP-LRB 0401 as a model organism.

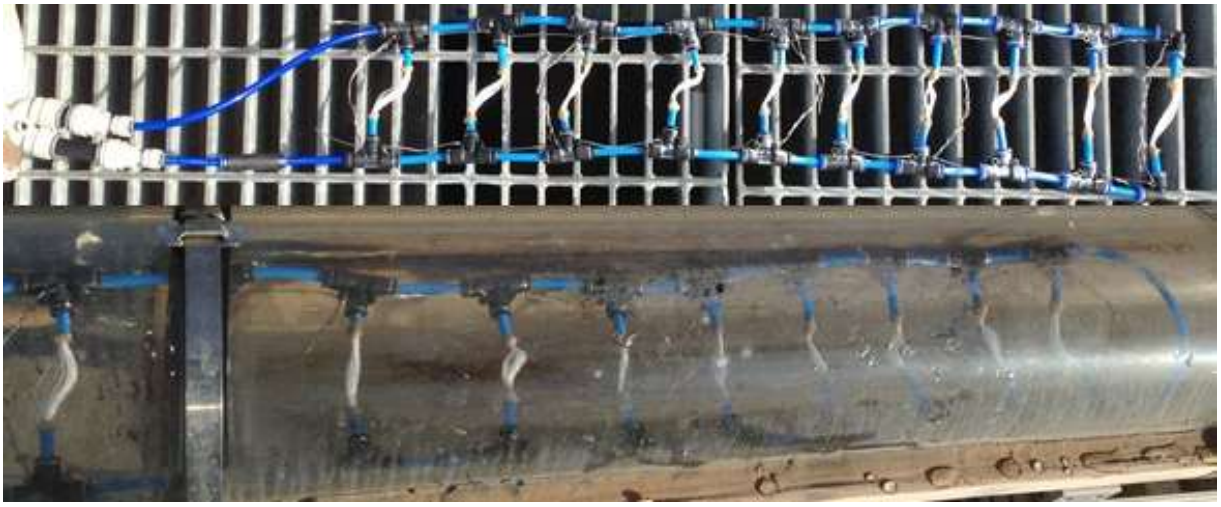

Figure 16: Image of the MC unit design and its placement inside the PBR.

Figure 17 shows productivity values for a 5-day experiment. The peak productivity reached about 5 g DW/m^2-day, although some values were negative. We discovered that mixing in the cylindrical PBRs was insufficient to keep the biomass in suspension. Thus, the low and negative productivities were the result of biomass settling inside the PBR, not poor photosynthesis. Settling in the cylindrical PBRs was an artifact of the fact that the 75-L PBRs were design originally for the cultivation of cyanobacteria, not algae; cyanobacteria are much more easily kept in suspension.

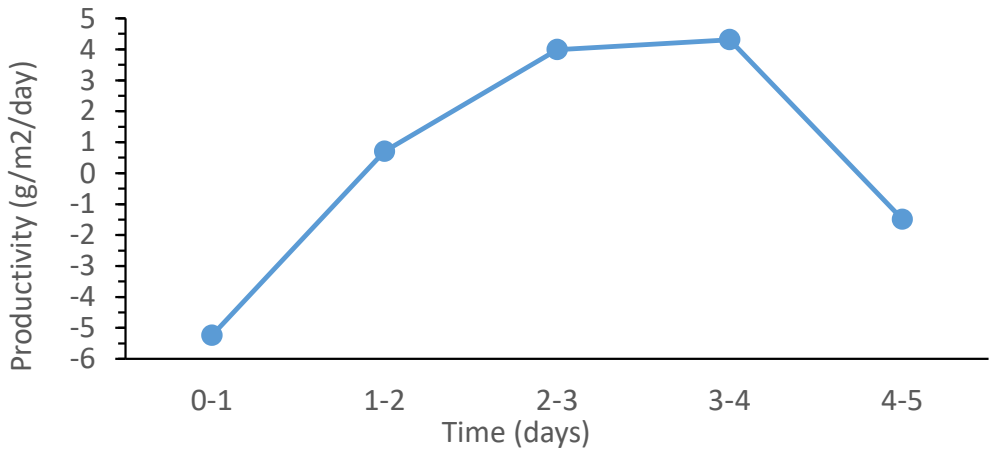

Figure 17: Biomass productivity of LRB-0401 during initial design testing. he MC unit design and its placement inside the PBR.

Figure 18 shows productivity and pH for a follow-up 7-day experiment. The pH was maintained near the set point for the most part during daylight periods, but during the later part of the experiment, CO_2 demand from the culture, including settled biomass, caused the pH of the culture to increase above the set point. This indicates that the surface area of the membranes needed to be increased to ensure sufficient CO_2 delivery. Biomass productivities were as high as 9 gDW/m^2-day, but also showed some low values related to setting. As the Team decided to focus on the 1,500-L open raceways, we did not invest more effort towards overcoming the mixing deficiency in the 75-L PBRs.

Key Outcome: Short-term productivity and pH control were satisfactory, but poor mixing prevented us from evaluating long-term productivity.

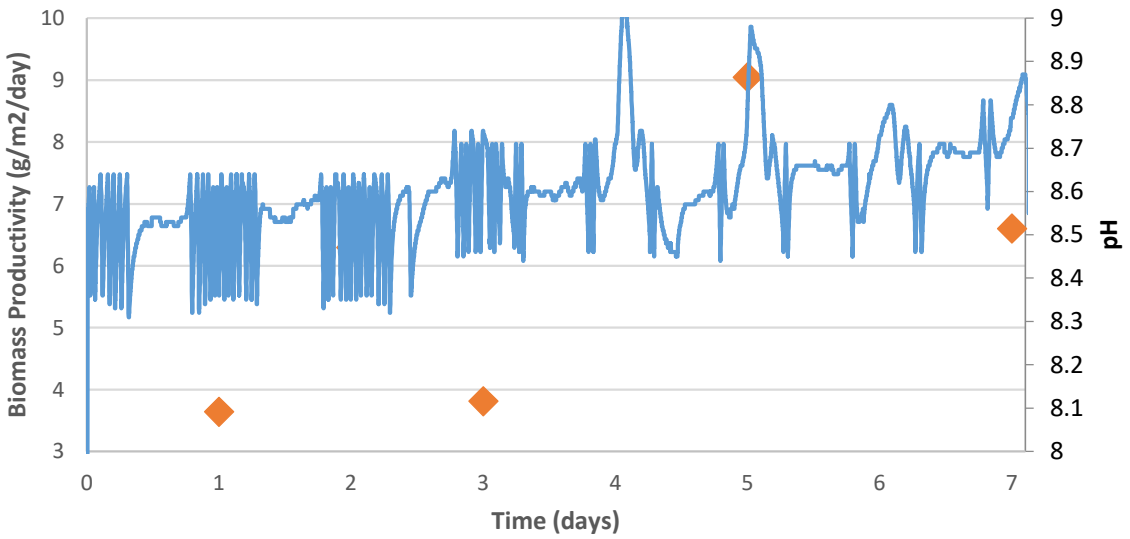

Figure 18: Biomass productivity (orange) and pH (blue) of LRB-0401 during initial design testing. The pH set point was 8.6 for days 1 and 2 and 8.7 for the remainder. Note that the large changes in productivity were due to significant settling, which prevented accurate quantification.

Task 8 – Scaling up MC to outdoor 1500-L raceway ponds

For scaling up to the 1500-L raceways, one of the major changes in membrane design was a shift from individual fiber bundles to sheets, which are easier to scale for modules useful at commercial scale. **Figure 19** shows the membrane design and placement in the AzCATI raceways; a close up is shown in **Figure 20**. The membranes were designed with an approximate surface area of 0.56 m^2 consisting of 1600 fibers, 0.4 m in length. The membranes had a metal frame for stability and to ensure membranes remained submerged.

To evaluate the membranes' CO_2 flux, abiotic testing similar to indoor abiotic tests were performed in one raceway. We filled the raceways with 900-L of tap water and added 50 g of Na_2CO_3 to increase the alkalinity to ~200 mg/L, which avoided any complications from precipitation. Results from the sheet-based fibers, shown in **Figure 19**, indicated that a flux up to 3000 g-CO_2/m^2-fiber/day was achievable with a pressure of 7 psig. This flux is similar to or greater than what we achieved in the laboratory for closed-end fibers operating with 100% CO_2 (**Figure 9**).

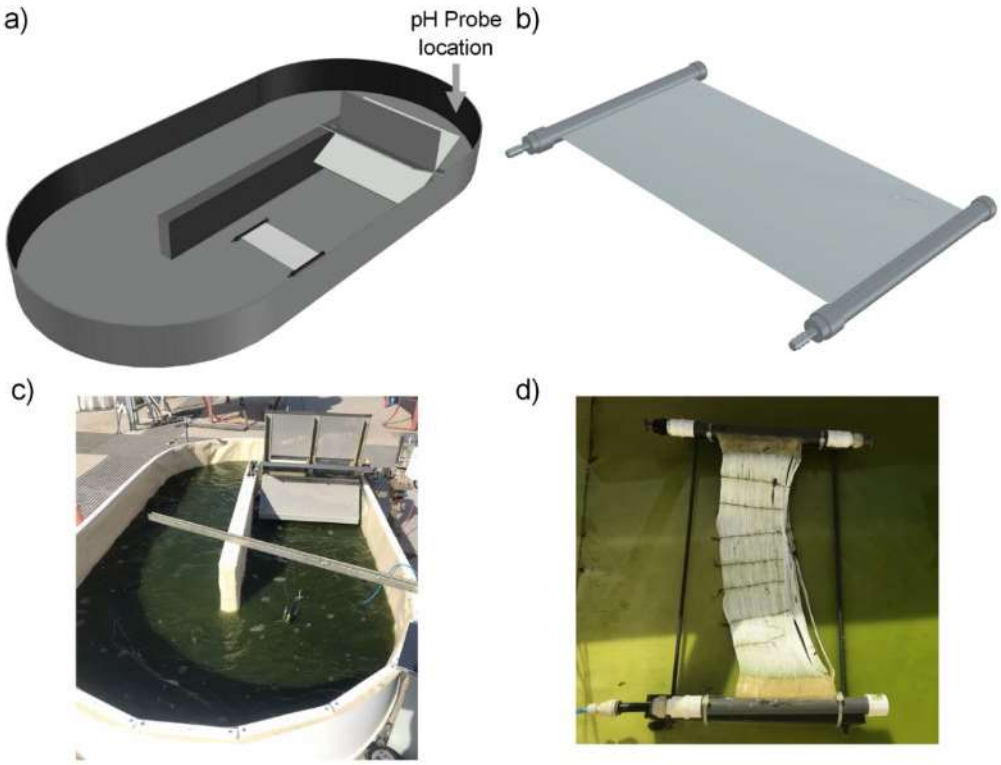

Figure 19: a) and **b)** show the conceptual placement and design of the MC unit in the raceway, while **c)** and **d)** provide images of actual placement.

Figure 20: Development of an MC module for the 1500-L raceways at AzCATI.

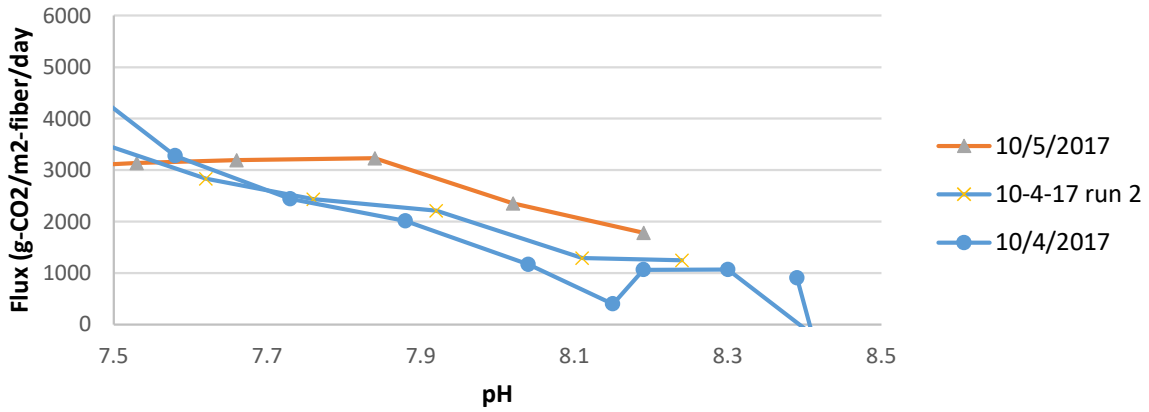

Figure 21: CO_2 flux through fibers during abiotic testing of the membrane carbonator.

Task 9 – Design and construction of integrated ACED system into PBR and continuous operation.

Because of challenges with algae settling in the 75-L tubular PBRS and longer than expected development times for the MSS system, the team shifted its focus for integration on the 1500-L raceway ponds; this was agreed to by DOE at our Go/No go site visit, since the 1500-L raceways are more relevant and scalable. The full-scale air-capture and storage system was constructed and tested in a high bay laboratory.

Key Outcome: A problem of water getting into the MC fibers when not CO_2 not being delivered (e.g., at night) was uncovered; it was solved during subsequent operation in the raceway ponds.

Task 10 – Design, construction, and operation of an integrated ACED system into an open raceway pond.

Air capture and storage subsystem

A number of challenges were uncovered during construction and initial operation of the direct air capture and storage system that, in general, can be expected for a system having its complexity and that is constructed in a short timeframe. Ultimately, several long runs enabled data to be collected to evaluate the performance of the resin and storage process.

Membrane carbonation subsystem

Because the amount of CO_2 produced and the duration of production of the direct air capture and storage system as constructed were insufficient to support the high growth required of the algae, the MC system was evaluated in 1500-L ponds using the 100% CO_2 supply available at the AzCATI facility and compared to cultivation by delivering CO_2 by sparging. **Figure 19** provides pictures of the outdoor

raceways with the MC system installed. **Table 2** provides information related to notable events during the experiments, including percent harvested, culture crashes, and other special circumstances.

Table 2: Description of key events that occurred during experimentation and correlate to specific points in **Figure 22**.

Experiment	Key Event	Date	Elapsed Time (days)	Event Note
3	17	4/22/18	4	Harvested 75% of the culture. Supplied ¼ BG-11 for the total volume. Cultures were supplied with ammonium bicarbonate instead of sodium nitrate.
	18	4/23/18	5	Low biomass concentrations, ammonia toxicity, and high light intensity caused a decrease in AFDW. MC2 did not recover.
	19	4/27/18	9	Harvested 75% of the culture. MC1 biomass was used to restart MC2 raceway.
	20	5/2/18	14	MC-2 culture crashed due to contamination.
	21	5/4/18	16	Experiment ended due to contamination.

A semi-continuous harvesting experiment was conducted from April 18 to May 4, 2018 using ammonium bicarbonate as the nitrogen source. **Figures 22** shows AFDW, areal productivity, pH, CO_2 delivery, and % CUE for cultures. Growth on ammonium bicarbonate creates a net zero change in alkalinity, which, compared to growth on sodium nitrate increase the CUE, as DIC in the medium was not increasing. However, growth on ammonium presents additional limitations associated with high pH values. The pKa for ammonium and ammonia is ~9.35, and ammonia (the non-ionized (free) form) is toxic and volatile [2, 8, 9]. The experiment was conducted with a pH setpoint of 8.5 to maintain a slight carbon limitation in the culture. However, pH 8.5 allows some free ammonia, which led to the loss of the culture in MC2 and a decrease in biomass concentration in MC1 and the sparged raceways (Key Events 17 and 18 in **Figure 22**). However, the biomass recovered, and the overall biomass productivity for the experiment was 6.7 ± 6.0 $g \cdot m^{-2} \cdot d^{-1}$. In addition to the satisfactory productivity, a main outcome of these experiments was the CUE, which was 106 ± 45% for MC1. The ability of the MC1 culture to achieve greater than 100% CUE was due to two factors. One was using ammonium bicaronate at the N source to prevent a steady increase in DIC. Two was that the pH setpoint was high enough that the culture pulled CO_2 from the atmosphere in addition to the MC-supplied carbon.

Key Outcome: Membrane carbonation demonstrated ≥ 100% CUE and consistent performance throughout the outdoor experiment in 1500-L raceway ponds.

Task 12 – Performance evaluation, modeling, and final display.

Outdoor performance data was evaluated to understand the impact of outdoor operation compared to earlier indoor experiments.

CO_2 delivery subsystem

Table 3 provides a summary of key results from 4 different biological experiments conducted at AzCATI and includes details on productivity, environmental conditions, nitrogen source, fiber performance, and carbon utilization efficiency for sparging and MC. The major shift in flux shown in the table occurred during Experiment 2, as the MC units were replaced with newly built modules. With the second round of prototypes, the methodology and manufacturing steps decreased the number of fibers that plugged during the gluing stage. This increased the overall flux of CO_2 per installed surface area.

One of the largest challenges in utilizing a closed-end fiber unit is the accumulation of inert gases and humidity. Running pure CO_2 still has a small accumulation of N_2 and O_2. Additionally, the polyurethane tubing from the system connection point may have exchanged gasses with the atmosphere [12]. This did not have a large impact during the day, but lack of photosynthetic activity during the night or extended cloud coverage decreased the flow of CO_2 being delivered to the fibers and accentuated the challenge of inert gases. This topic will be addressed in our upcoming DOE project DE-EE0008517.

Another factor that can lead to decreased MC performance is the accumulation of water vapor in the fibers. This can become a significant problem as the culture and gas temperatures fluctuate diurnally. When the temperature in the culture decreases at night, the humidity inside of the fibers increases above 100%, causing condensation in the internal macropores, which adds mass-transport resistance to the flux of CO_2. We evaluated this effect by testing the flux of the fibers prior to starting experiment 1, with dry fibers, versus at the end of experiment 1, with fibers that had been immersed for 48 days. The initial fluxes were 1570 and 1410 g-CO_2·m^{-2} fiber SA·d^{-1} for MC1 and MC2, respectively, while the fluxes at the end of experiment 1 were 860 and 760 g-CO_2·m^{-2} fiber SA·d^{-1}, respectively. This was a 46% decrease in fiber performance due to long-term accumulation of water vapor with closed-end operation. The buildup of water vapor can be mitigated by occasional venting.

Table 3: Summary of key results from multiple experiments at AzCATI. Average values ± S.D. Initial and final flux are averages of the first and final 3 days, respectively.

	Experiment 1	Experiment 2a	Experiment 3	Experiment 4
Dates	01/23 to 3/11/18	3/16 to 4/11/18	4/18 to 5/4/18	5/18 to 6/5/18
pH Setpoint	8.5	8.5	8.5	8.0
Average temp (°C)	13.5 ± 3.1	17.6 ± 4.3	20.3 ± 4.8	23.1 ± 5.1
Average Light ($kWh \cdot m^{-2} \cdot d^{-1}$)	4.4 ± 1.1	6.2 ± 0.7	7.2 ± 0.8	8.3 ± 0.3
Nitrogen source	Nitrate	Nitrate	Ammonium bicarbonate	Ammonium bicarbonate
Biomass Productivity (g·m-2·d-1)	2.96 ± 1.92	10.19 ± 3.64	6.68 ± 6.01	11.76 ± 6.88
MC Pressure (psIg)	16	10-16	16	16
Initial fiber flux ($g\text{-}CO_2\ m^{-2} \cdot d^{-1}$)[b]	860 ± 60	920 ± 430	2600 ± 1100	1760 ± 380
Final fiber flux ($g\text{-}CO_2 \cdot m^{-2} \cdot d^{-1}$) [b]	630 ± 100	2890 ± 720	2430 ± 110	2600 ± 470
Average fiber flux ($g\text{-}CO_2 \cdot m^{-2} \cdot d^{-1}$) [b]	775 ± 120	1360 ± 860	2220 ± 750	2290 ± 610
CUE MC1	78 ± 55%	67 ± 35%	106 ± 45%	51 ± 27%
CUE Sparging	-	25 ± 18%	36 ± 19%	17 ± 10%
CUE Ratio MC/Sparging		2.65	2.94	3.0

a Experiment 2 had the original MC module replaced after having several fibers cut by a raccoon.

b The area referenced in the membane flux is the total surface area of the fibers.

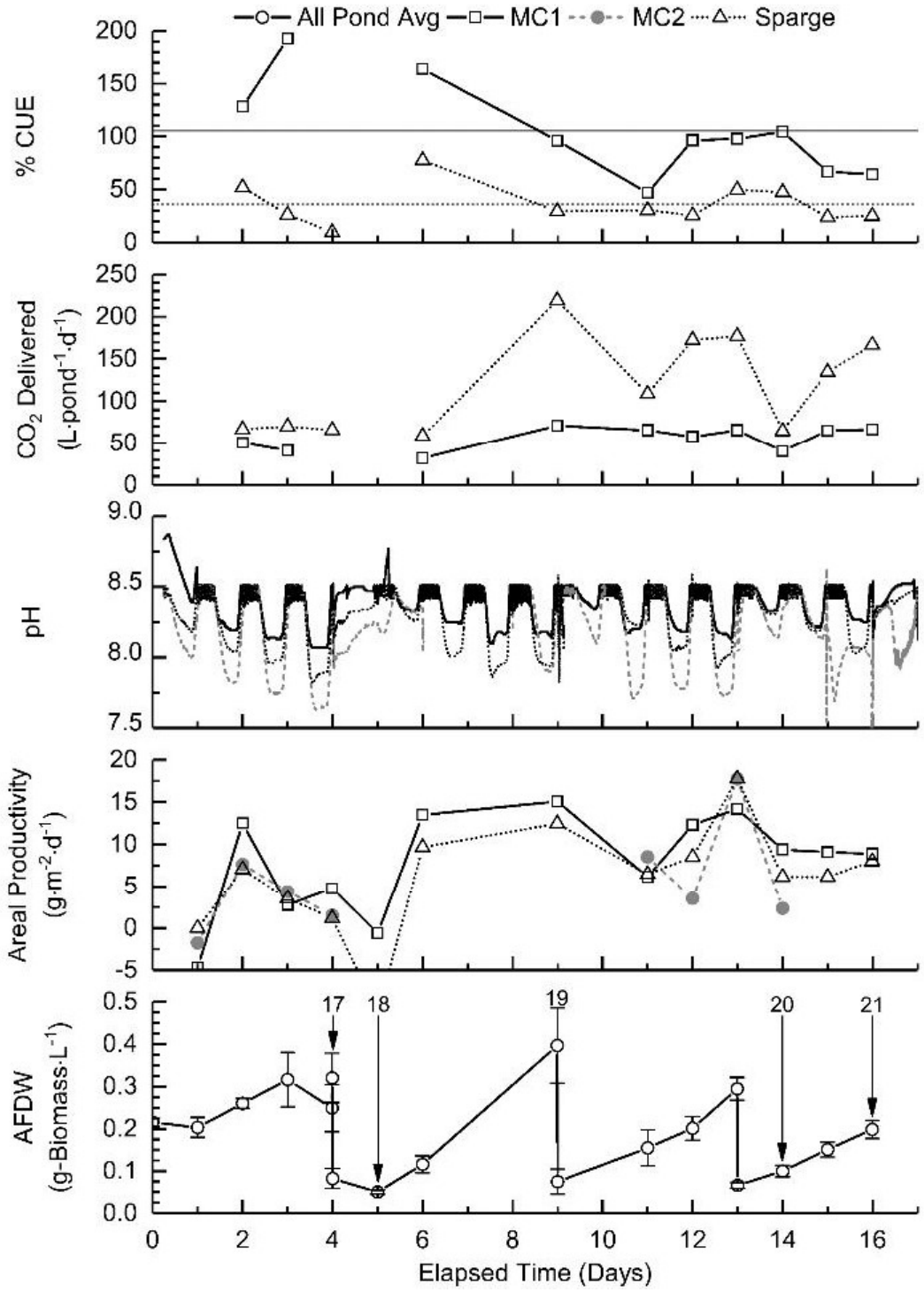

Figure 22: CUE, CO_2 delivery, pH, Areal productivity, and AFDW for cultures from Experiment 3, April 18 to May 4, 2018. The AFDW is the average with standard deviation for the three cultures, as the biological conditions were the same. MC1 and sparging were monitored for CO_2 delivery to calculate CUE. The horizontal line in the % CUE graph represents the average CUE for the experiment.

Key Outcomes: Membrane carbonation provided 2.5–3-fold higher CUE than a sparging control, and its CUE was > 100% when using ammonium bicarbonate as the N source. Buildup of water vapor could lower the CO_2 flux, and this effect can be mitigated by periodic venting.

CO_2 capture and storage subsystems

The performance of a direct air capture system was evaluated outdoors for about 9 months at the ASU Polytechnic Campus, where it was subjected to a wide range of environmental conditions. Due to software instability and hardware failures, system runs were generally 2 days or less until June 2018. Data for a 7-day run in June was analyzed in detail, and it represented a time of favorable hot and dry ambient conditions (**Figure 23**).

CO_2 captured into storage was positively correlated to temperature and wind speed and negatively correlated to relative humidity, as expected. The system produced an average of 20 g CO_2 per day while consuming 23.5 liters/day of water, resulting in an average ratio of 2,700 moles of H_2O per mole of CO_2 captured. This far exceeded the theoretical thermodynamic limit of 2:1 and the practical water-loss goal of 25 : 1 mol/mol. The process as currently implemented introduced a significant excess of water that was shed to the atmosphere. In addition, many of the cycles only collected a small fraction of the CO_2 available, but would still have to air dry the collectors once they had been made wet. Excess water also increased the resin drying time and therefore affected overall performance. As noted, our target was to release about 25 water molecules per CO_2 molecule. Thermodynamic data on the resin show that the water participating in the moisture swing was between 2 and 10 moles per mole of CO_2. Any additional water may have been added to the resin, but it was not directly contributing to the moisture swing. Thus, eliminating efficiencies should bring water use to the goal.

We evaluated the reasons for the inefficiencies. Analyzing the concentration of CO_2 released from the resin over time showed that many regeneration runs terminated prematurely because of a sensitivity of the algorithm to noise in the Infrared Gas Analyzer (IRGA) measurement. Regeneration runs stopped after 10 to 15 minutes, rather than going for long exposure times; this means that much more CO_2 was captured than was successfully delivered into storage. While such shutoffs curtail CO_2 collection, they do not reduce water evaporation during the collection cycle. One of the lessons learned is to add more diagnostic tools to the device. This will help analyze the performance and suggest improvements, but it also would make it possible to advance the algorithmic control of the system operation, by making more informed decisions. As a specific example consider an additional bypass of the carbonator system. Such a bypass would make it possible in conjunction with the already installed gas analyzer to determine the CO_2 equilibrium pressure in the MSS tank, and in each of the separate carbonate storage tanks. This knowledge in turn could make it possible to optimize the carbonator performance much more effectively then in this first version.

The blower speed circulating CO_2 from the resin to the carbonator was varied during delivery and found that most CO_2 was captured during the initial higher speed phase. The transfer rate into storage was highest (~90 mg/min or ~65 g/day, the latter number assumes 50% of the time in regeneration) into the highest storage tank for the most productive runs, which delivered CO_2 for nearly 4 hours, while delivery to the medium and low storage tanks were much shorter (13–27 min) and delivered very little CO_2.

Even though the blowers require energy, the total power consumption of the capture and carbonator system was quite small. The big energy consumer in the system is the distillation column. In order to achieve CO_2 concentrations higher than originally intended, the amount of water boiled was quite large. Further work is needed to quantify the energy consumption of all steps in detail, but overall, the big energy consumption is in the distillation column. Mechanical movement of parts took very little energy, blower speeds were small, but could like be reduced significantly further.

The resin performance was degraded by chloride from tap water accumulating in the resin (**Table 4**). The performance could be completely restored with two successive washes in 1 M Na_2CO_3. Adding Na_2CO_3 to the supply water reservoir also increased resin performance in the field by minimizing chloride accumulation. The CO_2 delivered from storage by thermal release was as much as 40 – 50 g per day. The concentrations ranged from 60–80%. One unintended consequence of adding sodium carbonate to the water has been a significant amount of scaling in the water reservoir. However, the system showed surprising resilience to scaling.

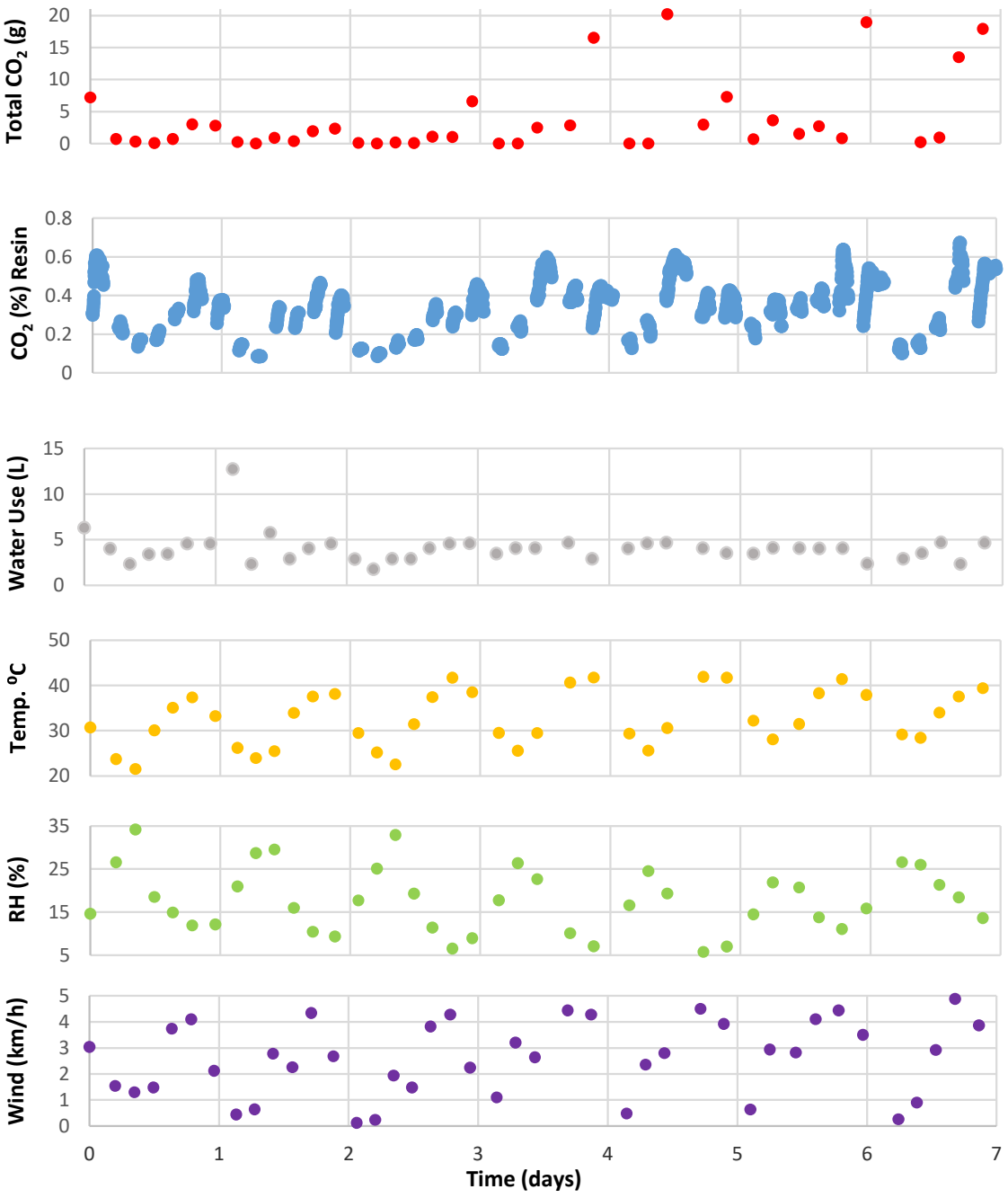

Figure 23. Total CO_2 captured into storage (red) and concentration of CO2 (%) released from the resin (blue) and water consumed (grey) per cycle over the 7 day period analyzed along with the corresponding average environmental condition for each cycle, including temperature (yellow), relative humidity (green) and wind speed (purple).

This demonstration showed that the novel process is feasible, but it also showed that much work remains to be done to improve the process to the point that it achieves the results seen the individual units at bench scale test. In addition, the performance at bench scales needs to be improved.

Due to time and resource limitations, this first implementation ran afoul on a number of integration issues. Early on, software issues plagued the performance of the system. Frequent failures in the software would stop collection runs prematurely, and result in outages. In its original form, the software had memory leaks, which slowed the computer and in some cases led to the crash of the operating system. After short run time, internal resource limitations would cause delays, which in turn forced safety shutdowns. Carbonator operation was most severely affected. As a result of myriad integration issues and resulting delays, the systems total operational time became much longer than originally anticipated. In the end this resulted in failures of subsytems, like heaters which were intended for a 30 day use, and had to operate for roughly a ten times longer period. In addition, the focus on system integration issues, prevented us from gaining true run time experience.

The system succeeded in exposing CO_2 filter units to the air, moving them back and forth into the regeneration unit, where the filters would be inundated in water and once wet were allowed to release the CO_2 they collected. The CO_2 in the regeneration chamber would reach between 0.5 and 2% CO_2 concentrations, and the CO_2 was then brought in contact with a series of carbonate brines, which acted as storage for the system. The carbonate was then moved into a distillation column to produce a mixture of CO_2 and water vapor for downstream use.

As a whole the system demonstrated that it can perform the task, but more work is required to reach performance levels commensurate with what has been achieved on the lab scale. When CO_2 from the MSS was available it was fed directly to the raceway pond.

One of the positive outcome of the long operational period has been the observation that the sorbent material is remarkably resilient. Even at the end a nine months exposure to the elements the washed resin material performed essentially as well as new material. This is in spite of the fact that the system was not protected from the intense Arizona sun. Indeed, UV damage to the plastic pipes for the water plumbing system and other plastic parts of the system is quite visible. Yet, the sorbent material performed well.

Table 4. Field resin performance as a function of days in the field, chloride concentration in the tap water and tote water refill tank before and after a 1M Na_2CO_3 wash. New resin has a 175 ppm swing.

Date	**Days in Field (approx.)**	**Performance (ppm) / % of new**	**After 1 M Na2CO3 wash / % of new**	**Tapwater [Cl^-]**	**Tote Water [Cl^-]**	**Na2CO3 in Tote Water?**
Feb 2018	60	20 ppm / 11%	100 ppm / 57% (1x wash)	144 ppm	240 ppm	No
Mar 6, 2018	90				345 ppm	Yes
April 24, 2018	150	55 ppm / 31%	90 ppm / 51% (1x wash)	259 ppm	369 ppm	Yes
Aug 2-4, 2018	240	60 ppm / 34%	170 ppm / 97% (3x wash)	173 ppm	637 ppm	Yes
Aug 3, 2018	0 (new)	175 ppm / 100%				

The collector performed mechanically in the way it was supposed to. The computer controlled system was able to raise the filter units on its scissor lift to the full exposed level and drop them down into the regeneration box based on exposure time. The system continued to operate over nine months of frequent raising and lowering. The computer control successfully integrated weather alerts, and local wind data to assure that the sail-like structure would be secured inside the regeneration box, whenever wind conditions posed a risk.

The scissor-lift failed once, when the sensor indicating the end of the lowering failed to engage and the motor kept pulling the unit back up, spooling the cable up in the reverse direction. Apart from this one glitch, the system behaved as designed, and even after nine months of operation, it is still intact.

The collector unit demonstrated relatively low CO_2 concentrations in the regeneration step, which was expected as the volume of the chamber was not well matched to the volume of the filters. Due to the large volume, it takes quite an amount of CO_2 to fill the chamber. This emptying of the resin lowers the partial pressure of CO_2 that is achievable. Another potential for CO_2 losses are leaking of outside air into the chamber. This possibility has not yet been investigated.

Another reduction in performance arose from the high sodium chloride levels in the local tap water. This resulted in an ion exchange with the resin material in the filter which effectively turned the active carbonate/bicarbonate resin into an inactive chloride resin. The team was able to address this problem by adding sodium bicarbonate to the wash water. The concept is simple: The anion composition on the resin is very similar to that in the water. For tap water it is quite easy to overwhelm the chloride concentration with carbonate or bicarbonate. Either one works equally well, and the resins will transform the brine into a mild bicarbonate solution in any case. Once the resin was predominately in the carbonate/bicarbonate form, its ability to collect CO_2 was restored. Nevertheless, at the end of a nine-months run, the salt concentration in the water tote had become too high. We have recently developed a strategy to maintain the water in the system at a dilute-enough level.

The carbonators successfully collected CO_2. We can measure the difference in the CO_2 concentration between the gas entering the carbonator and the gas leaving the carbonator. From this, together with the gas flow velocity, we can calculate the amount of CO_2 that has been collected in the brine. For the successful runs this number reached about 90 mg/min, which was still much less than would be expected from a fully loaded resin that releases CO_2 into the regeneration chamber. Future experiments will have to determine whether this performance loss was due to a low performance of the regenerator chamber, the resin was still wet when it returns to the regenerator, or we have encountered a bottleneck at the carbonator itself.

Key Outcomes:

1. The team demonstrated that the MSS system can take CO_2 from the atmosphere and deliver compressed gas to a consumer. The system still significantly under-performs its design goals. Some of the reasons for the underperformance have been identified and likely can be fixed. Others, still need to be explored.
2. Total CO_2 captured into storage was positively correlated with temperature and wind speed and negatively correlated with relative humidity, as expected.
3. The resin proved to be resilient to long-term outside operation. No attempt was made to protect the resin from the elements. Apart from picking up salts, which can be washed out, the resin maintained its original performance characteristic through nine months of operating exposure.
4. Water consumption was much higher than the design goal. Immersion in water tended to over-wet the resin. We showed in the laboratory that this aspect can be improved by increasing the hydrophobicity of the resin material. It is also expected that more efficient CO_2 collection will also improve the H_2O : CO_2 ratio.
5. Most CO_2 delivery cycles stopped prematurely, which means that only a fraction of the total CO_2 captured was delivered into storage.
6. Even the best cycles still underperformed the expectations from the bench-scale.
7. Energy consumption was dominated by the thermal release column. For CO_2 concentrations in excess of 90% other concepts for regeneration need to be explored.
8. Tap water contamination caused problems for resin immersion, but the team demonstrated a way of overcoming these problems.

Task 6 – Preliminary Techno-Economic Analyses (TEA).

A preliminary TEA was performed to evaluate trade-offs during system design. The process model (**Figure 24**) and capital expense breakdown and total subsystem costs (**Figure 25**) were developed first. A baseline scenario assumed costs for implementation of the prototype system replicated in large quantities with no improvement from lab results. This yielded a cost estimate of $910 per metric tonne of bioavailable CO_2 (i.e., in liquid culture media). A tornado chart was developed to investigate which

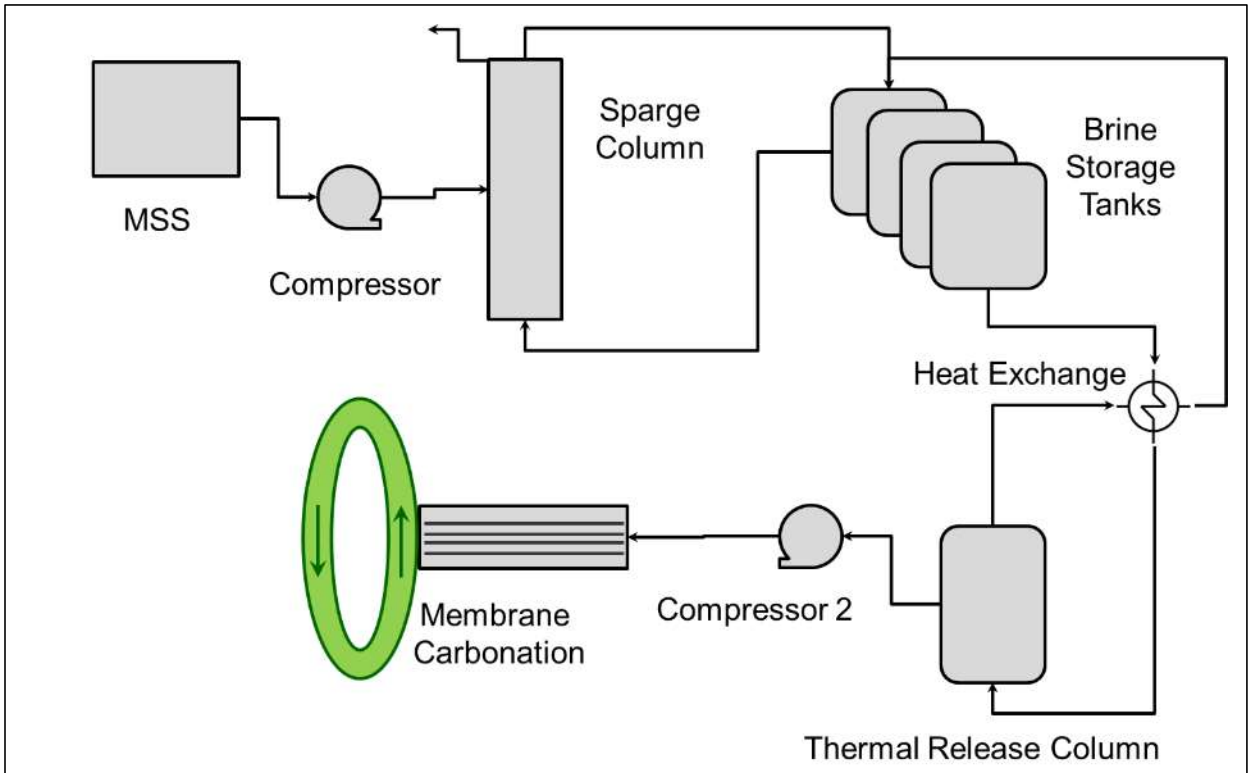

Figure 24. Process flow diagram of the ACED system highlighting the various subsystems modeled.

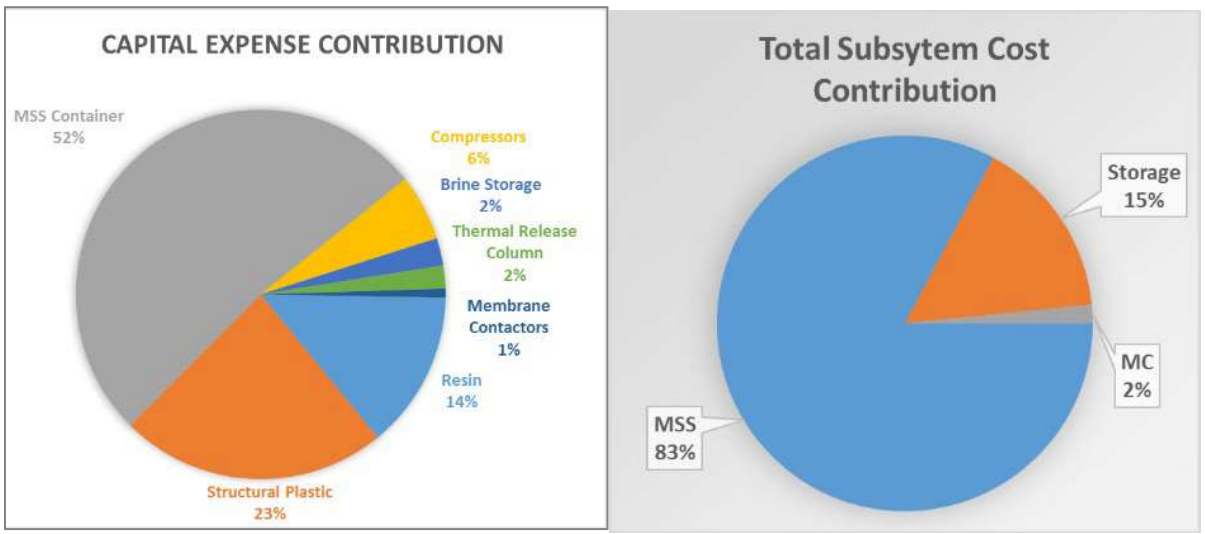

Figure 25. Breakdown of capital expenses (left) and total subsystem cost in ACED system.

parameters could have the greatest impact on reducing cost (**Figure 26**). The tornado chart helped the team to focus its efforts on the most important cost factors, which are identified in the outcomes below.

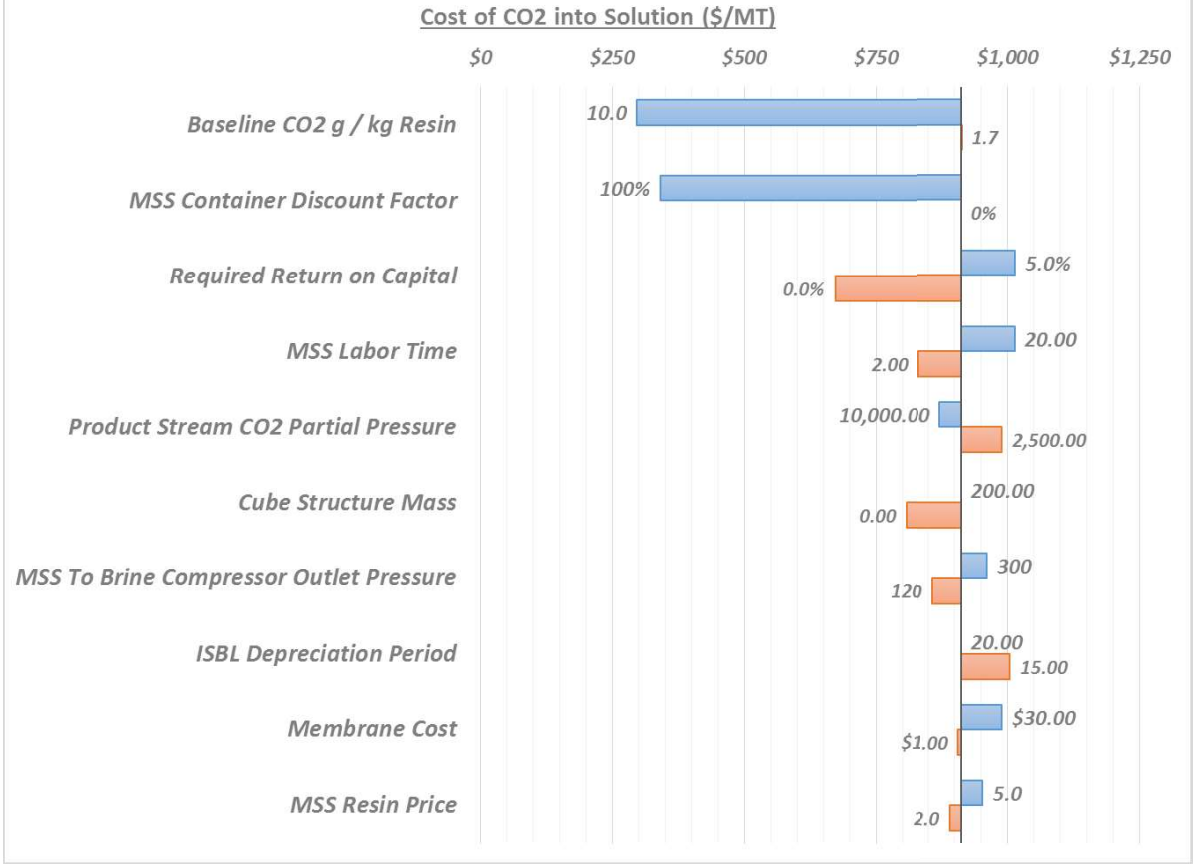

Figure 26. Tornado chart of important technoeconomic parameters in the ACED system.

Key Outcomes:

1. Resin productivity was the most important factor in determining the overall CO_2 cost.
2. It is critical to have a large fraction of the MSS resin product (the "cube") be composed of resin materials costs rather than machining and overhead costs.
3. The MSS container needs to deploy the maximum mass of working resin at minimal cost.
4. Compressing and sparging low concentration CO_2 is costly and needs to be optimized.
5. The cost of MC is minor, which means that the CO_2-delivery benefits of MC are obtained at low marginal cost.
6. Fouling of the membrane carbonator is a risk, as its cost is determined largely by a loss of CO_2 flux.

Task 11 – Final Techno-Economic Analyses.

Because of challenges operating the CO_2 capture and storage subsystem, the CO_2 delivery system was not run with CO_2 captured from the air. Insufficient integrated data was available for updating the TEA model so the final TEA considered the CO_2 delivery subsystem separate from the CO_2 capture and storage subsystems.

CO_2 Capture and Storage

For the CO_2 capture and storage subsystem, the model was updated to reflect a design change from compressing and sparging CO_2 into the storage brine to the constructed prototype that uses a lower pressure fan to blow the collected CO_2 across an oscillating fabric carbonator that is wetted with the brine solution which did not change the overall economics at $930/tonne CO_2. The capital expense contributions are shown in **Figure 27**.

Key Outcomes: The fabric carbonator used to deliver captured CO_2 into storage had lower performance than sparging that it offset its lower operating costs. Potential is great to improve the performance of this nascent technology in the future to achieve lower cost than sparging.

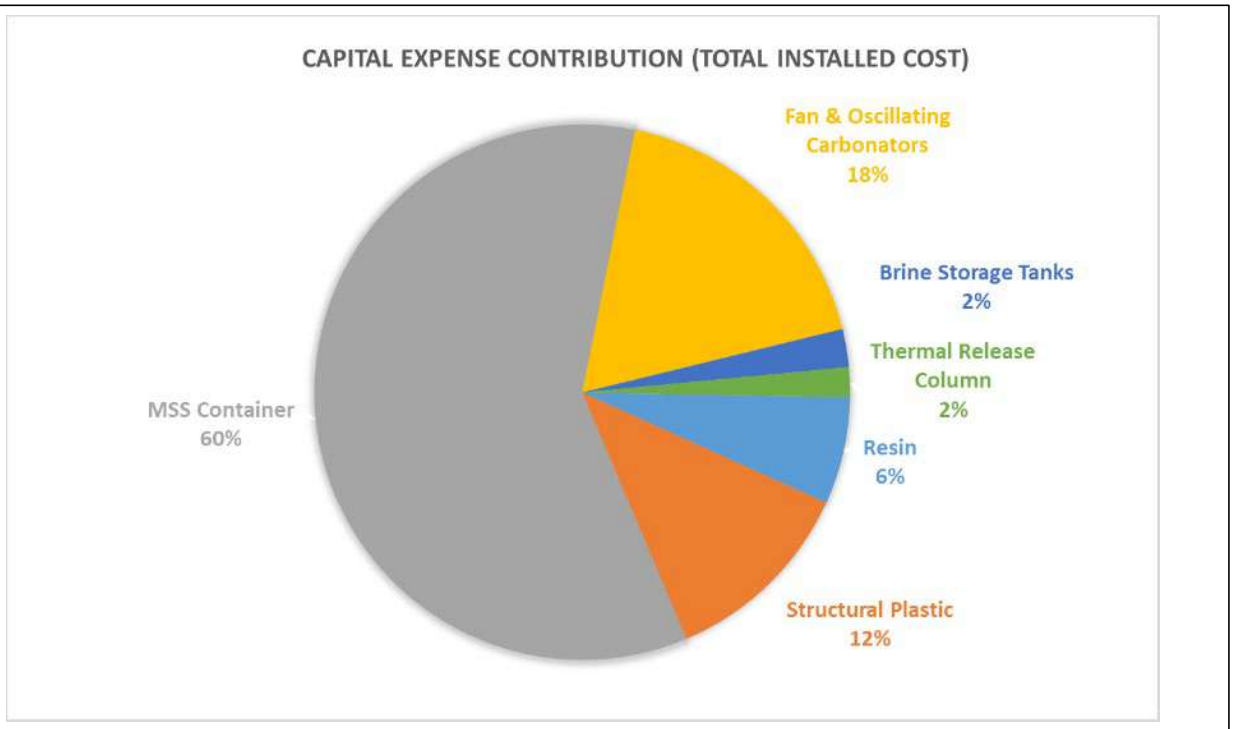

Figure 27. Breakdown of capital expense for MSS technology.

CO_2 Delivery

For the CO_2 delivery system (MC), its performance is compared with a competing technology that sparges CO_2 into a 2-m-deep sump at a transfer efficiency about 77%. As shown in **Figure 28**, the cost of operating MC always is less than with the 77%-efficient sump sparger. A delivery fluxes greater than 1800 gCO_2/m^2-d has an installed cost of only about $3/MT CO_2 delivered. This compares to 78%-efficient sump sparging at $15/MT CO_2. The costs are roughly equal only when the CO_2 delivery flux is smaller than about 300 gCO_2/m^2-d, which is very low for MC.

Key Outcomes:

1. MC is projected to add <$3/ton cost when CO_2 is $50/tonne.
2. MC is lower cost than sump sparging under all expected scenarios.

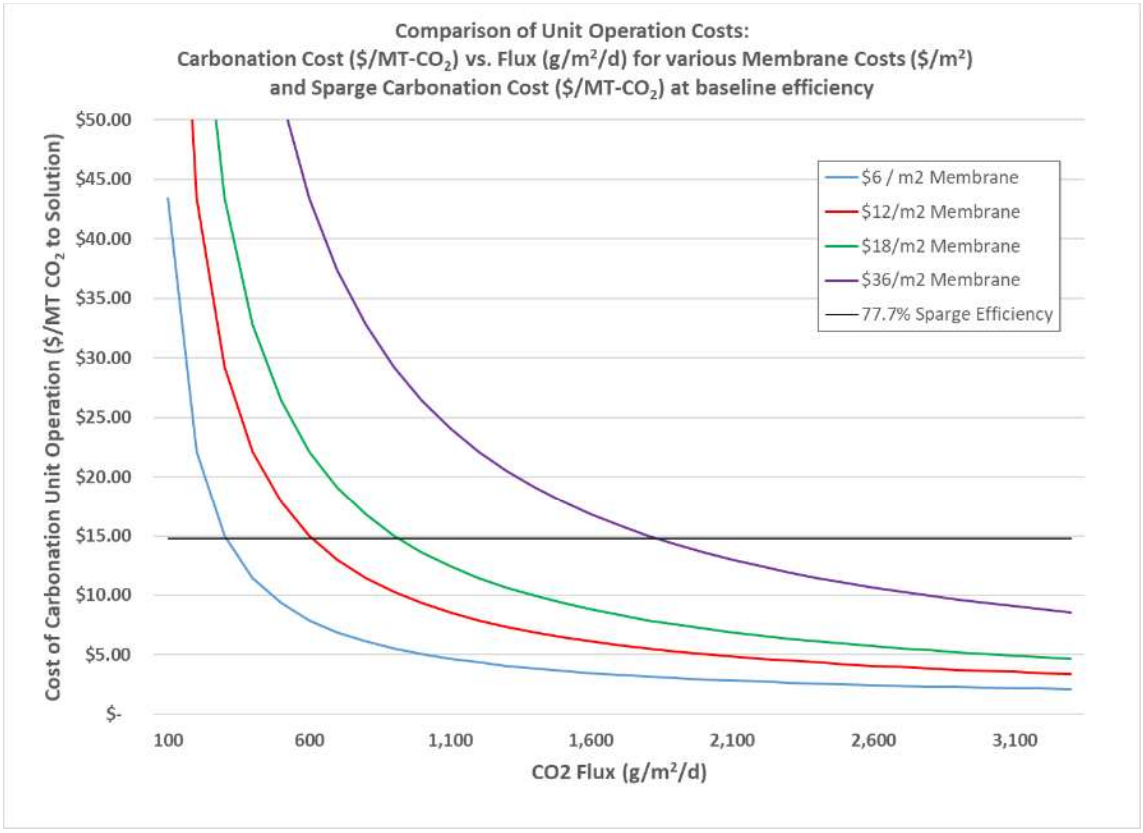

Figure 28. CO_2 flux of membrane and sump sparger vs. Total Cost to Deliver CO_2 for several membrane costs. $\$6/m^2$ is a reasonable target for "n-th plant" production of similar membranes.

Comparison of Accomplishments and Project Goals and Objectives

Each of the tasks described previously were completed successfully with the following exceptions:

1. **No integration testing in 75-L photobioreactor**. Testing in the 75-L photobioreactors was cut short following a recommendation from DOE to focus on cultivation in the 1500-L raceways after microalgae settling was observed to arise from the larger size of algal species used (*Scendesmus actus*) compared to the cyanobacteria (*Synechocystis*) for which the 75-L PBRs were designed.
2. **No integration testing in 1500-L photobioreactor**. The CO_2 supplied by the capture and storage subsystems was insufficient to support cultivating microalgae because of lower than expected performance and system downtime due to operational challenges. Microalgae was cultivated using pure CO_2 delivered by MC technology and compared to traditional spargers.

Products Developed

Technologies

Prototype systems were developed for:

1. MSS technology for capturing CO_2 from ambient air.
2. Technology for storing and extracting CO_2 from carbonate/bicarbonate brines.
3. MC technology for delivering CO_2 to microalgae.

Invention/patent applications

1. **Microalgae-driven CO_2 removal from mixed gases using hollow-fiber membranes**. Disclosed on Dec. 12, 2018 to Skysong Innovations for patent preparation. Inventors: Everett Eustance, Bruce Rittmann, Yen-Jung Lai, Tarun Shesh, Justin Flory. iEdison #0488301-18-0068.
2. **Use of Hydrophobic Coatings on Direct Air Capture Sorbents Used for Carbon Dioxide Removal from Air**. Provisional patent filed on Oct 30, 2018. Inventors: Allen Wright, Klaus Lackner. iEdison #0488301-18-0069.

Publications

One manuscript on CO_2 modeling has been submitted for publication entitled "Characterization of CO_2 Flux Through Hollow-Fiber Membranes Using pH Modeling" by Tarun Shesh, Everett Eustance, Yen-Jung Sean Lai and Bruce E. Rittmann. Two additional manuscripts on outdoor cultivation and bleed valve operation, along with a manuscript on modeling gas dynamics inside the MC fibers, will be submitted very soon.

Computer Modeling

Model for CO_2 delivery in hollow fiber membranes:

Model Description

A model was developed to calculate CO_2 flux, mass-transfer coefficient (K_L), and volumetric mass-transfer coefficient (K_La) based on carbonate equilibrium, alkalinity of the solution, and changes in pH. The model provides an accurate and rapid method of evaluating operating strategies to deliver CO_2 into solution based on real-time measurement of pH changes as CO_2 is delivered to an abiotic carbonate solution. A key assumption for the development of this model was constant total alkalinity of the solution.

Performance Criteria

The concentration of gaseous CO_2 in the supply stream or the CO_2 partial pressure, the configuration of the membrane module including fiber length and number of fibers, hydrodynamic conditions in the reactor, and the mode of operation (open- versus closed-end) were found to be influential in altering CO_2 delivery rates.

Test results

To verify the accuracy of the model developed, samples were taken from a sodium carbonate solution at regular pH intervals to measure DIC using a TOC-V instrument. **Figure 9** shows that the model-predicted DIC concentrations matched the measured DIC values down to a pH of 7.5.

Theory behind model

A pH-based method of evaluating flux of CO_2 delivery takes advantage of the fact that DIC exists as several interconvertible chemical forms based on the pH of the solution: dissolved carbon dioxide ($CO_{2(aq)}$), carbonic acid (H_2CO_3), bicarbonate (HCO_3^-), and carbonate (CO_3^{2-}). CO_2 dissolves in water to form $CO_{2(aq)}$, which is converted to H_2CO_3. The sum of H_2CO_3 and $CO_{2(aq)}$ is termed $H_2CO_3^*$. When the water contains base (or alkalinity), $H_2CO_3^*$ dissociates to form HCO_3^- and then CO_3^{2-} if enough base is present. The law off mass action was applied to each reaction. Then, the ionization fractions for key species, $H_2CO_3^*$, HCO_3^- and CO_3^{2-} were calculated based on equilibrium reactions for each reaction. The increase in the total concentration of DIC (C_T) was then computed based on the constant total alkalinity, and the change in pH over time due to the acidification effect of CO_2 addition. The DIC concentration could then be converted into a flux based on the reactor volume, membrane module configuration (number of fibers, fiber length, fiber diameter), and time. The driving force for CO_2 transfer is provided by a high concentration gradient between the gas and the liquid phase. During the process of mass-transfer, the CO_2 gas molecule experiences resistance at every stage in series which is calculated as the overall resistance to the rate of CO_2 transfer. The rate at which CO_2 is transferred from the gas phase to the liquid phase is proportional to the driving force and the mass-transfer area. Thus, having computed the flux of CO_2 delivery and knowing the mass-transfer area, the mass-transfer coefficient (K_L), and subsequently the volumetric mass-transfer coefficient (K_La) was computed.

Mathematics used

Gaseous CO_2 undergoes three chemical reactions with four chemical species upon dissolution in water:

$$H_2O_{(l)} + CO_{2(aq)} \overset{K}{\leftrightarrow} H_2CO_{3(aq)} \overset{K_1}{\leftrightarrow} HCO^-_{3(aq)} + H^+_{(aq)} \overset{K_2}{\leftrightarrow} CO^{2-}_{3(aq)} + H^+_{(aq)}$$

Applying the law of mass action to each reaction yields:

$$K = \frac{[H_2CO_3]}{[CO_2]}$$

$$K_1 = \frac{[H^+]\ [HCO_3^-]}{[H_2CO_3^*]}$$

$$K_2 = \frac{[H^+]\ [CO_3^{2-}]}{[HCO_3^-]}$$

Since very little CO_2 reacts with water to form carbonic acid, the concentration of dissolved $CO_{2(aq)}$ is much greater than that of H_2CO_3 leading to the following equation based on a K value of 650:

$$[CO_{2(aq)}] = 650\ [H_2CO_3]$$

The above equation coupled with the definition of $H_2CO_3^*$, results in

$$(0.998) \times [H_2CO_3^*] = [CO_{2(aq)}]$$

The mass balance equation to compute DIC is

$$C_T = [H_2CO_3^*] + [HCO_3^-] + [CO_3^{2-}]$$

A proton-condition equation is

$$[H^+] = [OH^-] + [HCO_3^-] + 2\,[CO_3^{2-}]$$

The ionization fractions can be calculated as

$$\alpha_0 = \alpha_{H_2CO_3^*} = \frac{[H^+]^2}{[H^+]^2 + [H^+]\,K_1 + K_1\,K_2} = \frac{[H_2CO_3^*]}{C_T}$$

$$\alpha_1 = \alpha_{HCO_3^-} = \frac{[H^+]\,K_1}{[H^+]^2 + [H^+]\,K_1 + K_1K_2} = \frac{[HCO_3^-]}{C_T}$$

$$\alpha_2 = \alpha_{CO_3^{2-}} = \frac{[H^+]\,K_1\,K_2}{[H^+]^2 + [H^+]\,K_1 + K_1K_2} = \frac{[CO_3^{2-}]}{C_T}$$

The driving force for carbon dioxide transfer (ΔC) is based on the measured dissolved CO_2 concentration ($C_{CO2(aq)}$) and the CO_2 concentration in the liquid phase that would equilibrate the gas phase ($C^*_{CO2(aq)}$). The latter was computed using Henry's law having calculated the partial pressure of CO_2 (P_{CO2}) using the composition of carbon dioxide used in the inlet stream and the pressure of the gas supplied.

$$C^*_{CO_{2(aq)}} = H^{cp} \times P_{CO_2} = H^{cp} \times \%CO_2 \times P$$

Substituting the above equation into the law of mass action equations allows us to relate the aqueous-phase concentrations to P_{CO2}

$$[HCO_3^-] = \frac{K_1\,H^{cp}\,P_{CO_2}}{[H^+]}$$

$$[CO_3^{2-}] = \frac{K_1\,K_2\,H^{cp}\,P_{CO_2}}{[H^+]^2}$$

The analytical definition of alkalinity is

$$[Alk]_0 = [HCO_3^-] + 2\,[CO_3^{2-}] + [OH^-] - [H^+]$$

The concentration of protons in the solution was calculated based on the measured pH of the solution

$$[H^+] = 10^{-\mathrm{pH}}$$

The concentration of OH^- was computed from the mass-action equation for water dissociation

$$K_W = [H^+]\,[OH^-]$$

Then, C_T was calculated using

$$C_T = \frac{[Alk]_0 - \frac{K_W}{[H^+]} + [H^+]}{\alpha_1 + 2\alpha_2}$$

The concentration of DIC (C_T) was then expressed as the mass of DIC in the media based on the reactor volume and CO_2 molecular weight,

$$m_{CO_2} = MW_{CO_2} \times C_T \times V$$

Having m_{CO2} and time (t), the transfer rate of CO_2 in units of g-CO_2 m^{-2} of fibers per unit time was calculated using

$$J_{CO_2} = \frac{\left(m_{CO_2}\right)_{i+\Delta t} - \left(m_{CO_2}\right)_i}{SA \times \Delta t}$$

The surface area of the membrane module (SA) was computed using the number of fibers, fiber length, and fiber diameter,

$$SA = \pi n l D$$

The change in concentration of DIC over time was calculated using

$$N_{CO_2} = \frac{\left(m_{CO_2}\right)_{i+\Delta\,t} - \left(m_{CO_2}\right)_i}{V \times \Delta t}$$

K_La was calculated using

$$K_L a = \frac{N_{CO_2}}{C^*_{CO_{2(aq)}} - C_{CO_{2(aq)}}}$$

K_L was calculated using

$$K_L = \frac{J_{CO_2}}{\Delta C}$$

The effective gas-liquid interfacial area per unit volume (a) was computed using

$$a = \frac{K_L a}{K_L}$$

Peer review status

This model has been submitted for peer review, but has not yet been revised or published.

Operating environment

The model was developed and executed on a Dell Inspiron 15 7000 model laptop with an Intel Core i5-8250U processor and 8GB RAM running Windows 10 and Excel 2016.

User guide

Current model format does not support providing additional documentation.

Appendices

Techno-Economic Evaluation of Carbon Dioxide Mass transfer using Hollow Fiber Membrane Contactors for Algal Biomass Production

The importance of CO_2 as an economic input

The Techno-Economics team investigated the relative economic performance of the membrane carbonation technology in comparison to other, state-of-the-art technologies. As a primary nutrient for algal cultivation, CO_2 expenses are a significant contribution to the final cost of algal biomass production and algal biodiesel production. The primary challenge in analysis is that there is still significant uncertainty around what long term CO_2 delivery strategies, costs, and carbon utilization efficiencies (CUE) will eventually be achieved. In order to understand the relative contribution costs of CO_2 to a biodiesel product, we show sensitivity analysis based on the production model from 2012 Harmonization Report [DOE Biomass Program][1].

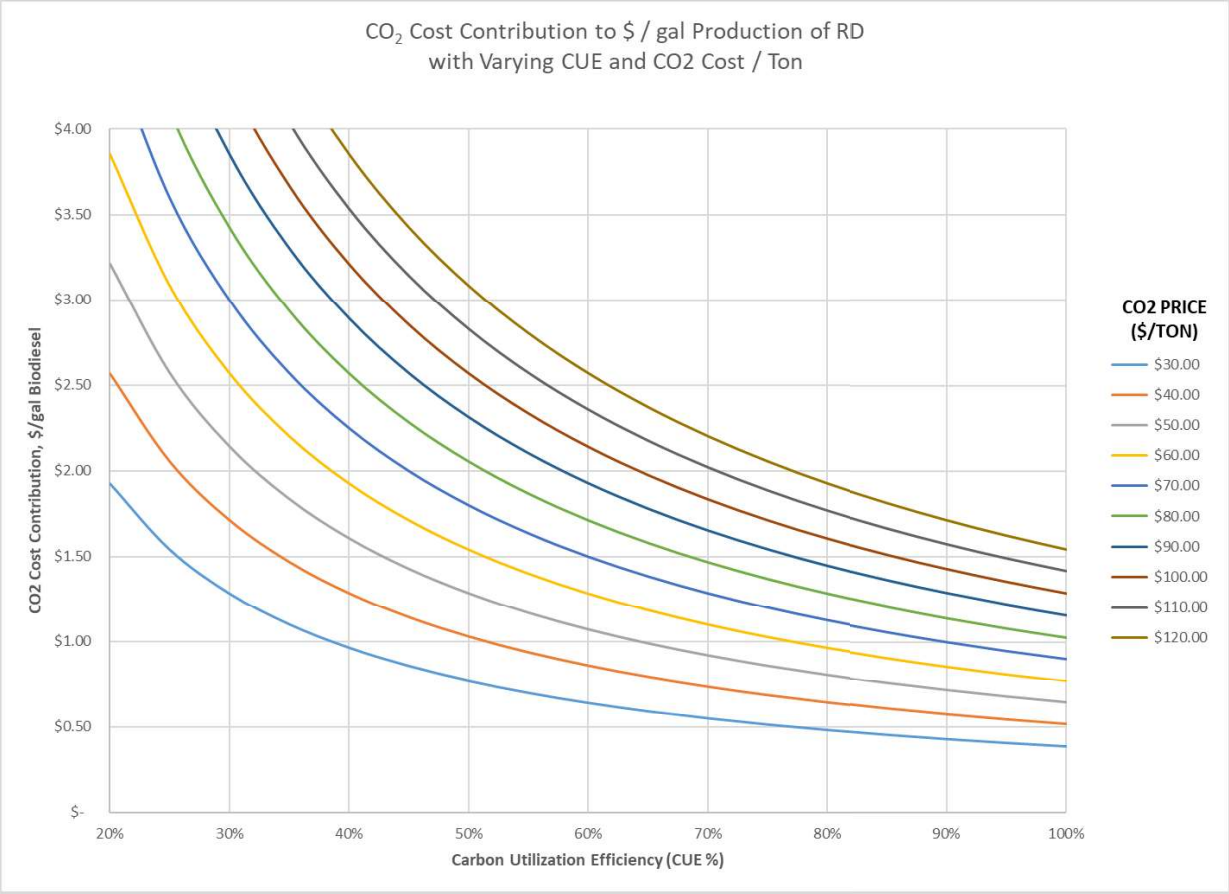

Figure 2. Cost Contribution of Carbon Dioxide to One Gallon of Renewable Diesel

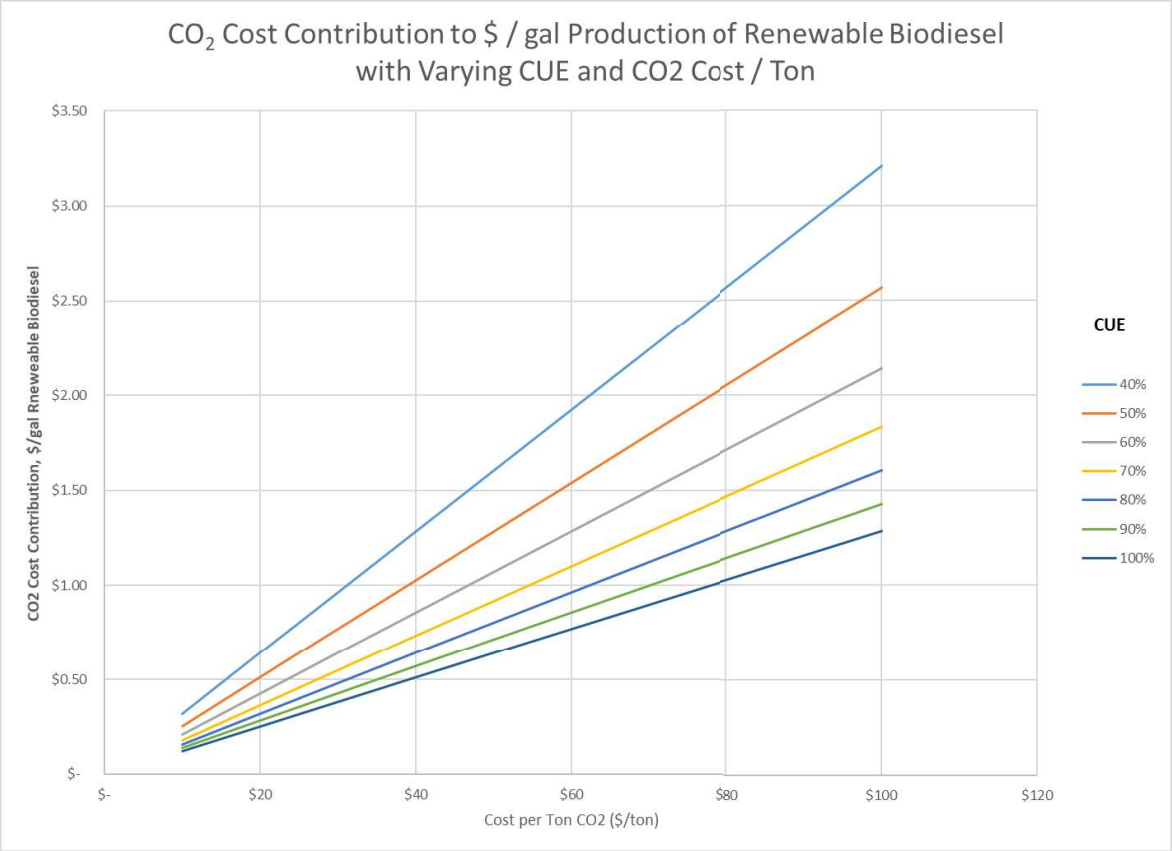

Figure 3. Cost Contribution of Carbon Dioxide to One Gallon of Renewable Biodiesel

Figure 1 and Figure 2 show two visualizations of CO_2 cost contribution to the total cost of a gallon of Renewable Biodiesel (RD) production. As stated, there is significant uncertainty around the correct amortized (in the case of Capital Expense assessments) expense or cash price for a given volume of CO_2. In our experience, a typical long term target for CO_2 is roughly estimated at $40–60 per ton (plant gate), which is derived from cost engineering for amine-based scrubbing processes. Based on supply contracts to ASU and AzCATI, we believe the price of compressed, bottled CO_2 to be in the range of $600–800 / ton, which is clearly not feasible long term. The overall conclusion, though, is that CO_2 cost and CUE will be primary contributing factors to any algal bioenergy production processes.

Current Methods and Statistics for CO_2 Delivery in Algal Cultivation

In open pond cultivation Techno-Economics, it is assumed that inorganic carbon must be transported into solution for the organisms to use. This is due to large imbalance between CO_2 requirements of growing algal cultures and minimal CO_2 transport that occurs at the interface between the atmosphere and cultivation media (i.e., the surface of the pond). Only roughly 5% of the carbon required by the growing biomass can be delivered by culture surface gas transfer while maintaining maximal growth rates.

There are several methods to actively transport CO_2 into growth media that have been proposed for implementation at large scale (1000-10,000 acres): sparging via porous stones or drilled/sealed pipes, sparging via stirrer blades, bubble columns, airlift columns, silicone tubing, polymer hollow fiber

membranes, and gas exchangers. A comparison of the relative advantages and disadvantages of these methods can be found in Carvalho 2006. In the case of transport via sparging, two large problems can arise that inhibit transport efficiency. [2] First, limited residence time of the bubble surface in solution before it reaches the surface can result in significant losses of CO_2 and resultant low CUE to the atmosphere. Second, biofouling of the sparger can result in larger bubble sizes and/or blocked pores, resulting in degraded mass transport efficiency and higher pressure drop and pressurization costs. Various methods have been proposed to increase residence time and thus the efficiency of transport from gas phase CO_2 to dissolved inorganic carbon. The most mechanically feasible seems to be countercurrent injection of CO_2 using a sump baffle, but the resulting hydrodynamic performance can be poor. Mendoza (2013) estimated inclusion of a sump baffle increased paddlewheel power consumption by roughly six times.[3]

In the literature, the typical CUE for production systems TEA is assumed to be roughly 90%, an assumption we believe is aggressive. Assuming complete recovery of DIC from solution during the harvest phase, this allows for approximately 5% loss due to surface offgassing and 5% loss directly in the sump sparge. The highest sump mass transfer efficiencies our team saw in the literature was reported by deGodos (2014) as 94% using liquid velocities of > 0.35 m/s, 10% CO_2 flue gas sparge rates of 100 L/s, and pH of 8 in a 1 m deep, 1 m wide sump located 1.8 m down-stream from the paddlewheel of a 100 m^2 raceway.[4] Mass transfer rates of 50 g/min were observed using 0.22 m/s liquid velocity, 50 L/s sparge rate, and pH 8. Doubling sparge rate from 50 L/s to 100 L/s decreased CO_2 removal efficiency from 96% to 76%, which speaks to the challenges in optimizing a fixed system. In that pilot environment, reducing pH to 6 reduced efficiencies and mass transfer rates by as little as 5% and by as much as 50%.

The above results compare extremely favorably with a carbonation column experiment and mathematical model described by Putt (2010). The team constructed a 3.1 m carbonation column with theoretical transfer efficiency of 90% using 5% CO_2. The recorded results show efficiencies of 83% (pH 9-10) and 82% (pH 8-9). The team estimated based on their model that a 3.0 foot (0.9 m) well sparging with 3 mm bubbles would have a transfer efficiency of only 48%.[5]

The challenges with estimating CO_2 mass transfer rates is discussed extensively in Weissman (1988), especially Appendix I (and Appendix II (Augenstein). The changing geometry of ascending bubbles, movement of bubble swarms relative to liquid flow, driving force from biological activity, bubble size distribution, water velocity, and CO_2 concentration (pure vs. ~10% flue gas) all effect transfer rates and efficiency. The conclusion is that only a pilot facility should be used to estimate scaled CO_2 transfer rates. However, Weissman estimates the CO_2 removal rates (or stripping rates) of a downstream sump to be approximately 12.5% per second with a bubble rise rate of 30 cm/s, requiring 7 m of rise to remove 95% of CO_2.[6] Since sumps of that depth are prohibitively expensive to excavate, a gas collection and recycle loop was proposed above the sump. Based on mass transfer theory, it is possible the excellent performance noted by de Godos with flue gas was due to the close proximity of the sump to the paddlewheel and smaller scale of the pond. In order to illustrate the relationship between column depth and stripping rates, we have included the chart below using the following equations to determine efficiency:

Variables

r = stripping rate (1/s)

P = partial pressure CO_2 (atm)

v_B = bubble ascend rate (30 cm/s) [Weissman, Putt]

D = column depth

η = sparger efficiency

Equations

$$\frac{dP}{dt} = -rP$$

$$\eta = 1 - e^{-r\frac{D}{v_B}}$$

Sparge Efficiency										
		Stripping Rate (1/s)								
		0.1	0.125	0.15	0.175	0.2	0.225	0.25	0.275	0.3
Column Height (cm)	25	8%	10%	12%	14%	15%	17%	19%	20%	22%
	50	15%	19%	22%	25%	28%	31%	34%	37%	39%
	75	22%	27%	31%	35%	39%	43%	46%	50%	53%
	100	28%	34%	39%	44%	49%	53%	57%	60%	63%
	125	34%	41%	46%	52%	57%	61%	65%	68%	71%
	150	39%	46%	53%	58%	63%	68%	71%	75%	78%
	175	44%	52%	58%	64%	69%	73%	77%	80%	83%
	200	49%	57%	63%	69%	74%	78%	81%	84%	86%
	225	53%	61%	68%	73%	78%	82%	85%	87%	89%
	250	57%	65%	71%	77%	81%	85%	88%	90%	92%
	275	60%	68%	75%	80%	84%	87%	90%	92%	94%
	300	63%	71%	78%	83%	86%	89%	92%	94%	95%
	325	66%	74%	80%	85%	89%	91%	93%	95%	96%
	350	69%	77%	83%	87%	90%	93%	95%	96%	97%
	375	71%	79%	85%	89%	92%	94%	96%	97%	98%
	400	74%	81%	86%	90%	93%	95%	96%	97%	98%
	425	76%	83%	88%	92%	94%	96%	97%	98%	99%
	450	78%	85%	89%	93%	95%	97%	98%	98%	99%
	475	79%	86%	91%	94%	96%	97%	98%	99%	99%
	500	81%	88%	92%	95%	96%	98%	98%	99%	99%

Table 1. Comparison of Sparger Efficiency with Various Stripping Rates and Column Heights

As mentioned before, Weissman estimated stripping rates of 0.125/s. Putt estimated stripping rates of 0.22/s based on a mathematical model and bubble column data. As mentioned, the stripping rate is dependent on bubble swarm physics (bubble size, relative liquid velocity, depth correction factors). Complicating matters further is extrapolating the data collected under abiotic scenario to liquids containing microalgae and growth media. In addition to changing mass transport coefficients, the presence of various ions in solution may impact surface tension and thus alter bubble coalescence

properties. In making a very specific TEA comparison to sparging, more research is necessary to estimate precise sparge efficiencies and stripping rates.

In practice with shallow ponds, experience at ASU/AzCATI shows that up to 80-90% of sparged CO_2 can be lost in open ponds of minimal depth (~20 cm). This is in rough agreement with Table 1. Similar numbers are cited in De Godos (2014) for shallow open ponds. These numbers are so clearly unfeasible economically that we assume the proper comparison point for our membrane carbonation technology must be versus a sparge sump, not a shallow sparger. There is certainly opportunity to compare techno-economics against proprietary designs of silicone tubing coils, gas exchangers, and bubble columns. Since we do not have access to confidential cost information for these products, we have elected not to compare the membrane carbonation module economics to these products at this time.

Baseline Case: Sump Sparging Analysis

In order to evaluate the membrane carbonation technology's potential for commercialization, we compare the performance against two scenarios: a sparge sump with an operating depth of 1.0 meter and one with 2.0 m depth. These sumps are estimated to be operating in large scale raceways (larger than 2 acres in cultivation area). Typically, these sumps are placed close downstream to the paddlewheel in a pilot scale raceway. In this way, the sparger efficiency can be increased by culture turbulence and the resulting higher mass transfer coefficients.[vii]

For the purposes of our Techno-Economic comparison, our baseline estimate is that a large scale sump of depth 1.0 m would transfer 52.8% of input CO_2 into DIC with no impact on required paddlewheel power. This number is taken from the above calculations (Table 1) using the appropriate depth and Putt's estimation of a stripping rate of 22%/s. Similarly, we estimate the 2.0 m deep sump would transfer 78% of CO_2 into DIC. We additionally assume no discernable positive or negative impact to productivity, e.g., through cell rupture effects (negative) or vertical culture mixing (positive).

The cost of operating the sparge sump is composed of the operating expenses and amortized capital expenses, standardized to a metric tonne (MT) of CO_2 successfully transported into DIC. We estimate the operating costs of the sparger to be composed of the input CO_2 costs and the electricity required to compress the CO_2 gas. For both this scenario and the membrane carbonation scenario (to be discussed below), we estimate the cost of CO_2 gas at the point of the sparger to be $51.47/MT. This number is the sum of the assumed $50/MT-$CO_2$ (farm gate) plus an amortized $1.47/MT for distribution of CO_2 within the farm complex[1,viii]. In order to determine the compression costs of the gas, we assume the operating pressure to be the sum of operating pressure at a given depth (ρgh) and the sparger's pressure drop[2]. This gives us an estimated total gauge pressure of 25.5 kPa (3.7 PSIG) when operating at 2.0 meters and 15.7 kPa (2.28 PSIG) at 1.0 m. We base the capital costs of the sparger on the Atlantic Diffusers models

[1] This number is calculated using our assumed real discount rate of 5.04%, the average weighted average cost of capital for the farming/agriculture industry. Real discount rates can be approximated as the nominal disount rate minus the antipated rate of inflation. We then amortize over 30 years the $6MM in CO_2 costs Davis (2016) estimates for CO_2 distribution in an open pond production farm. The number is then standardized per metric tonne of CO_2 delivered in that model.

[2] AzCATI uses Atlantic Diffusers' Fine Bubble Tube Diffusers in operation. The data sheet for the AB-70012 indicates a pressure drop of 23.75 in-H20 (5.9 kPa) when operating in the middle (10 SCFM) of its 3-17 SCFM range.

found at AzCATI. Amazon.com places the price of a 3–17 SCFM tube diffuser at approximately $70. Given the large amount of gas these devices can transfer and the very low capital costs, we assume the amortized capital costs of the sparger to be negligible.

The calculations for the two sump sparger scenarios are shown below:

Sparger Assumptions			
Cost of CO2 (Farm Gate)	$	50.00	$/MT
Cost of CO2 (Distribution)	$	1.47	$/MT
Cost of CO2		51.47	$/MT
Depth of Sparger		100.00	cm
Temperature of Gas, Sparged		25	C
1 atm in PA		101325	Pa
Sparger Calculations			
Sparger Conditions			
Depth of Sparger		100.00	cm
Head Loss in Sparger		5.91	kPa
Total Pressure Sparger (gauge)		15.72	kPa
Ideal Compression			
moles in 1 MT CO2		22727	mols CO2
kWh to Compress 1 MT CO2		2.26	kWh/MT
Practical Energy Requirements			
Compressor Efficiency		80%	
Total Energy Requirements		2.82	kWh/MT
Cost of Electricity	$	0.06	$/kWh
Total Cost of Compression	$	0.17	$/MT
Sparger Efficiency Calculations			
Sparger Stripping Rate		22.5%	%/s
Bubble Ascend Rate		30.00	cm/s
Sparger Efficency- Mass Transport		52.8%	
Total Cost of Sparging			
Total Cost of CO2 to Sparger		51.64	$/MT
Total Cost of CO2 to Solution		**97.88**	**$/MT**

Sparger Assumptions			
Cost of CO2 (Farm Gate)	$	50.00	$/MT
Cost of CO2 (Distribution)	$	1.47	$/MT
Cost of CO2		51.47	$/MT
Depth of Sparger		200.00	cm
Temperature of Gas, Sparged		25	C
1 atm in PA		101325	Pa
Sparger Calculations			
Sparger Conditions			
Depth of Sparger		200.00	cm
Head Loss in Sparger		5.91	kPa
Total Pressure Sparger (gauge)		25.52	kPa
Ideal Compression			
moles in 1 MT CO2		22727	mols CO2
kWh to Compress 1 MT CO2		3.51	kWh/MT
Practical Energy Requirements			
Compressor Efficiency		80%	
Total Energy Requirements		4.39	kWh/MT
Cost of Electricity	$	0.06	$/kWh
Total Cost of Compression	$	0.26	$/MT
Sparger Efficiency Calculations			
Sparger Stripping Rate		22.5%	%/s
Bubble Ascend Rate		30.00	cm/s
Sparger Efficency- Mass Transport		77.7%	
Total Cost of Sparging			
Total Cost of CO2 to Sparger		51.74	$/MT
Total Cost of CO2 to Solution		**66.60**	**$/MT**

Table 2. Comparison of Two Sparger Scenarios, 1.0m and 2.0m Depths

From the calculations, it is clear that the vast majority of the expense of operating the sparger is from the input CO_2 and the CO_2 lost to sparge inefficiencies. As the price of the supplied CO_2 increases, the cost of the CO_2 lost to the atmosphere becomes increasingly important. In the baseline case, our use of \$50/MT-CO_2 is an optimistic number appropriate for long term biofuels production forecasts. With respect to initial target markets, "food grade" CO_2 used in the cultivation of nutraceutical microalgae products would have dramatically higher costs. As mentioned previously, AzCATI's small volume contract for bottled CO_2 is at approximately \$600-800/MT.

One important item we have not included in this calculation (or the membrane carbonation model) is the capital cost of the compressor(s). The challenge with this item is that it is heavily dependent on the scale and layout of the cultivation operation. Capital costs for compressors generally show economies of scale that materialize in a decreasing \$/KW as total power increases. So many specific design decisions and calculations are necessary in optimizing the cost of a CO_2 distribution system that we hesitate to provide a potentially misleading general case.

Membrane Carbonation Assumptions

Cost estimation of the performance of the membrane carbonation technology is the primary purpose of this report. As with the costs of sparging, the calculations for costs are not terribly complex, but the assumptions have tremendous uncertainty. The techno-economics team has attempted to reduce this uncertainty by narrowing the windows for confidence intervals for the assumptions. A justification for key assumptions follows.

Cost of CO_2: The assumption for the cost of CO_2 at the start of the membrane carbonation unit operation is assumed to be $51.47/MT, the same as for the sparging operation. The CO_2 concentration is assumed to be 100%. This is justified above.

Membrane Flux: The baseline flux for the membrane in this analysis was chosen to be 1661 g/m^2/day. The unit is estimated to operate for 12 hours per day, resulting in a flux of 831 g/m^2 per calendar day. This number was selected as it represents the average of the four experimental values resulting from raceway experiments 1, 2a, 3, and 4. It is evident from that section of the report that flux is incredibly dependent on CO_2 concentration, fiber geometry optimization, valve/venting configuration, and operating pressure. This results in a wide range of TEA results for the membrane carbonation process as a function of process operating conditions.

The reality of operating the membrane over the course of a year would look quite different than our simple model. Similar to many capital expense challenges in cultivating algae, the primary hurdle is dealing with seasonal fluctuations in CO_2 demand. One benefit of the membrane carbonation method is that flux rate can be increased by increasing the operating pressure. Thus we would expect that a fixed membrane asset could be optimally sized by 1) examining the expected yearly cycle of carbon dioxide demand, 2) calculating flux rates as a function of pressure, 3) calculating total operating expenses / tonne of CO2 delivered as a function of pressure, 4) delivering the necessary amount of carbon dioxide at the lowest price using the appropriate pressure control algorithm and ideally sized membrane cassette. There is also the opportunity to integrate forward looking weather sensors to turn the carbonation devices on/off early or later than instantaneous demand would merit. All of these concepts have not been examined in this TEA, but are desired for future analysis.

Membrane Cost: Estimating the high volume production costs of a batch-produced prototype is challenging. In order to bracket the potential low and high costs for our hollow fiber membrane (HFM), we examined products that share similar production processes and form. The membrane we currently use is a triple layer hollow fiber consisting of a nonporous urethane layer laminated between two microporous polyethylene layers. Typically, porous single fiber membranes are fabricated using a spinning process utilizing a doping fluid, bore fluid, spinneret, and coagulation bath.[ix] A single layer membrane requires a simpler spinneret geometry than a double or triple layer membrane. However, similar to many extrusion processes, once the expensive die is manufactured, the unit production costs are relatively similar for simple and complex product geometries. Conversations with experts at ASU in hollow fiber membrane spinning confirmed that overall production costs for our triple layer membrane would be similar to single layer membranes at comparable volumes.

With this information in hand, we then hope that the long term production costs of hollow fiber membranes for transport of CO_2 would be similar to other hollow fiber membranes produced in large volumes. One use of HFMs this team has experience is in the membrane bioreactor (MBR), used in processing domestic wastewater. Use of polypropylene porous fibers for ultrafiltration has become so common that the item is a commodity product. These fibers can be found on Alibaba.com supplied from Chinese manufacturers at costs (including module) of \$3–10 / m^2. GE Water (now Suez Water Technologies) has offered the ZeeWeed HFM for many years, which is a hollow braid coated with a PVDF membrane. A typical implementation can be found in the ZeeWeed 500D module, an outside-in flow, 1.9 mm OD fiber assembly containing roughly 34 m^2 of fiber surface area.[x] Public documents showing bids to municipal water authorities reveal unit prices of \$1189, yielding a price of \$24-\$35/m^2. [xi, xii]

Another growing application of HFMs is in biogas upgrading. Many membrane vendors and integrators exist. In the literature, a cost of \$20/m^2 is estimated for a polyvinylamine/polyvinylalcohol (PVAm/PVA) blend membrane.[xiii] This author's analysis of a study showing Capital Investments for European biogas separation units (EG Evonik's polyamide-based membrane) yields a similar estimate.[xiv]

Although it is challenging to guess the "soft-costs" of these operations, it seems reasonable to estimate that total production costs of HFMs (including module/packing) could be as low as \$3–10/m^2. For this TEA, we use an estimate of \$6/m^2 for an "n-th plant" total installed cost of capital. The cost of installation for both the sparger and membrane are not included in this analysis, but are likely similar as they require similar plumbing effort.

Membrane Lifetime: Membrane lifetime is extremely important in determining the amortized cost of capital. We use an estimated lifetime of 10 years. This is based on Cote (2011), which used GE Water warranty data to estimate a life of at least 10 years for installations of the GE ZeeWeed PVDF membrane.[xv] The PVDF fiber in the MBR application was specifically chosen due to its resilience to that operating environment which requires frequent pond cleaning with chlorine. In general, the typical failure mode for the product was in the mechanical module attachments (potting, structure), not the fiber. Until better lifetime analysis is available on our membrane, this data point serves as an excellent proxy for membranes in high-duty environments.

Discount Rate: The primary cost item in the "Total Cost of Ownership" for the Membrane Carbonation unit operation is the amortization of the capital expense of the hollow fiber membrane. This item is a function of Total Capital Investment, lifetime, and applied discount rate. We apply a discount rate of 5.04%, which is the average weighted average cost of capital (WACC) for the agricultural/farming industry as provided by Damodaran.[xvi] In Damodaran's methodology, WACC is determined by using the weighted average cost of equity and after-tax debt applied to the Debt/Equity ratio of a given industry or firm. The cost of equity is estimated using the Capital Asset Pricing Model (CAPM), which applies a risk premium to the risk-free borrowing rate as a function of the risk premium and industry beta. The after-tax debt rate is calculated as (1 – Tr) x Dr, where Tr is the marginal tax rate and Dr is the corporate debt rate, which is itself a function of stock price volatility. It should be noted that Farming/Agriculture as a sector has a low cost of capital due to having a higher-than-average Debt to Equity ratio and lower market volatility. A case could be made that the appropriate WACC to use for biofuel production is the Oil and Gas Production industry's cost of capital rate of 7.76%, since crude oil price volatility is the

primary source of revenue risk for both. In future efforts, we may consider using a blended WACC as a function of specific assets and revenue models involved. It should be noted that the WACC for the entire market is currently 5.81% (excluding financials).

Cost of Electricity: The cost of electricity is assumed to be $.06/kWh which is in line with EIA industrial rates for the Gulf Coast (Texas, Louisiana, Alabama, Mississippi), which is considered to be a likely location for algal biomass production. The industrial rate for Arizona are similar, peaking at roughly $.07-$.08 in summer.

Membrane Carbonation Results

An estimate for the total cost of the membrane carbonation unit operation follows. Recall that the input to this process is 1 atm, 100% CO_2 supplied at a cost of $51.47/MT. As we discuss results, we draw a distinction between the total cost to deliver 1 MT of CO_2 to solution (includes the cost of 1 MT of CO_2, electricity, lost CO_2, amortized capital, etc.) and the cost of the unit operation (Total Cost minus 1 MT of CO_2).

Membrane Assumptions			
Cost of CO2 (Farm Gate)	$	50.00	$/MT
Cost of CO2 (Distribution)	$	1.47	$/MT
Cost of CO2		51.47	$/MT
Membrane Flux		1,661.00	g / m^2 / d
Membrane Cost	$	6	$/$m^2$
Membrane Lifetime		10.00	years
Real Discount Rate		5.04%	
Membrane Efficiency		100%	

Membrane Calculations		
Membrane Calculations		
Membrane Flux - calendar day	830.50	g / m2 / d
Membrane Flux - yearly	0.303340	MT / m2 / y
Lifetime Flux		
Lifetime CO2 Delivered to solution (MT)	3.03340	MT / m2
Levelized Cost Calculations (membrane + CO2 losses)		
Real Discount Rate	5.04%	
Levelized Cost / MT	**$54.04**	$/MT-CO2
Cost Contribution of the Membrane	**$2.57**	**$/MT**
Compression Costs		
Membrane Operating Pressure (gauge)	101.325	kPa
kWh to Compress 1 MT CO2	10.84	kWh/MT
Compressor Efficiency	80%	
Total Energy Requirements	13.55	kWh/MT
Total Cost of Compression	0.81	$/MT
Total Cost of CO2 to Solution	**$54.85**	**$/MT**
Total Cost of Membrane Unit Operation	**$3.38**	**$/MT**

Table 3. Total and Incremental Cost to Deliver Carbon Dioxide via Membrane Carbonation

The assumption for these calculations are provided below.

Shared Assumptions				Reference
Real Discount Rate		5.04%		Farming/Agriculture estimated WACC, http://people.stern.nyu.edu/adamodar/New_Home_Page/datafile/wacc.htm
Cost of Electricity	$	0.06	$/kWh	EIA.gov rough averages, Gulf Coast
Cost of CO2 (Farm Gate)		50.0	$/MT	Various
Compressor Efficiency		80%		Peters, M. S., Timmerhaus, K. D., West, R. E., Timmerhaus, K., & West, R. (1968). *Plant design and economics for chemical engineers* (Vol. 4). New York: McGraw-Hill.
Membrane Assumptions				
Membrane Flux - daily		1,661.00	g / m^2 / d	Experimental :Eustance, Lai, 2018
Membrane Cost	$	6	$/$m^2$	Team Estimate
Membrane Lifetime		10.00	years	Cote, P., Alam, Z., & Penny, J. (2012). Hollow fiber membrane life in membrane bioreactors (MBR). *Desalination , 288* , 145-151.
Membrane Efficiency		100%		Experimental :Eustance, Lai, 2018
To Biomass Efficiency		90%		Experimental :Eustance, Lai, 2018
Membrane Operating Pressure (gauge)		101.325	kPa	Experimental :Eustance, Lai, 2018
Sparger Assumptions				
Diffuser Cost	$	70.00		Atlantic Diffusers AB - 70012 (amazon.com, atlanticblowers.com data sheet)
Diffuser Rate		10	SCFM	Atlantic Diffusers AB - 70012 (amazon.com, atlanticblowers.com data sheet)
Diffuser Rate (g/d)		*757,431*	*grams-CO2/day*	Calculation
Diffuser Pressure Drop		5.90995	kPa	Atlantic Diffusers AB - 70012 (amazon.com, atlanticblowers.com data sheet)
Sparger Stripping Rate		22.5%	%/s	Putt
Sparger Operating Depth		200.00	cm	Davis 2016
Bubble Ascend Rate		30.00	cm/s	Putt, Weissman
CO2 Delivery Systems (Davis 2016)				
Capital Expense of CO2 of Delivery System	$	6,500,000		Davis 2016
Annual MT of CO2 Delivered		376,256	MT	
CO2 System Life		30	years	
Capital Recovery Factor		*0.065*		Calculation
CO2 System Annual Maintenance Charge		2.0%		Peters, M. S., Timmerhaus, K. D., West, R. E., Timmerhaus, K., & West, R. (1968). *Plant design and economics for chemical engineers* (Vol. 4). New York: McGraw-Hill.
Levelized Cost of Distribution to Pond	*$*	*1.47*		Calculation

Table 4. Assumptions Used in Membrane Carbonation Calculations

Overall, we see the cost of the carbonation unit operation for membrane carbonation to be $3.38 / MT of CO_2 delivered to solution and $14.78/MT for the 2 m deep sparge sump. It is difficult to estimate exact error rates for these estimates, but typical first-order estimates typically are in the -15 to +30% range. In the case of the membrane, the capital costs of the membrane dominate and thus are the primary source of error. In the case of the sparger, the cost of the lost carbon dioxide dominates, and the ability to predict the price of CO_2 dominates the uncertainty.

The most important comparison to make for the two different technologies to examine the cost of the carbonation operations using a varying membrane cost assumption. This is because there is currently the most uncertainty around the future cost. In the chart below, we estimate the membrane carbonation unit's total cost ($ per MT of CO_2 delivered to solution) for various membrane costs ($/$m^2$). The straight lines show estimates of the cost of operation for 2 m sparge sumps operating at various efficiencies. The cost of sparging is obviously independent of the cost of the membrane. This chart

allows us to see where, all else equal, the operator would be indifferent between the two technologies given the baseline assumptions given previously.

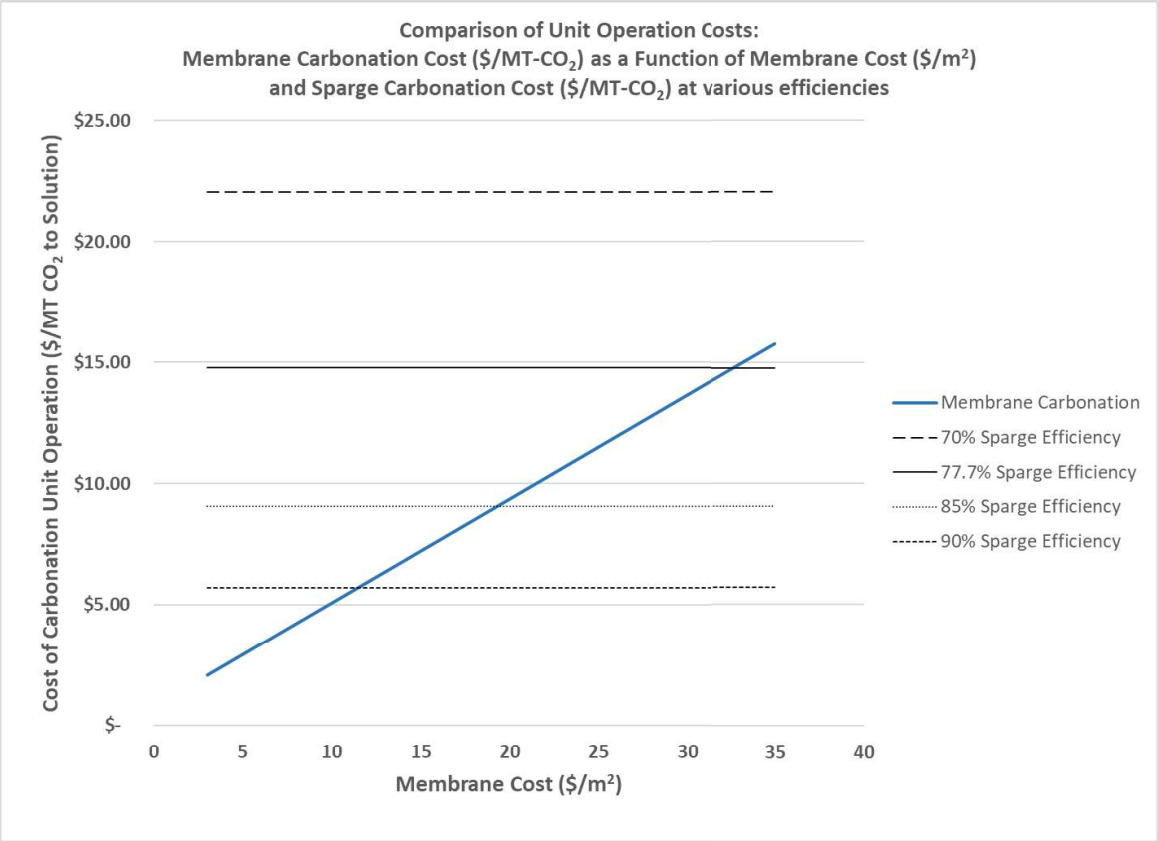

Figure 4. Membrane Cost vs. Total Cost of Carbon Dioxide Delivery in Membrane Carbonation

In these scenarios, we see that the membrane would need to cost less than $33/m^2 in order to be cost effective with a 77.7% efficient 2.0 m sparge sump (22.5%/s stripping rate).

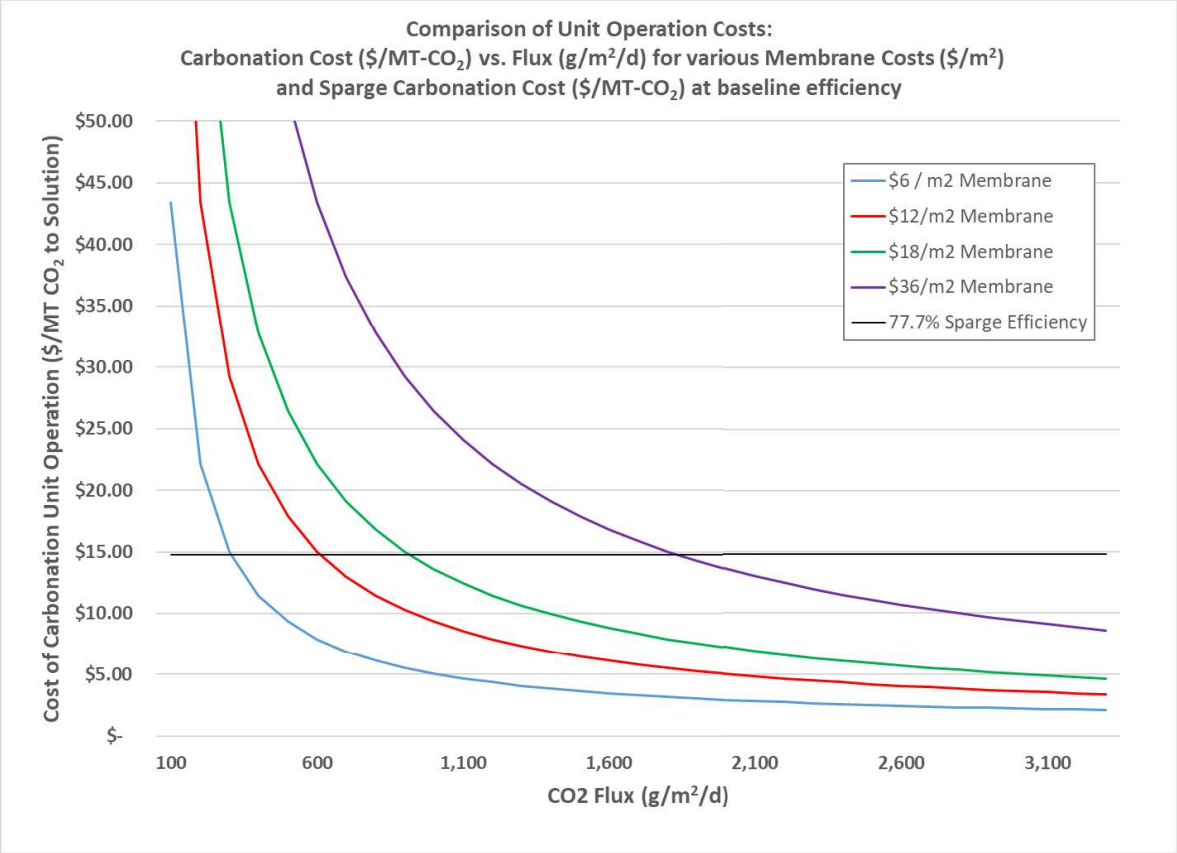

Figure 5. Carbon Dioxide Flux Rate vs. Total Cost to Deliver Carbon Dioxide

Similarly, we compare the performance of a 77.7% efficient 2.0 m deep sump sparge with the membrane carbonation process. For various assumed costs of capital, we show the relationship between CO_2 flux ($g/m^2/d$) and unit operation cost ($/MT-$CO_2$-to-solution). The cost of operating the membrane is always lower than the 77.7% efficient sparger at delivery fluxes greater than 1800, 800, 611, 297, and 150 $g/m^2/d$ flux with installed costs of $36/m^2, $18/m^2, $6/m^2, $12/m^2, and $3/m^2, respectively.

The last analysis we examine is a comparison of sparging and membrane carbonation for several scenarios. The parameters are chosen based on the author's familiarity with this field and general cost curves to represent different phases of maturity:

Scenario I: Shallow sparge (25 cm) with a low calculated carbon transfer efficiency (17%). This is calculated from the previous equations and stripping rates. The cost of the CO2 represents bottled prices delivered from a gas supplier such as Linde or Praxair. The membrane prices represent very low volumes that might be achieved in pilot facilities. The discount rate is appropriately high for a small, high risk operation.

Scenario II: This is an identical scenario to Scenario A, but the estimated sparge efficiency is increased. It has been noted in the literature that very shallow sparges have higher efficiency than expected in the first second of bubble ascent (~30cm) due to complex interactions.

Scenario III: This is an intermediate scale comparing a 2.0 m sparge with membrane carbonation at $120/MT for CO2 supply. This cost corresponds with high volume contracts delivered by tank car from the above gas suppliers.

Scenario IV: This represents a "perfect" scenario for sparging where its relative weaknesses are mitigated by a deep sparge. The price of CO_2 is minimal, corresponding to a short pipeline from a collocated facility which does not invoice for CO_2. This is unlikely, but an interesting edge case to examine. Discount rates represent those achieved by the least risky borrowers (municipalities, regulated utilities, subsidized industries).

	Unit	I	II	III	IV
Sparge Depth	cm	25	25	200.0	600.0
Sparge Efficiency	%	17%	30%	78%	98.9%
CO2 Purchase Price	$/MT	500	500	120	5
Membrane Price	$/$m^2$	1000	1000	25	6
Discount Rate	%	15%	15%	10%	4%
Unit Cost of Sparging	$/MT-$CO_2$	$ 2,440	$ 1,174	$ 35	$ 3
Unit Cost of MC	$/MT-$CO_2$	$ 658	$ 658	$ 14	$ 2

Table 5. Scenario comparison.

With the exception of Scenario IV, the membrane carbonation appears to provide a lower total cost to the operator in each situation. This bodes well for the commercialization opportunities of the technology, as it could provide an immediate cost benefit for customers at early, mid, and late stages of adoption.

REFERENCES / ENDNOTES

Davis, R., Fishman, D., Frank, E. D., Wigmosta, M. S., Aden, A., Coleman, A. M., ... & Wang, M. Q. (2012). *Renewable diesel from algal lipids: an integrated baseline for cost, emissions, and resource potential from a harmonized model* (No. ANL/ESD/12-4; PNNL-21437; NREL/TP-5100-55431). National Renewable Energy Lab.(NREL), Golden, CO (United States).

[1] Carvalho, A. P., Meireles, L. A., & Malcata, F. X. (2006). Microalgal reactors: a review of enclosed system designs and performances. *Biotechnology progress*, *22*(6), 1490-1506.

[1] Mendoza, J. L., Granados, M. R., De Godos, I., Acién, F. G., Molina, E., Banks, C., & Heaven, S. (2013). Fluid-dynamic characterization of real-scale raceway reactors for microalgae production. *Biomass and Bioenergy*, *54*, 267-275.

[1] De Godos, I., Mendoza, J. L., Acién, F. G., Molina, E., Banks, C. J., Heaven, S., & Rogalla, F. (2014). Evaluation of carbon dioxide mass transfer in raceway reactors for microalgae culture using flue gases. *Bioresource technology*, *153*, 307-314.

[1] Putt, R., Singh, M., Chinnasamy, S., & Das, K. C. (2011). An efficient system for carbonation of high-rate algae pond water to enhance CO2 mass transfer. Bioresource technology, 102(3), 3240-3245.

[1] Weissman, J. C., & Goebel, R. P. (1987). *Design and analysis of microalgal open pond systems for the purpose of producing fuels: a subcontract report* (No. SERI/STR-231-2840). Solar Energy Research Inst., Golden, CO (USA).

[1] Kumar, K., Mishra, S. K., Shrivastav, A., Park, M. S., & Yang, J. W. (2015). Recent trends in the mass cultivation of algae in raceway ponds. *Renewable and Sustainable Energy Reviews*, *51*, 875-885.

[1] Davis, R., Markham, J., Kinchin, C., Grundl, N., Tan, E. C., & Humbird, D. (2016). *Process design and economics for the production of algal biomass: algal biomass production in open pond systems and processing through dewatering for downstream conversion* (No. NREL/TP-5100-64772). National Renewable Energy Lab.(NREL), Golden, CO (United States).

[1] Peng, N., Widjojo, N., Sukitpaneenit, P., Teoh, M. M., Lipscomb, G. G., Chung, T. S., & Lai, J. Y. (2012). Evolution of polymeric hollow fibers as sustainable technologies: past, present, and future. *Progress in Polymer Science*, *37*(10), 1401-1424.

[1] https://www.gewater.com/kcpguest/documents/Fact%20Sheets_Cust/Americas/English/FSpw500D-MOD_EN.pdf

[1] City of Modesto, Proposal Number 186238-2, Original Project Number 500475, September 7, 2017.

[1] https://www.mi-wea.org/docs/Session%202%20-%20Joe%20Hebert.pdf

[1] Deng, L., & Hägg, M. B. (2010). Techno-economic evaluation of biogas upgrading process using CO2 facilitated transport membrane. *International Journal of Greenhouse Gas Control*, *4*(4), 638-646.

[1] http://www.sgc.se/ckfinder/userfiles/files/SGC270.pdf

[1] Cote, P., Alam, Z., & Penny, J. (2012). Hollow fiber membrane life in membrane bioreactors (MBR). *Desalination*, *288*, 145-151.

[1] http://people.stern.nyu.edu/adamodar/New_Home_Page/datafile/wacc.htm (updated January 2018)

Final Techno-Economics Report on MSS Prototype Performance

Overview

Our previous report examined the economics of the Membrane Carbonation (MC) operation in great depth. This report focuses on the ability of the MSS (Moisture Swing Sorption) to economically capture, concentrate, and deliver carbon dioxide gas. While the objective of the overall project was to integrate the two technologies into an Atmospheric CO_2 Enrichment and Delivery (ACED) system, our prototype and theoretical process design did not explore any synergies between MSS and MC subsystems. The final TEA effort analyzed the costs of each unit process separately and simply added costs for the end-to-end process. In order to model the hypothesized synergies from the MSS-MC integrated system, we would need currently unavailable experimental data detailing the composition of vented gases from the MC system and subsequent reintroduction to the MSS system.

Since the ACED development team is currently focused on designing and operating a prototype, some abstractions have been made while attempting to perform cost engineering on the system. The costs considered in the TEA model are those we view as core to the ACED technology, regardless of final implementation. In this particular case, we have chosen not to model certain expenses like liquid pumps, piping, instrumentation, electrical wiring, and service facilities, opting instead to use accepted multipliers on itemized major capital expense items (Perry's Chemical Engineers' Handbook §9; Jelen's Cost and Optimization Engineering, 1991; Peters, Timmerhaus, West, 2011).

The construction and operation of the MSS prototype over the course of this project did little to inform our projections for the long-term techno-economic prospects for the technology. Since the prototype suffered many operational challenges that would not occur in a production environment, the performance measures do not feed well into an idealized model. For example, the laboratory experiments at the beginning of this project indicated the resin could concentrate atmospheric CO_2 levels to roughly 5% to 10% at a rate of roughly 1.0 to 2.0 g-CO_2/kg-resin/hour. The prototype was not designed to maximize these metrics and as such delivered perhaps 0.35 g-CO_2/kg-resin/hour at a concentration of 0.4% to 1%.

While the economic outcome for the process flow analyzed in this document is not optimistic, the TEA performed over the course of this project has encouraged the MSS team to evaluate other strategies that will likely reduce costs dramatically.

Process Definition

The figure of merit we use to evaluate economic performance is US Dollars per Metric Tonne of Carbon Dioxide gas successfully evolved from the Thermal Release Column. **Figure 1** (Simplified Process Flow) illustrates the simplified process which was constructed to perform TEA. This process diagram has been

modified since the Preliminary Techno-Economics Report to reflect the new figure of merit as well as some configuration changes.

The target production of the facility is 100,000 MT per year of CO_2 into solution, a number on the same order of magnitude as previous TEA efforts on biofuel production via algae harvest (Davis et al, 2011). We make no attempt to conduct TEA on algal growth, harvest, or biodiesel production, as that research is far outside the boundaries of this research.

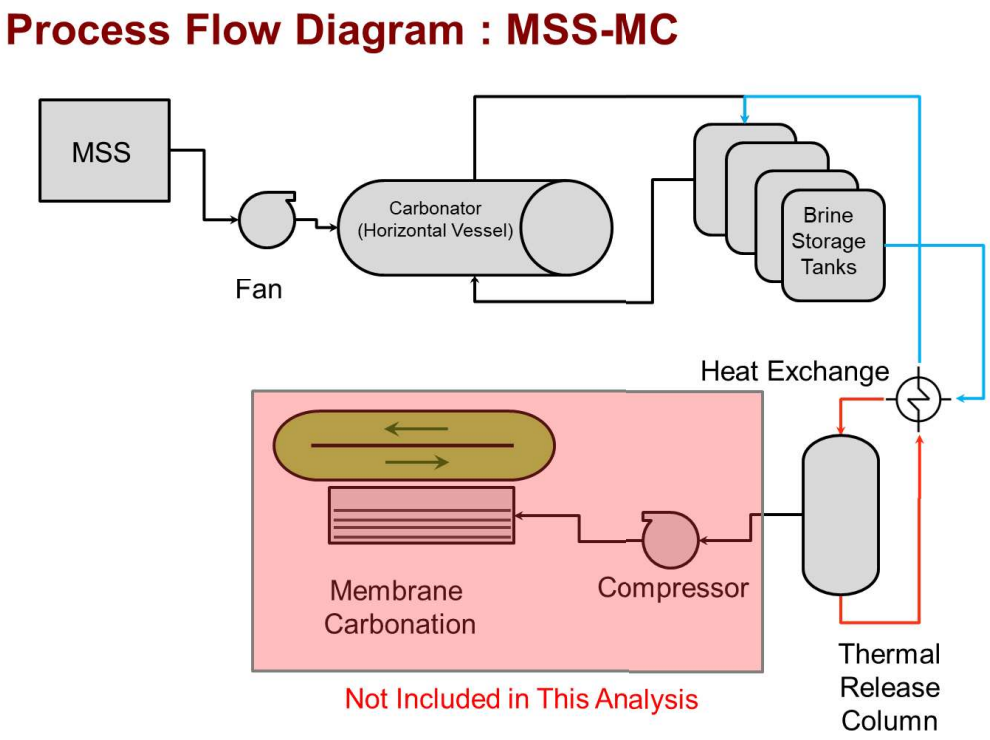

Figure 6. Simplified Process Flow

Figure 1. Simplified Process Flow Diagram assists the Techno-Economic analyst in estimating mass flows and capital requirements. A detailed Piping and Instrument Diagram was not created for the purposes of this analysis since the effort tends to limit flexibility in making hypothetical changes to the system.

The process begins with a module to capture and concentrate atmospheric CO_2 using a moisture swing sorption (MSS) process. The harvested CO_2 is delivered into a Carbonate/Bicarbonate brine storage tank until CO_2 is required by algal growth. Previous TEA models assumed the CO_2 from the MSS is sparged into the brine tanks. The current PFD reflects the current design of the prototype, which uses a lower pressure fan to blow the collected CO_2 across an oscillating fabric carbonator which is wetted with the brine solution. To recover the stored CO_2, brine is sent to a Thermal Release Column, where it is heated

by both natural gas burner and heat exchange with hot effluent from the column. This is the point where the output is analyzed for the techno-economic figure of merit ($/MT-$CO_2$).

Energy and Mass Balance

The characteristics (mass, volume, composition, etc.) of input and output streams for each subprocess are calculated in a spreadsheet using Microsoft Excel 2013 based on key performance parameters (KPP) for each component. KPPs for components unique to this project (MSS, MC) were sourced from the respective design and development teams. Statistics for common components like heat exchanges were taken from Chemical Engineering handbooks and literature. Please refer to Table 1 for a detailed list of many KPPS.

A. The primary characteristic driving TEA of the MSS is the productivity of the resin in capturing CO_2. Lab experiments yielded a productivity of roughly 1.67 g CO_2 per kg of resin per hour. Operational challenges with the prototype have made measurement of the CO_2 yield difficult. The very few measurements of the productivity of the resin in the prototype yielded a rate of 0.35 g/kg-resin/hour, which dramatically increases the predicted cost of the system. The other KPP which impacts the energy and capital expenses of the MSS is the partial pressure of CO_2 in the product stream. In the preliminary report, we had hoped to achieve 5000 Pa CO_2 (~5%), but the IRGA sensors in the fabric carbonator indicate a partial pressure of approximately 0.4% to 1% CO_2. This would increase the size and power of the blowers required to evacuate the MSS chamber while the resin is submerged.

B. **Centrifugal Radial Fan –**Centrifugal Radial Fans were sized to move the required volume of product stream from the MSS chamber to the fabric carbonator. In the absence of simulation data to optimize with, they are sized 25% above straight-line requirements in order to "catch up" after rain days. The necessary power to run these fans is added to the utility-electricity charge.

C. **Horizontal Fabric Carbonator –** The size of the fabric carbonators was estimated using a straight-line extrapolation of the performance of the prototype in mass of CO_2 transferred to solution per unit volume per unit time. We calculated the volumetric flow of CO_2 into solution, then converted to a KPP of g-CO_2/m^3/minute. The equipment required is thus expressed in a volume (m3) of fabric carbonator required. The fabric carbonator is a novel piece of equipment. For the purposes of estimating cost, we use a $/$m^3$ metric consistent with horizontal low pressure tanks. The prototype carbonators are actuated by an oscillating chain drive. For the purposes of this TEA, we did not estimate actuation power costs, but these would certainly be non-zero.

D. **Brine Storage Tanks –** The brine storage tanks were sized according to a user-controlled number of days of CO_2 requirement, designed to make CO_2 available to the algae when the MSS productivity cannot keep pace and maximize CO_2 capture efficiency when the algae demand is insufficient. The number of tanks to size can be changed by the analyst.

E. **Heat Exchange –** The CO_2 rich stream coming from the brine tanks is heated by the CO_2 poor stream coming from the Thermal Release Column. A generic heat exchanger was sized according to accepted Heat Transfer Coefficients and desired T_{in}/T_{outs} for the various fluids.

F. **Thermal Release Column –** The performance of the Thermal Release Column is still under investigation, but preliminary estimates suggest roughly half of the carbon stored in the bicarbonate solution is extracted by heating the fluid. The size of the reactor is based on an expected solution residence time and required flow rate.

Cost Engineering

Total capital expenses are calculated based on the itemized equipment list created in the previous step. In scenarios where cost data is not available in the present year for certain items, the 2018 cost is approximated using the CEPCI (Chemical Engineering Plant Cost Index), which is analogous to an inflation index.

The primary source used for common equipment costs is Peters, Timmerhaus, and West (2011). For example, using this resource, a heat exchange can be sized based on type and surface area.

Quantities of consumables (e.g., electricity) are assigned costs based on numbers sourced from an appropriate agency (US EIA, published utility rates).

Cost estimates for the MSS unit were based on two methods:

1) The "cubes" which compose the active surface of the MSS are currently created from sheets of resin held apart by a thermoformed structural plastic. The TEA team believes there is significant optimizations possible for economical Design-to-Manufacture on this item. Therefore, the device is abstracted to a few key assumptions:
    - Productivity of the resin (g-CO_2 / kg-resin / hour)
    - Cost per kg resin ($/kg)
    - Ratio of resin materials costs to total manufactured cost
    - Cost per kg structural thermoplastic ($/kg)
    - Ratio of structural plastic materials costs to total manufactured structure cost
2) The MSS container as currently costed/envisioned is an assembly consisting of a watertight plastic box, foul weather winch, supporting structure (various lengths of square steel framing tube), and sail scissor bars (various lengths of steel bar stock). Allowances were made for fasteners and labor fabrication/assembly time.

Given the above methods, the MSS was costed by calculating the required mass of resin to support the CO_2 demand. The resin and thermoplastic support costs were estimated by mass. A geometric relationship was established to determine how much resin would be enclosed by a 1 m^3 container. This is easily calculated given each resin cube contains 100g of resin, 200g of structural plastic, and measures

10 cm on each side. Finally, estimates for the container were created by determining the price of each component in the Bill of Materials using part cost resources such as McMaster-Carr.

A more thorough TEA would examine the large scale manufacturing expenses of the scissor-lift & chamber using advanced part-costing techniques. We do not recommend going down this path because the prototype sail/container design as currently imagined will never reach reasonable cost goals. Also, the process of "dunking" the resin in water wastes large amounts of water and causes the resin to become waterlogged.

Results and Discussion

This investigation into the techno-economics of the MSS system demonstrates that significant cost and performance improvements must be made in order to economically deliver CO_2 gas at a target cost below $100 / tonne.

For the purposes of communicating our results, we will define three scenarios:

- The "Prototype" scenario uses performance assumptions based on experimental results observed. Expenses (Capital and Operating) are commensurate with the scale of the analysis. As noted, the efficiencies and performance in the prototype in the field was often $1/10^{th}$ that observed in the lab.
- The "Baseline" scenario uses lab results for performance parameters of new equipment. On the cost side we assume that the MSS Container prototype is deployed en masse, essentially taking the prototype design and putting thousands into the field. Although this scenario is not realistic, it is ideal from the TEA analyst's standpoint, as we can identify via sensitivity analysis key area of uncertainty that need to be researched and/or flagged for the development team.
- The "Aspirational" scenario explores what assumptions are necessary to achieve certain cost targets. Although there are a multitude of scenarios that could reach any given cost target, we present one to give the reader a general sense of what could be an economical implementation of the MSS technology.

Prototype Scenario

The "Prototype' scenario yields an estimate of ~3,500 / MT-CO_2(g) or $3,185 / ton-$CO_2$(g). Of this, only roughly $25/tonne is consumables expenses (electricity, water, bicarbonate consumed). The very low productivity of the resin causes the model to require an enormous capital investment in resin and resin support structure. As a result, there are incredibly high values for items driven by total capital employed (capital charges, depreciation, maintenance, property, insurance). We won't examine this scenario too closely, because it doesn't yield helpful insights beyond the already acknowledged primacy of resin productivity as the most important key performance parameter. A comparison of the key performance parameters used in the scenarios is found in *Table* 2.

Baseline Scenario

The baseline scenario yields an estimate of $931 per tonne of CO_2(g) [$844/ton-$CO_2$(g). The Total Product Cost estimate follows in *Table 1. "Baseline" Scenario - Total* Product Cost.

Table 6. "Baseline" Scenario - Total Product Cost

PLANT STATISTICS		
Feed	Atmospheric Air	
Analysis Date	2016	
Location	Arizona	
Capacity	100,000.0	MT / Yr
Operating Rate	95%	
Throughput	95,000.0	MT / Yr
Product	CO_2 in Solution	

CAPITAL COST	$ (Millions)	% of Plant
ISBL (Inside Battery Limits)	532.76	100.0%
OSBL (Outside Battery Limits)	-	0.0%
Total Plant Capital	532.76	**100.0%**
Other Project Costs	126.26	23.7%
Total Project Investment	659.02	**123.7%**
Working Capital	6.59	1.0%
Total Capital Employed	**665.61**	**124.9%**

PRODUCTION COST SUMMARY								$ Per MT	$ Per Ton	Annual Cost (USD Millions)
						Units per MT	*Price ($ / Unit)*			
RAW MATERIALS		Sodium Bicarbonate		kg		1.58	0.250	0.40	0.36	0.04
TOTAL RAW MATERIALS								*0.40*	*0.36*	*0.04*
UTILITIES		Electricity		MWh		0.008	59.1	0.48	0.44	0.05
		Process Water		MT		552.6	0.025	13.82	12.53	1.31
		Natural Gas		Mcf		0.88	6.530	5.76	5.22	0.55
TOTAL UTILITIES								*20.06*	*18.19*	*1.91*
TOTAL VARIABLE COST								**20.45**	**18.55**	**1.94**
DIRECT FIXED COSTS		Wages			$1,117,675			11.77	10.67	1.12
		Supervision	15%	of Wages				1.76	1.60	0.17
		Maintenance (Material & Labor)			2%	of ISBL		112.16	101.75	11
		Direct Overhead			45%	of Labor & Supervision		6.09	5.52	0.58
TOTAL DIRECT FIXED COSTS								*131.78*	*119.55*	*12.52*
ALLOCATED FIXED COSTS		Indirect Overhead			0%	of DFC		-	-	-
		Insurance, Property Tax, Land			3.00%	of Total Plant Capital		168.24	152.62	15.98
TOTAL ALLOCATED FIXED COSTS								*168.24*	*152.62*	*15.98*
TOTAL FIXED COSTS								**300.02**	**272.17**	**28.50**
TOTAL CASH COSTS								**320.47**	**290.72**	**30.44**
	Depreciation @		5%	for OSBL + OPC				66.45	60.29	6.31
			5%	for ISBL				280.40	254.37	26.64
	Total Depreciation							*346.85*	314.66	*32.95*
COST OF PRODUCTION								**667.32**	**605.38**	**63.40**
	Return on Capital Employed (including Working Capital)					3.8%		263.44	238.99	25.03
COST OF PRODUCTION + ROCE								**$ 931**	**$ 844**	**$ 88.42**

A "characteristic" of accepted chemical engineering cost estimation methods is that they are extremely sensitive to capital expense estimates. Since maintenance, insurance, property tax, and depreciation are all directly tied via accepted ratios to the Total Plant Capital estimate, each dollar of purchased capital can easily become three to five dollars of expense over the course of the capital's lifetime. This methodology is typically acceptable in a world where reactors, pumps, compressors, and distillation columns can be priced easily without detailed itemization from an EPC contractor. As an example of our methodology, since we do have a programmed service schedule for equipment, we simply assume the

yearly maintenance cost (material and labor) is 2% of the total ISBL equipment. This number is on the low side of typical ranges, but reflects a choice by the analyst to consider the low pressure/ low temperature nature of the operating conditions.

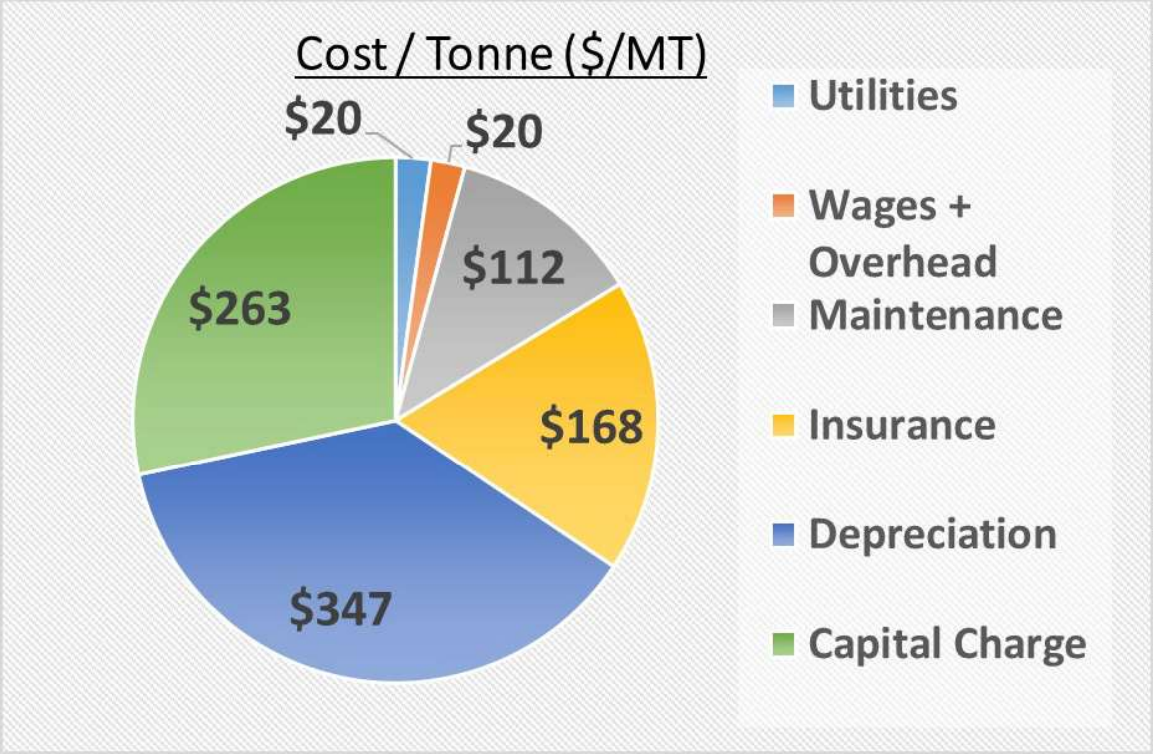

Figure 7. Breakdown of Expenses in Baseline Scenario

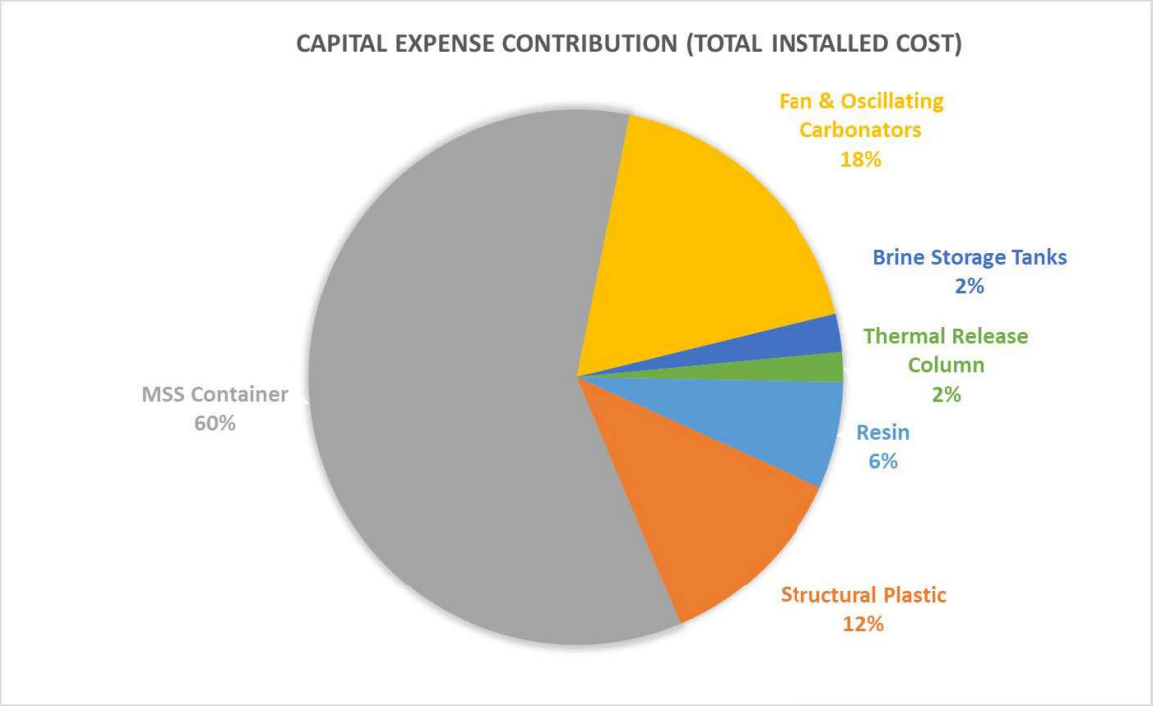

Figure 8. Breakdown of Capital Expenses in Baseline Scenario

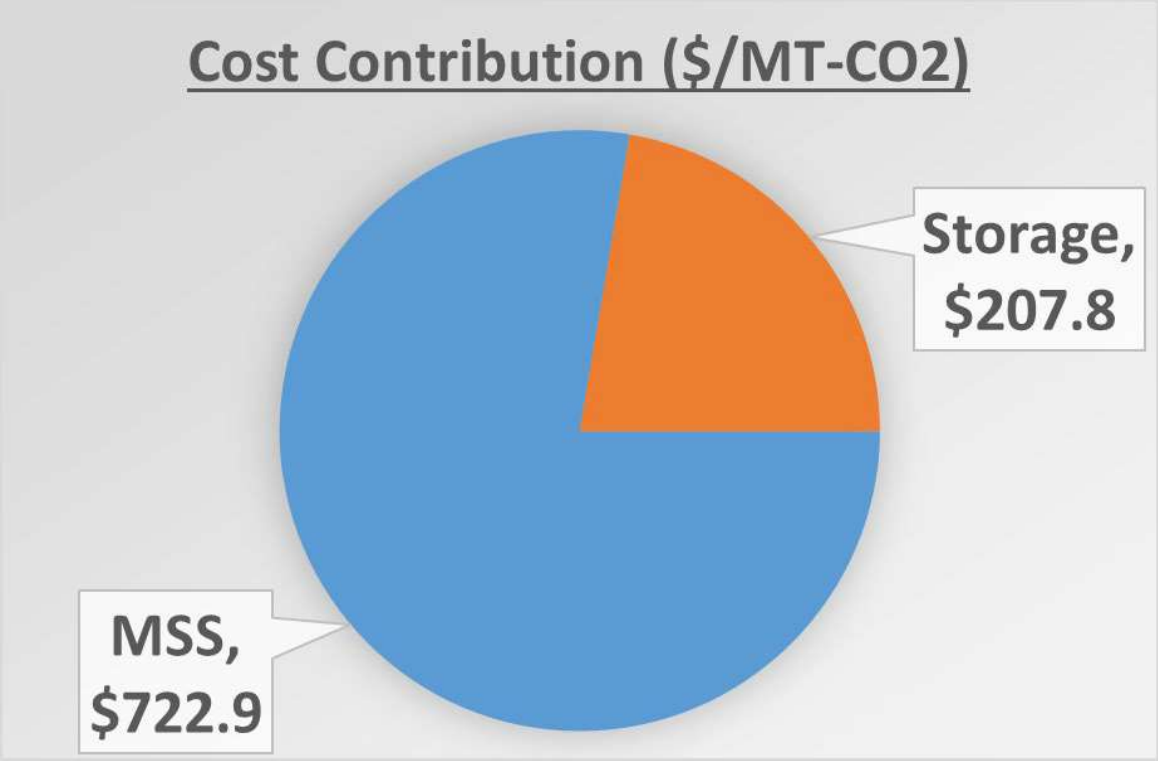

Figure 9. Subsystem Cost Contribution in Baseline Scenario

It is clear from **Figure 2** and **Figure 3** that the vast majority of expenses are derived from capital-expense-derived fixed costs rather than variable costs.

Figure 4. Provides a higher level view of the total cost contribution of each subsystem. This approach allocates depreciation, fixed costs, and finance charges according by capital expenses. Consumables such as electricity are allocated to the appropriate subsystem. The storage system includes all items following gas exit from the MSS (fan, oscillating carbonator, storage tanks, thermal release column).

The TEA model was designed to be somewhat abstract so we could tolerate a very large range of assumption values. Although we have no schematic of what the MSS would look like in this model, we can describe some critical performance metrics that should be achieved to meet a cost target of roughly \$100 / MT of CO_2 gas. To determine the most important parameters to examine, we deliver a "Tornado Chart" developed using the Crystal Ball (Oracle Corp.) software package:

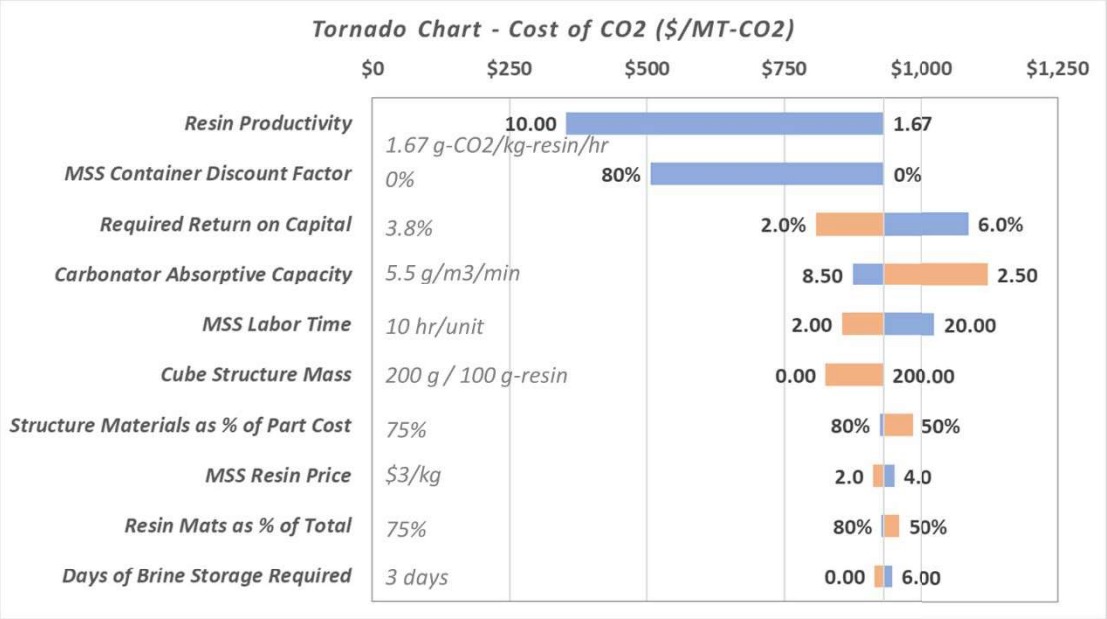

Figure 10. Tornado Chart

The Tornado Chart show the sensitivity of the model to the assumptions and range of the assumptions. The black vertical line shows the baseline estimate of approximately \$931 / MT. The values used in the baseline scenario are shown to the left in light gray. The blue and orange bars illustrate what the total cost estimate would be if only that variable were changed. For example, if the Required Return on Capital Employed (a charge assessed on total capital deployed) were increased from the baseline estimate of 3.8% to 6%, the cost per tonne would increase from \$931 / MT to roughly \$1088 / MT.

Although more than 20 parameters were examined, this chart show the top ten items which could contribute to an economically successful deployment. A description of the parameters follows:

- **Resin Productivity** : Mass of CO_2 released from a kilogram of resin per hour, averaged over a long period of time (many cycles). This accounts for daily temperature/moisture changes over the course of the year and downtime due to inclement weather.
- **MSS Container Discount Factor** : The container was costed using small volumes (~1000 units). Bulk production could reduce costs dramatically.
- **Required return on capital** : A capital charged added to ensure profitable operation of the plant. This is a substitute for adding a margin determined as a fraction of sale price.
- **Carbonator Absorptive Capacity** : The parameter for performance of the rotating fabric carbonator is grams-CO_2 per m^3 of carbonator volume per minute. This is a volumetric flux of CO_2 from gas into carbonate/bicarbonate brine relative to reactor size.
- **MSS Labor Time** : The manhours in total applied for assembly of the MSS container.
- **Cube Structure Mass**: In addition to the resin, the current device has supportive thermoplastic materials which act as spacers. There is currently 200g of spacers per 100g of "working" resin. An extruded 1-piece resin structure could conceivably have 0g of support structure.
- **Structure Materials as % of Part Cost:** The fraction of total part cost which is determined by thermoplastic structure materials costs. EG if 70% of cost is materials, 30% is processing and overhead.
- **MSS Resin Price :** Purchase price of the resin prior to processing
- **Resin Materials as % of Part Cost:** Similar to above, the fraction of total resin part cost determined by materials.
- **Days of Brine Storage :** Number of days of CO_2 delivery required to accommodate short term interruptions due to weather and total farm maintenance. This storage operates when the entire MSS unit operation must be shut down.

Aspirational Scenario

In order to achieve the aspirational goal of $100 / MT in the model, several key assumptions were modified. **By making the changes mentioned in Table 2, the estimated total product cost was $99 / MT of** CO_2 **provided.**

Table 7. Changes to Key Assumptions in the Aspirational Model

Key Assumption	Prototype Value	Baseline Value	Aspirational Value
Required Return on Capital	3.5%	3.5%	0.0%
Discount on MSS Container	0%	0%	90%
Resin Productivity	0.35 g/kg-resin-h	1.67 g/kg-resin/h	10 g/kg-resin/h
Cube Structure Mass per 100g Resin	200g	200 g	0 g
Carbonator Absorptive Capacity	5.5 $g/m^3/min$	5.5 $g/m^3/min$	10 $g/m^3/min$
Mols H20 per mol CO_2	2700	1350	4
Insurance, Tax (% of TCI)	3%	3%	1%

Using these new assumptions, we can provide a new Total Estimated Product Cost and associated breakdowns of cost contribution:

PLANT STATISTICS		
Feed	Atmospheric Air	
Analysis Date	2016	
Location	Arizona	
Capacity	100,000.0	MT / Yr
Operating Rate	95%	
Throughput	95,000.0	MT / Yr
Product	CO_2 in Solution	

CAPITAL COST	$ (Millions)	% of Plant
ISBL (Inside Battery Limits)	85.77	100.0%
OSBL (Outside Battery Limits)	-	0.0%
Total Plant Capital	85.77	**100.0%**
Other Project Costs	20.33	23.7%
Total Project Investment	106.09	**123.7%**
Working Capital	1.06	1.0%
Total Capital Employed	**107.15**	**124.9%**

PRODUCTION COST SUMMARY								$ Per MT	$ Per Ton	Annual Cost (USD Millions)
						Units per MT	*Price ($ / Unit)*			
RAW MATERIALS		Sodium Bicarbonate		kg		1.58	0.250	0.40	0.36	0.04
TOTAL RAW MATERIALS								*0.40*	*0.36*	*0.04*
UTILITIES		Electricity		MWh		0.008	59.1	0.48	0.44	0.05
		Process Water		MT		1.7	0.025	0.04	0.04	0.00
		Natural Gas		Mcf		0.88	6.470	5.71	5.18	0.54
TOTAL UTILITIES								*6.23*	*5.65*	*0.59*
TOTAL VARIABLE COST								**6.62**	**6.01**	**0.63**
DIRECT FIXED COSTS		Wages			$ 1,117,675			11.77	10.67	1.12
		Supervision	15%	of Wages				1.76	1.60	0.17
		Maintenance (Material & Labor)			1%	of ISBL		9.03	8.19	1
		Direct Overhead			45%	of Labor & Supervision		6.09	5.52	0.58
TOTAL DIRECT FIXED COSTS								*28.65*	*25.99*	*2.72*
ALLOCATED FIXED COSTS		Indirect Overhead			0%	of DFC		-	-	-
		Insurance, Property Tax, Land			1.00%	of Total Plant Capital		9.03	8.19	0.86
TOTAL ALLOCATED FIXED COSTS								*9.03*	*8.19*	*0.86*
TOTAL FIXED COSTS								**37.67**	**34.18**	**3.58**
TOTAL CASH COSTS								**44.30**	**40.19**	**4.21**
	Depreciation @		5%	for OSBL + OPC				10.70	9.71	1.02
			5%	for ISBL				45.14	40.95	4.29
	Total Depreciation							*55.84*	50.66	*5.30*
COST OF PRODUCTION								**100.14**	**90.84**	**9.51**
	Return on Capital Employed (including Working Capital)					0.0%		-	-	-
COST OF PRODUCTION + ROCE								**$ 100**	**$ 91**	**$ 9.51**

Table 8. "Aspirational" Scenario – Total Product Cost

Observations and Recommendations

As mentioned, the TEA did not improve or alter dramatically due to the operation of the MSS prototype. While many minor changes were made to the model, they did not dramatically alter the cost estimates. Observations follow:

1. The inclusion of the fabric carbonator over sparging an air/CO_2 mix was mostly a wash in overall costs, primarily substituting electricity costs for a low-energy, capital intensive unit operation. Although it was not specifically analyzed here, that substitution would positively impact environmental metrics in an LCA (Life Cycle Analysis). This team suspects there could be dramatic improvement in fabric carbonator performance realized if significant efforts were dedicated to engineering that device to maximize volumetric flux.

2. Resin productivity is the most important factor in determining the CO_2 cost. Although we know the MSS team is well aware of this fact, we emphasize for the reader that productivity should be increased by all means available, including high surface area to mass designs, resin composition, and operational optimizations like weather dependent cycling.

3. It is critical to have a large fraction of the MSS resin product (the "cube") be composed of resin materials costs rather than machining and overhead costs. Similarly, the mass of supporting plastic materials should be minimized to reduce materials and processing costs. A possibility could be an extruded shape which supports the resin, has a high surface area to mass ratio, and minimizes structural plastic material. This could also serve to minimize assembly and maintenance labor expenses.

4. The MSS Container (or Housing) needs to store and deploy the maximum mass of working resin at minimal cost. The final design should target a roughly \$150 / m^3 cost basis, including actuation, enclosure, and water storage.

5. Although we hesitate to dive too deeply into design recommendations on another team's technology, the TEA team does have some process recommendations based on a holistic understanding of the costs involved.

    a. An economic process would use an extruded resin product that requires very little (zero) support structure and has a high surface area to mass ratio.

    b. Moving from a batch process to a continuous process will be required to reach low cost targets.

    c. Actuating the resin (dunking) is an enormous source of complexity and cost (both CapEx and Maintenance). We would prefer to see working fluids (air, brine) pumped through an immobile reactor.

    d. This technology generates two potentially valuable waste products: water vapor and heat. Any technology that requires CO_2 and those items as inputs would synergize well with the MSS process.

Appendix, Assumptions used in Modeling

Scale			**Note:**
Target CO2 Production	100,000	MT / year	

Financial			
Required Return on Capital	3.8%		1)
OSBL + OPC Depreciation Period	20.00	Years	
OSBL + OPC Depreciation	5%		
ISBL Depreciation Period	20.00	Years	
ISBL Depreciation	5%		
Plant Overhead	60%	of Direct Fixed Costs	2)
Insurance, Property Tax, Land	3.00%	of Total Plant Capital	2)
Maintenance & Materials	2.00%	of ISBL	2)
Direct Overhead	45.00%	of Direct Labor & Supervision	2)
Indirect Overhead	0.00%	of Direct Fixed Costs	
Operating Rate	95%		
Working Capital % of Assets	1%	of Total Project Investment	3)

Utilities and Consumables Costs			
Electricity Cost	59.1	$ / MWh	4)
MSS Process Water Cost	0.025	$ / MT	
Sodium Bicarbonate	250	$ / MT	
Natural Gas - Industrial Rate	6.47	$ / Mcf	5)

MSS Module Expenses			
MSS Resin Price	$ 3.00	$ / kg	7)
Resin Mats as % of Total	75%	%	

Structural Plastic	$ 2.76	$ / kg	
Structure Materials as % of Part Cost	75%	%	8)
MSS Container Discount Factor	0%	%	
MSS Labor Time	10	hour	

MSS Module Expenses			
Cube Resin Mass	100	g	
Cube Structure Mass	2.00	g	
Cube Side Length	10.00	cm	
Resin Productivity	1.67	g/kg-h	9)
MSS Overcapacity	25%		
MSS To Brine Fan Count	4		
MSS To Brine Fan Outlet Pressure	102.1	kPa	
MSS To Brine Fan Efficiency	80%		
Product Stream CO2 Partial Pressure	5000.00	Pa	
MSS % Uptime	95%		
Carbonator Absorptive Capacity	5.50	g / m3 / min	9)
Moles of H20 used per Mole of CO2	1350	mols H20/mol CO2	10)

MC Module Performance			
Brine to MC Compressor Outlet Pressure	200	kPa	
Brine to MC Compressor Count	4		
Brine to MC Compressor Efficiency	80%		
Feed Stream CO2 Content	95%		
Membrane Cost	3.0	$ / m^2	
Membrane Flux	1,661.00	g / m^2 / h	10)
Membrane Uptime	50%		

Dissolution Efficiency	100%	10)
Membrane Lifetime	10.00	years

Storage Statistics		
Days of Brine Storage Required	3	days
Bicarbonate Molarity	1.00	M
Brine Tank Count	4.00	

Thermal Release Column Statistics		
Gas Release Efficiency	95%	
Brine Residence Time	300.00	s
Tc,in (CO2 Rich Brine Inlet)	20	°C
Tc,out (CO2 Rich Brine Outlet)	90	°C
Th,in (CO2 Poor Brine Inlet)	95	°C
Th, out (CO2 Poor Brine Outlet)	25	°C

Preliminary Labor Estimate		
Labor Hours per MT Product	0.50	Hours / MT
Labor Rate	$23.53	Hourly Rate
Supervision as % of Wages	15%	

NOTES:

1)	Average WACC, Utilities-Water, http://people.stern.nyu.edu/adamodar/New_Home_Page/datafile/wacc.htm
2)	Peters, Max Stone, et al. Plant design and economics for chemical engineers. Vol. 5. New York: McGraw-Hill, 2011.
3)	Two months of cash costs, roughly, no inventories
4)	EIA Arizona Industrial Rate Jan 2018 (3-23-2018)
5)	Arizona Industrial Price, EIA 2017 Year Average
6)	Team analysis based on vendor discussions
7)	Estimate, general thermoplastic resin with $.25/kg modification cost
8)	General Purpose ABS Apr-2018 (http://www.plasticsnews.com/resin/commodity-thermoplastics/current-pricing)
9)	Experimental results from laboratory
10)	Field Results (avg Summer 2018)

[1] Davis, R., Fishman, D., Frank, E. D., Wigmosta, M. S., Aden, A., Coleman, A. M., ... & Wang, M. Q. (2012). *Renewable diesel from algal lipids: an integrated baseline for cost, emissions, and resource potential from a harmonized model* (No. ANL/ESD/12-4; PNNL-21437; NREL/TP-5100-55431). National Renewable Energy Lab.(NREL), Golden, CO (United States).

[2] Carvalho, A. P., Meireles, L. A., & Malcata, F. X. (2006). Microalgal reactors: a review of enclosed system designs and performances. *Biotechnology progress*, *22*(6), 1490-1506.

[3] Mendoza, J. L., Granados, M. R., De Godos, I., Acién, F. G., Molina, E., Banks, C., & Heaven, S. (2013). Fluid-dynamic characterization of real-scale raceway reactors for microalgae production. *Biomass and Bioenergy*, *54*, 267-275.

[4] De Godos, I., Mendoza, J. L., Acién, F. G., Molina, E., Banks, C. J., Heaven, S., & Rogalla, F. (2014). Evaluation of carbon dioxide mass transfer in raceway reactors for microalgae culture using flue gases. *Bioresource technology*, *153*, 307-314.

[5] Putt, R., Singh, M., Chinnasamy, S., & Das, K. C. (2011). An efficient system for carbonation of high-rate algae pond water to enhance CO2 mass transfer. Bioresource technology, 102(3), 3240-3245.

[6] Weissman, J. C., & Goebel, R. P. (1987). *Design and analysis of microalgal open pond systems for the purpose of producing fuels: a subcontract report* (No. SERI/STR-231-2840). Solar Energy Research Inst., Golden, CO (USA).

[vii] Kumar, K., Mishra, S. K., Shrivastav, A., Park, M. S., & Yang, J. W. (2015). Recent trends in the mass cultivation of algae in raceway ponds. *Renewable and Sustainable Energy Reviews*, *51*, 875-885.

[viii] Davis, R., Markham, J., Kinchin, C., Grundl, N., Tan, E. C., & Humbird, D. (2016). *Process design and economics for the production of algal biomass: algal biomass production in open pond systems and processing through dewatering for downstream conversion* (No. NREL/TP-5100-64772). National Renewable Energy Lab.(NREL), Golden, CO (United States).

[ix] Peng, N., Widjojo, N., Sukitpaneenit, P., Teoh, M. M., Lipscomb, G. G., Chung, T. S., & Lai, J. Y. (2012). Evolution of polymeric hollow fibers as sustainable technologies: past, present, and future. *Progress in Polymer Science*, *37*(10), 1401-1424.

[x] https://www.gewater.com/kcpguest/documents/Fact%20Sheets_Cust/Americas/English/FSpw500D-MOD_EN.pdf

[xi] City of Modesto, Proposal Number 186238-2, Original Project Number 500475, September 7, 2017.

[xii] https://www.mi-wea.org/docs/Session%202%20-%20Joe%20Hebert.pdf

[xiii] Deng, L., & Hägg, M. B. (2010). Techno-economic evaluation of biogas upgrading process using CO2 facilitated transport membrane. *International Journal of Greenhouse Gas Control*, *4*(4), 638-646.

[xiv] http://www.sgc.se/ckfinder/userfiles/files/SGC270.pdf

[xv] Cote, P., Alam, Z., & Penny, J. (2012). Hollow fiber membrane life in membrane bioreactors (MBR). *Desalination*, *288*, 145-151.

[xvi] http://people.stern.nyu.edu/adamodar/New_Home_Page/datafile/wacc.htm (updated January 2018)